

Experimental Negative Triangularity activities on present-day devices and WPDES results related to DEMO NT

O. Sauter

With many contributions from colleagues and other tokamaks (but it is not an exhaustive review)

Slides from A. Balestri, J. Ball, O. Février, B. Labit, O. Sauter and S. Van Mulders

EPFL

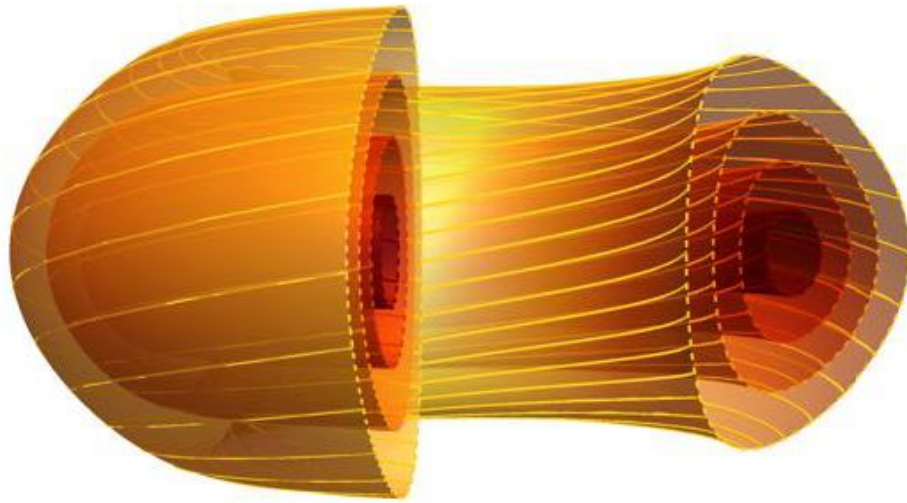


This work has been carried out within the framework of the EUROfusion Consortium, partially funded by the European Union via the Euratom Research and Training Programme (Grant Agreement No 101052200 — EUROfusion). The Swiss contribution to this work has been funded by the Swiss State Secretariat for Education, Research and Innovation (SERI). Views and opinions expressed are however those of the author(s) only and do not necessarily reflect those of the European Union, the European Commission or SERI. Neither the European Union nor the European Commission nor SERI can be held responsible for them.



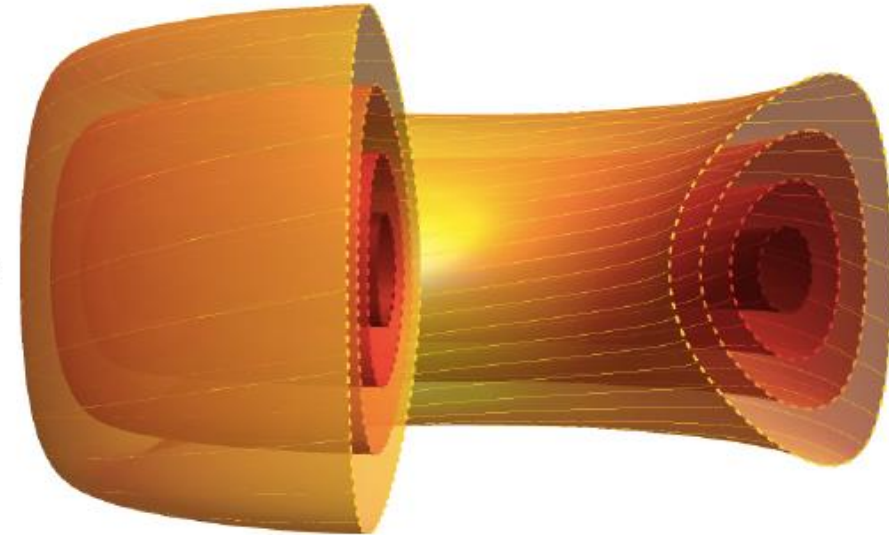
Assess a new operating regime for power plants

Positive Triangularity (PT) in H-mode



- 1) H-mode performance
 - 2) ELMs
 - 3) Standard H-mode SOL
- Everything else is similar

Negative Triangularity (NT) in L-mode



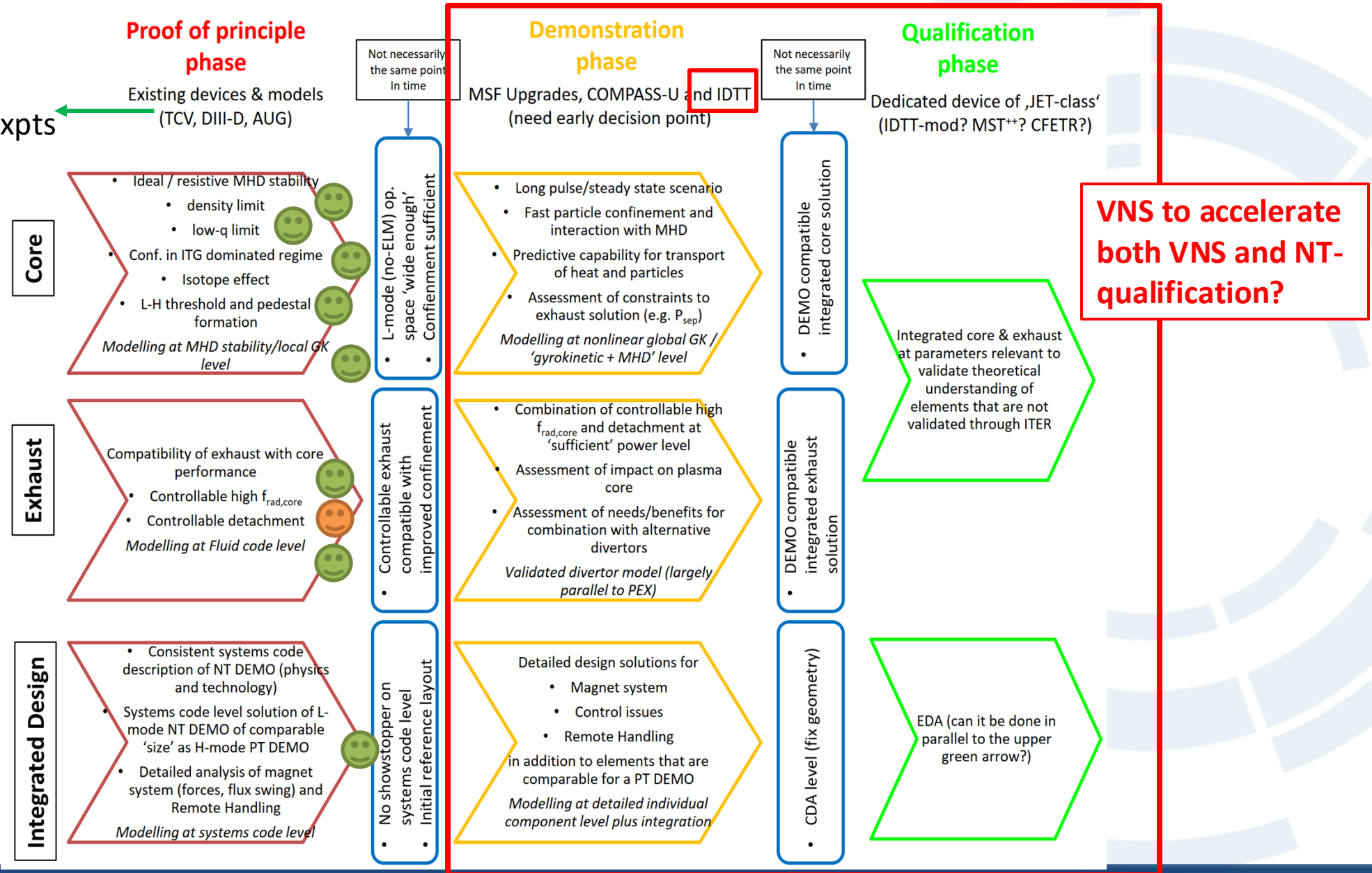
- 1) H-mode-**like** performance
 - 2) **No** ELMs
 - 3) **L-mode-like** SOL
- Everything else is similar



Strategy from ad-hoc group (2020): <https://idm.euro-fusion.org/?uid=2N29CN>

In addition:

JET, MAST-U and WEST expts
DTT-similarity expts





Special Issue on Advances in the Physics Basis of Negative Triangularity Tokamaks (<https://iopscience.iop.org/collections/ppcf-231109-412> 2024/2025 papers)

Modelling of power exhaust in TCV positive and negative triangularity L-mode plasmas

E Tonello et al 2024 Plasma Phys. Control. Fusion 66 065006

Comparison of detachment in Ohmic plasmas with positive and negative triangularity

O Février et al 2024 Plasma Phys. Control. Fusion 66 065005

Assessment of vertical stability for negative triangularity pilot plants

S Guizzo et al 2024 Plasma Phys. Control. Fusion 66 065018

Experiments and gyrokinetic simulations of TCV plasmas with negative triangularity in view of DTT operations

A Balestri et al 2024 Plasma Phys. Control. Fusion 66 065031

Experiments and modelling of negative triangularity ASDEX Upgrade plasmas in view of DTT scenarios

L Aucone et al 2024 Plasma Phys. Control. Fusion 66 075013

Physical insights from the aspect ratio dependence of turbulence in negative triangularity plasmas

A Balestri et al 2024 Plasma Phys. Control. Fusion 66 075012

Study of impurity C transport and plasma rotation in negative triangularity on the TCV tokamak

F Bagnato et al 2024 Plasma Phys. Control. Fusion 66 075019

System size scaling of triangularity effects on global temperature gradient-driven gyrokinetic simulations

Giovanni Di Giannatale et al 2024 Plasma Phys. Control. Fusion 66 095003

Effect of rotation on negative triangularity plasmas in DIII-D

C Chrystal et al 2024 Plasma Phys. Control. Fusion 66 105004

MANTA: a negative-triangularity NASEM-compliant fusion pilot plant

The MANTA Collaboration et al 2024 Plasma Phys. Control. Fusion 66 105006

Characterization of the ELM-free negative triangularity edge on DIII-D

A O Nelson et al 2024 Plasma Phys. Control. Fusion 66 105014

Overview of results from the 2023 DIII-D negative triangularity campaign

K E Thome et al 2024 Plasma Phys. Control. Fusion 66 105018

Pedestal properties of negative triangularity discharges in ASDEX Upgrade

B Vanovac et al 2024 Plasma Phys. Control. Fusion 66 115005

Examining transport and integrated modeling predictive capabilities for negative-triangularity scenarios

J McClenaghan et al 2024 Plasma Phys. Control. Fusion 66 115008

Plasma edge and scrape-off layer turbulence in gyrokinetic simulations of negative triangularity plasmas

T N Bernard et al 2024 Plasma Phys. Control. Fusion 66 115017

Power handling in a highly-radiative negative triangularity pilot plant

M A Miller et al 2024 Plasma Phys. Control. Fusion 66 125004

Characterization and controllability of radiated power via extrinsic impurity seeding in strongly negative triangularity plasmas in DIII-D

D Eldon et al 2025 Plasma Phys. Control. Fusion 67 015018

Characterizing the negative triangularity reactor core operating space with integrated modeling

H S Wilson et al 2025 Plasma Phys. Control. Fusion 67 015026

Investigation of triangularity effects on tokamak edge turbulence through multi-fidelity gyrokinetic simulations

A C D Hoffmann et al 2025 Plasma Phys. Control. Fusion 67 015031

Achievement of highly radiating plasma in negative triangularity and effect of reactor-relevant seeded impurities on confinement and transport

L Casali et al 2025 Plasma Phys. Control. Fusion 67 025007

Experimental characterization of turbulence properties in negative triangularity DIII-D plasmas

S D Stewart et al 2025 Plasma Phys. Control. Fusion 67 025032

First observations of edge instabilities in strongly shaped negative triangularity plasmas on DIII-D

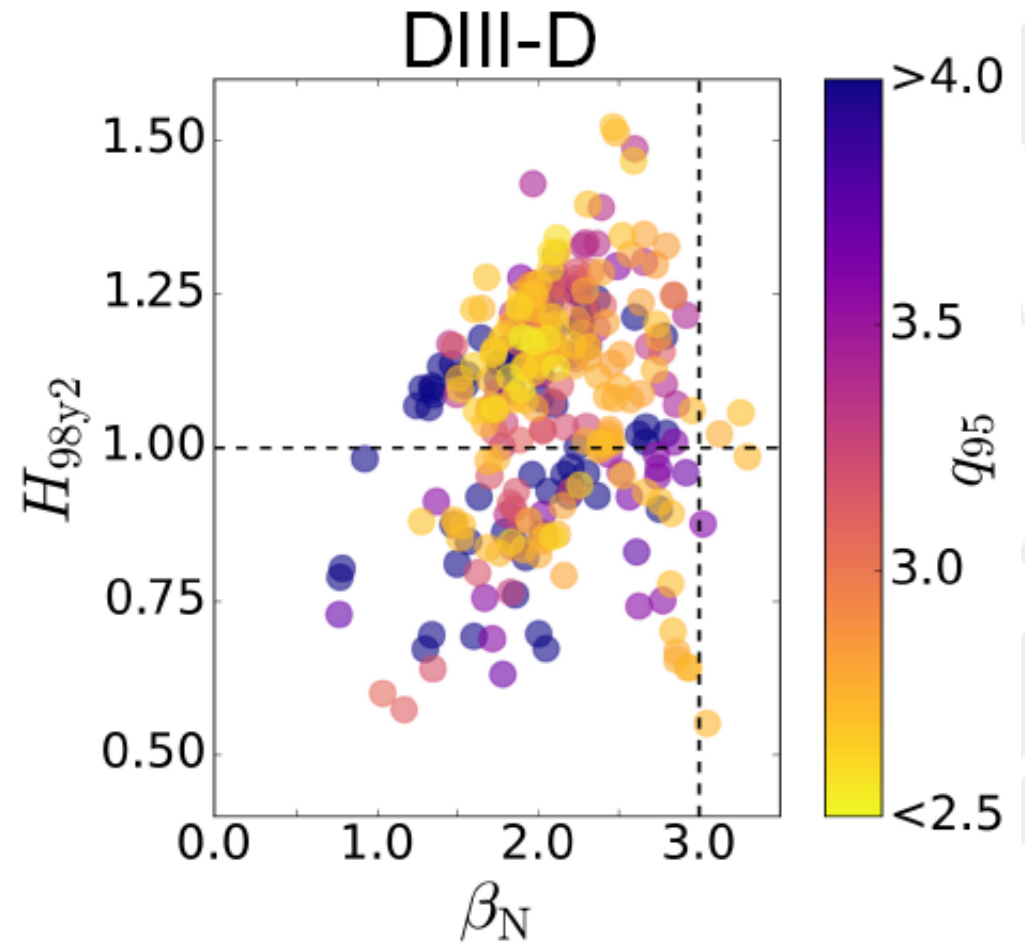
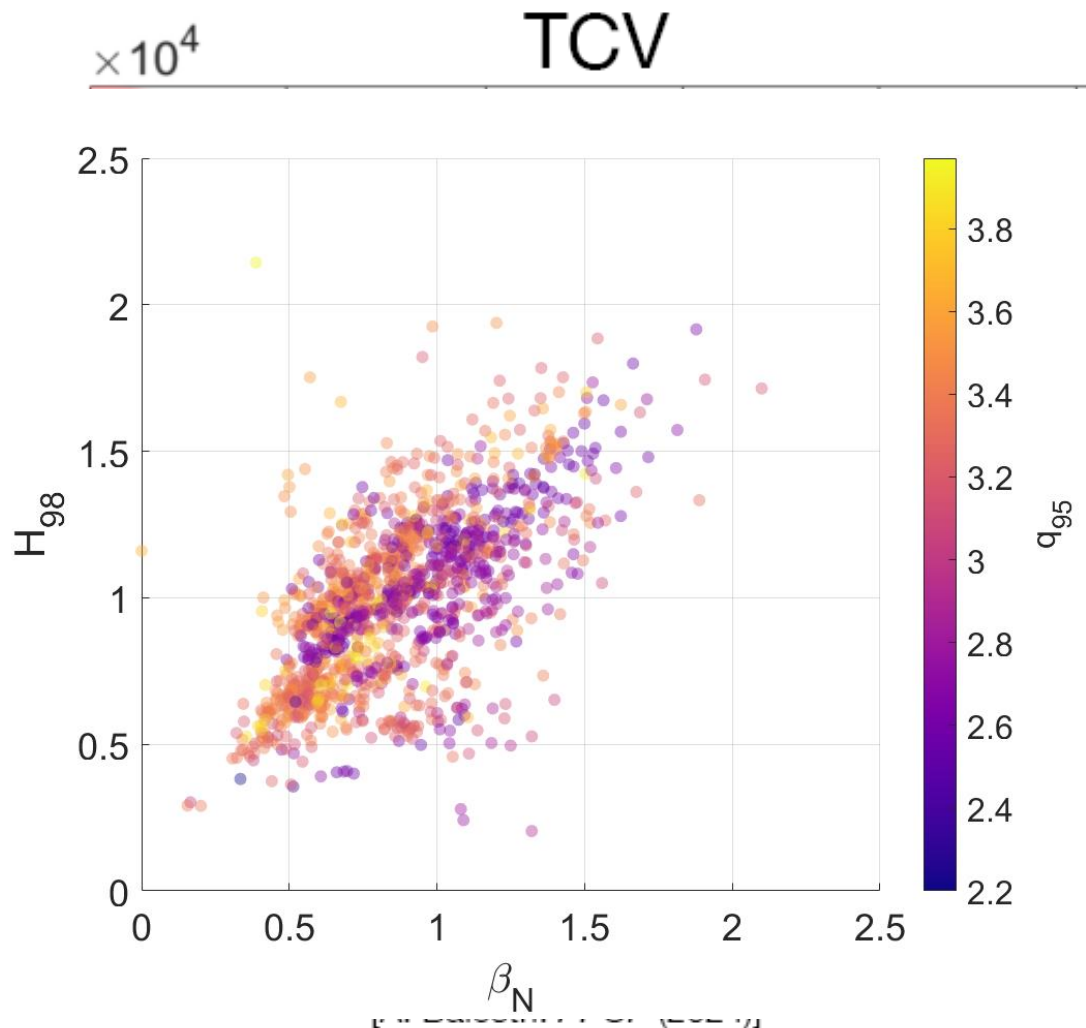
T Cote et al 2025 Plasma Phys. Control. Fusion 67 035033

Operation above the Greenwald density limit in high performance DIII-D negative triangularity discharges

O Sauter et al 2025 Plasma Phys. Control. Fusion 67 075009



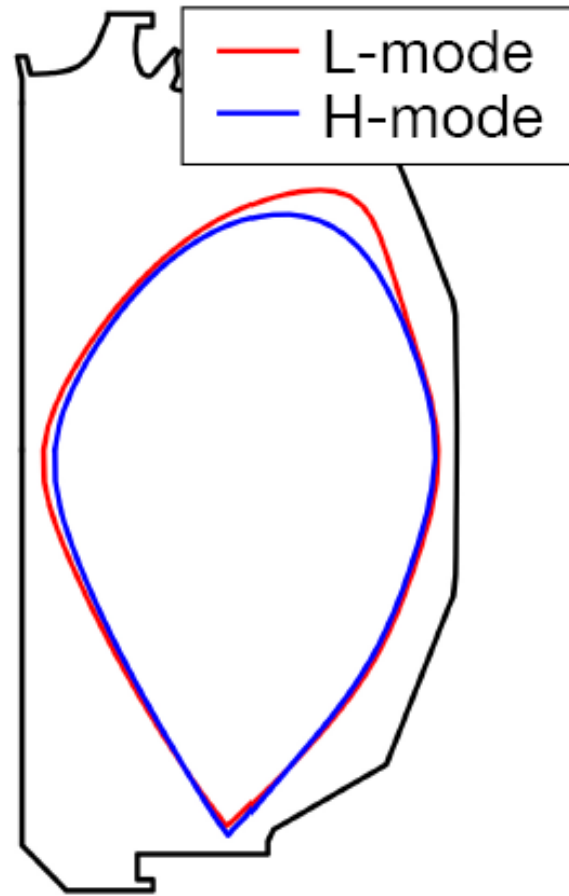
1) Core confinement



[C. Paz-Soldan. arXiv:2309.03689]

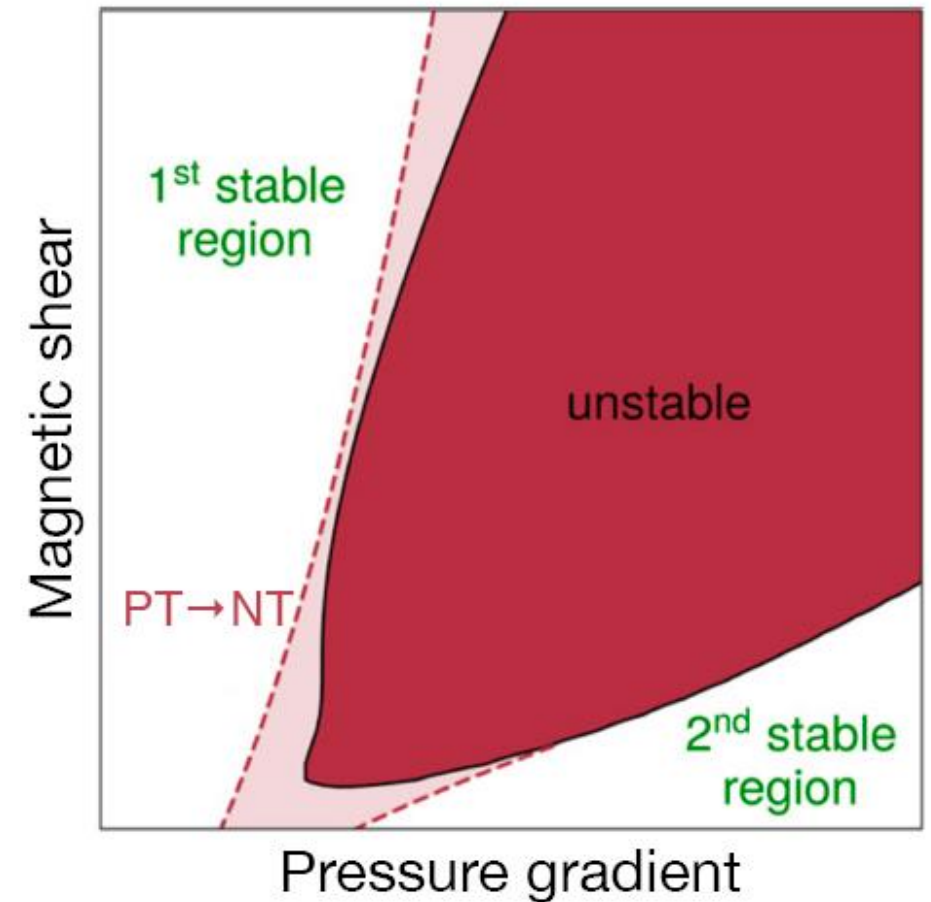


2) No L-H transition



[S. Saarelma. PPCF (2021).]

$\delta < 0$ closes access to $n = \infty$ 2nd stability region



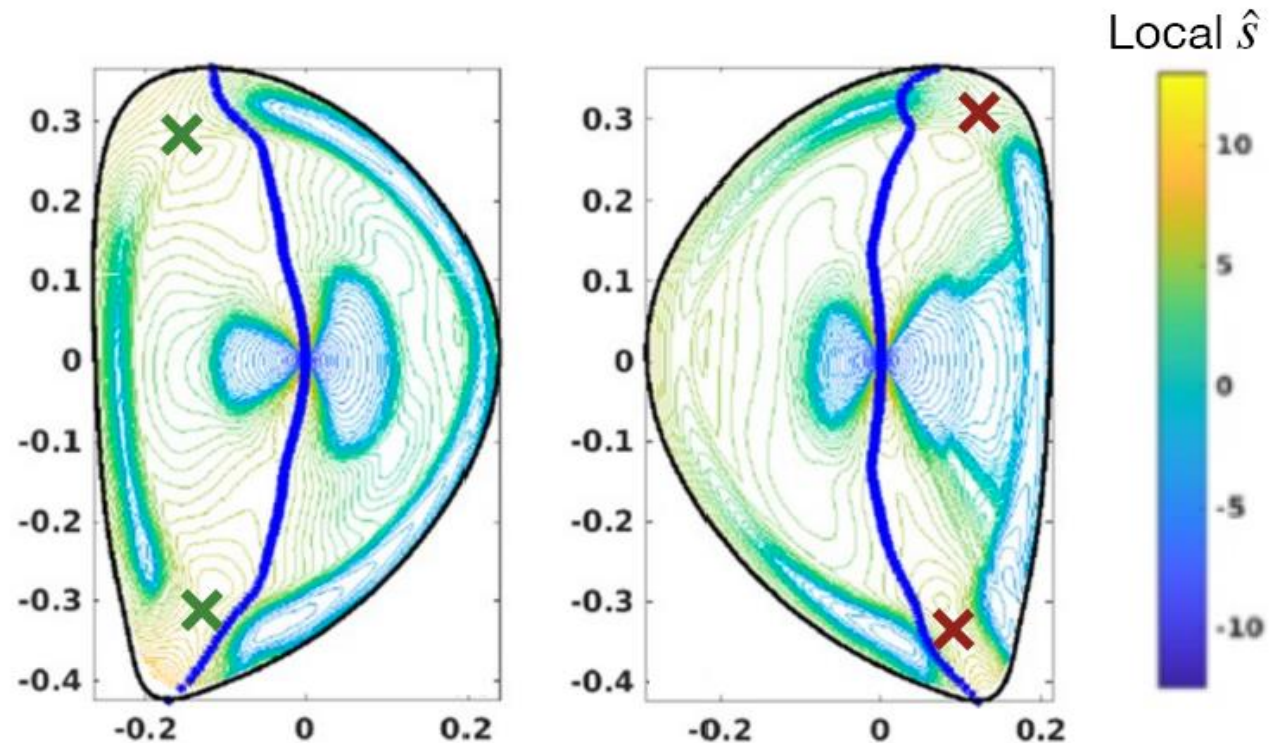


Transition to H-mode

- [1] A. Merle. *PPCF* (2017).
- [2] A. Marinoni. *Rev. Mod. Phys.* (2021).
- [3] S. Saarelma. *PPCF* (2021).
- [4] O. Nelson. *Nucl. Fusion* (2022), O. Nelson. *PRL* (2023).
- [5] O. Sauter. *IAEA* (2023).**
- [6] T. Happel. *Nucl. Fusion* (2023).

- Sufficiently negative δ closes access to the 2nd stability region for infinite-n ballooning modes, which is associated with the transition to H-mode^[1-5]
- Developed proxy for blocking the H-mode transition — when the maximum in the edge local magnetic shear crosses into the bad curvature region^[5]
- Can be used to explain ASDEX Upgrade results^[6]

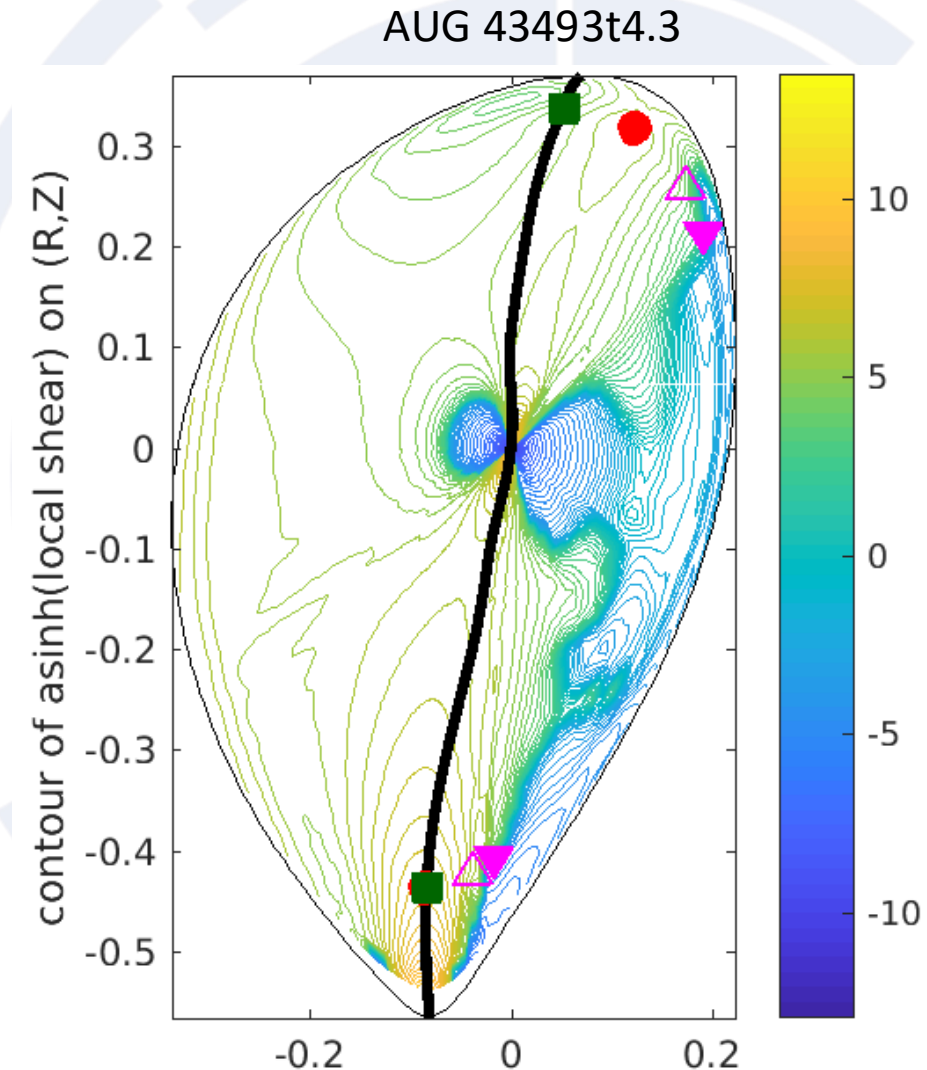
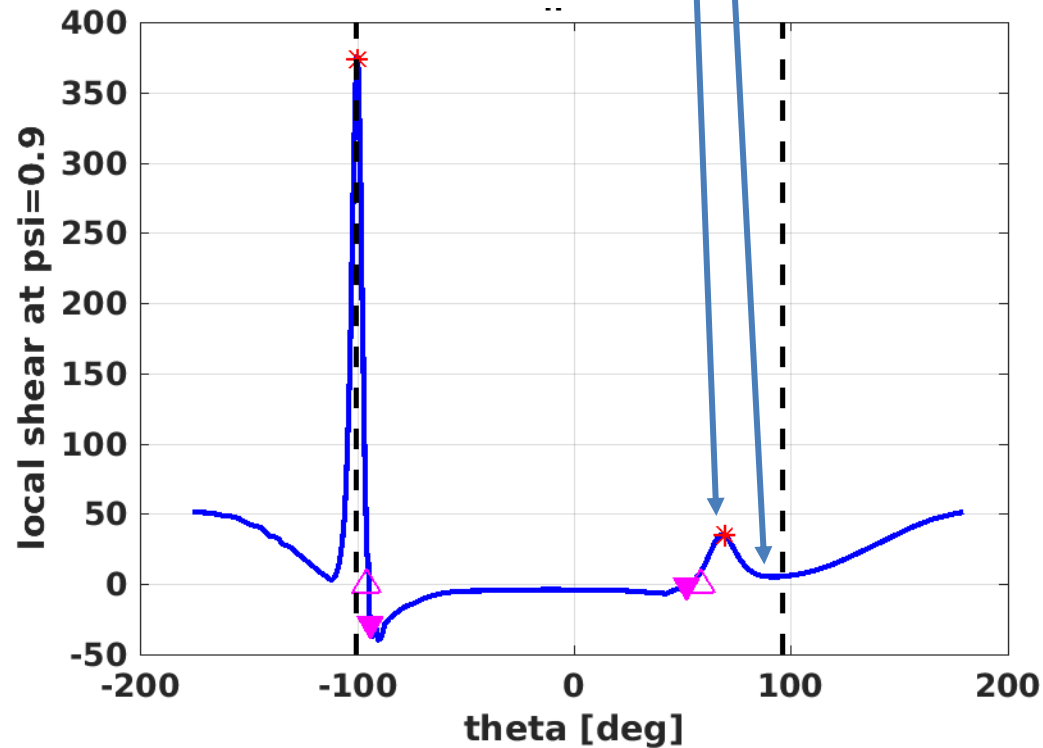
Ideal MHD, hence prediction to new machine "certain" and well validated





"Specificity" of the AUG shapes leading to residual ELMs

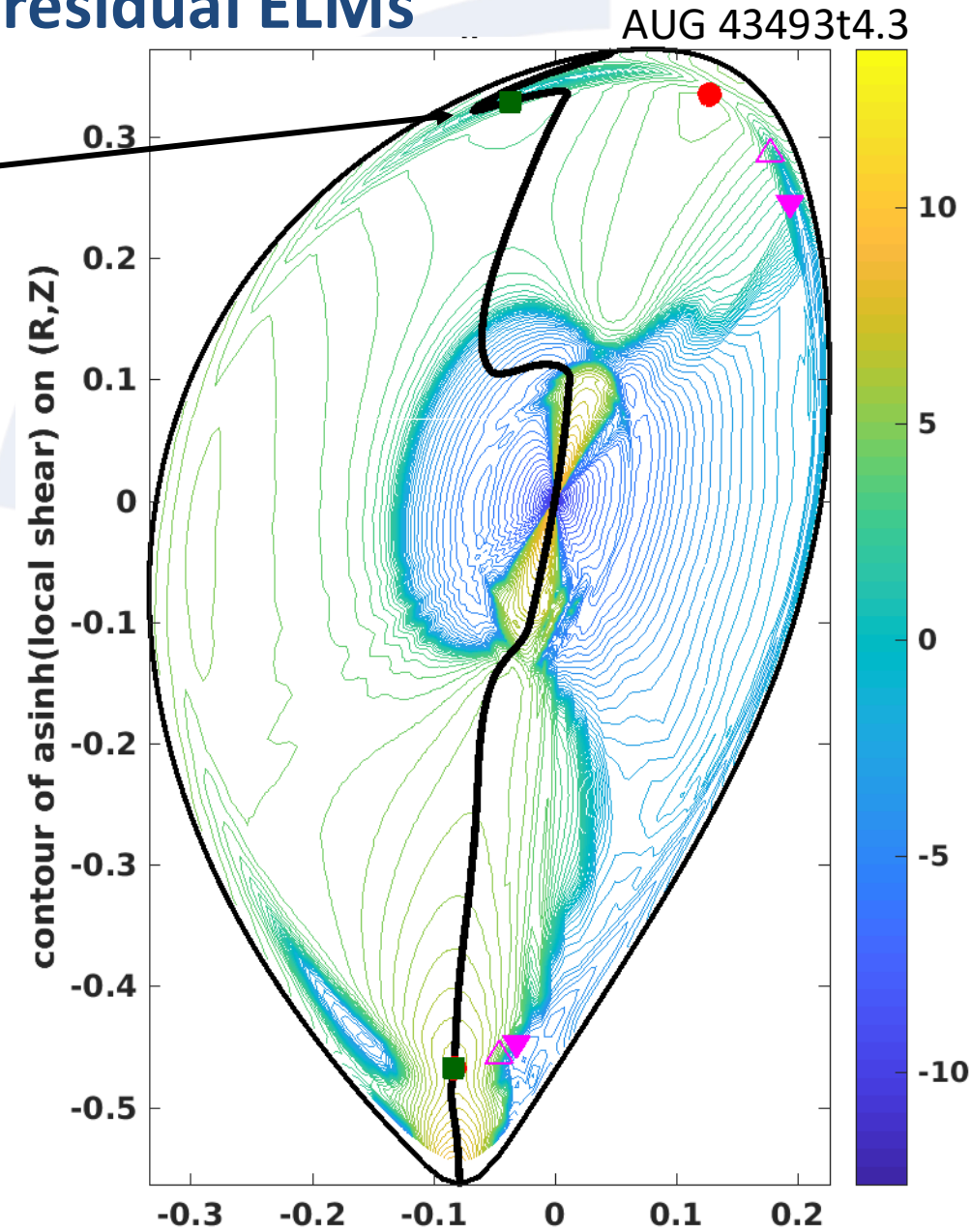
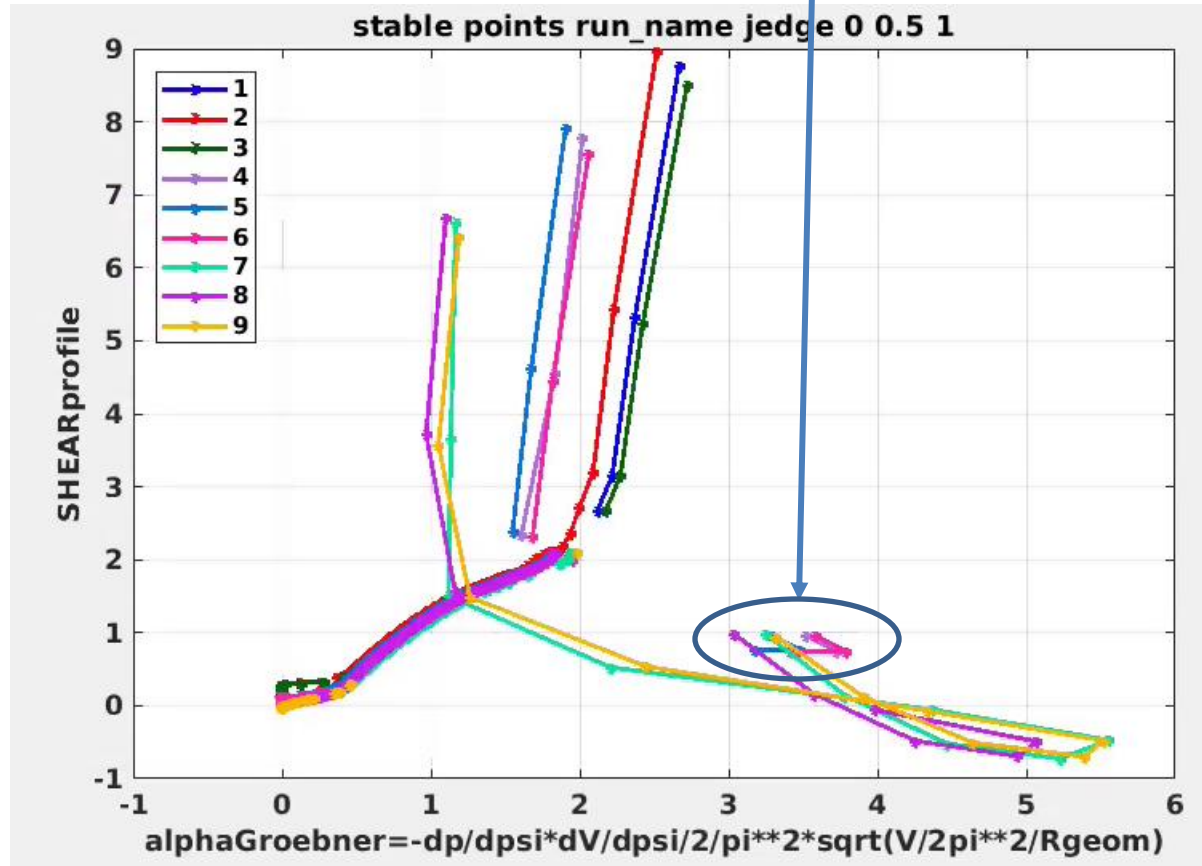
- AUG shapes are "oblique"/"tilted", requiring more negative d than TCV/DIII-D to close 2nd stability region
- Magnetic axis shifts "diagonally" with increasing β ($\Delta R \sim \Delta Z$)
- The local shear "hill" not very pronounced, easier to open
- *AUG results important to better understand other shape effects (squareness, etc)*





"Specificity" of the AUG shapes leading to residual ELMs

- Even this shape ($\delta = -0.47$) is marginal to avoid edge activity
- Good/bad curvature limit (solid line) strongly modified with edge BS current, usually not the case and will also affect transport



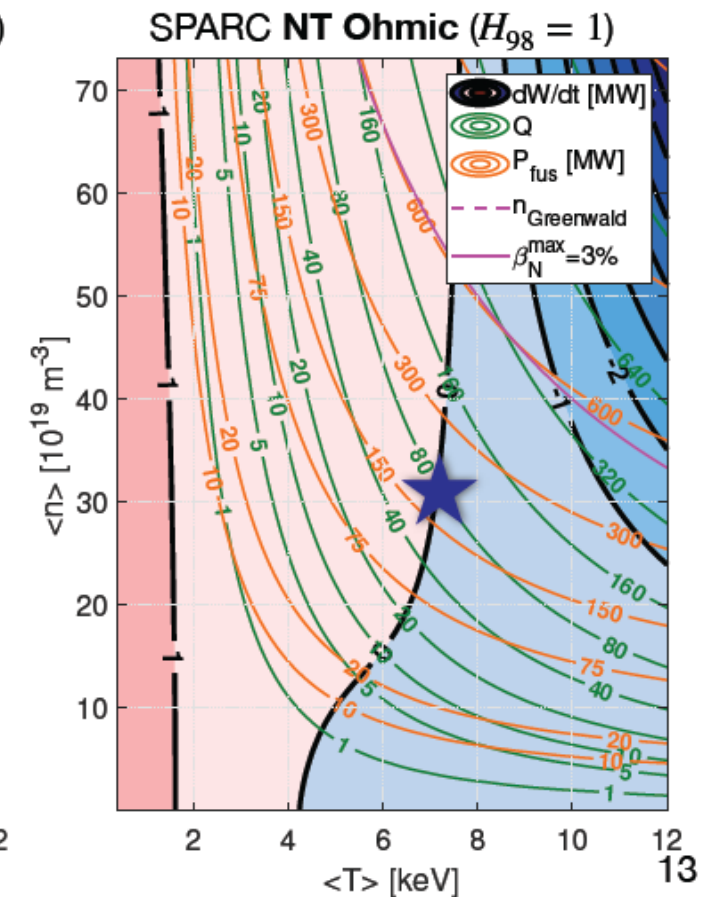
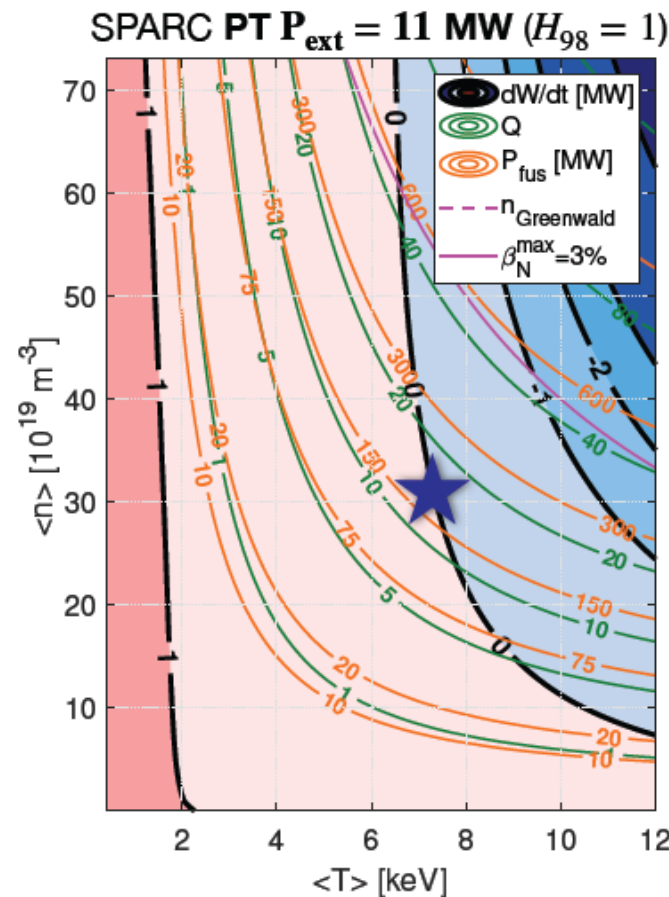


No need to exceed L-H power threshold

[1] A. Balestri. [10.1088/1741-4326/ae01bd](https://doi.org/10.1088/1741-4326/ae01bd)

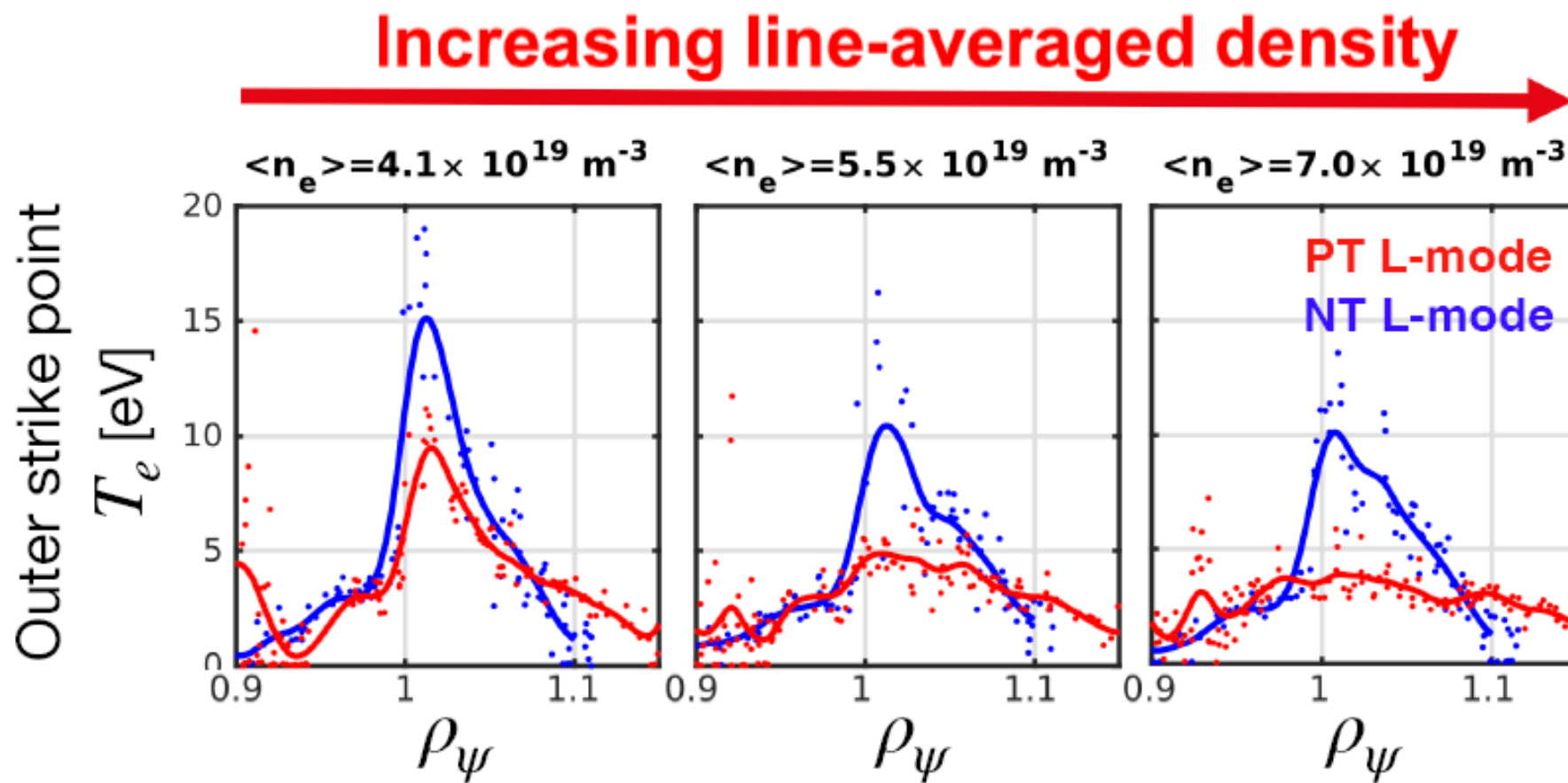
At 150MW P_{fus}

- Best to use minimum heating power that still enables significant α heating^[1]
- An Ohmically heated SPARC with a flipped triangularity may achieve $Q = 80$
- Most useful in high performance devices ($Q \gtrsim 10$), especially when B_0 is high





3) SOL dynamics



[O. Fevrier. *EPS* (2023).]



SOL width small in NT L-mode: good news! *(for confinement)*

- $\lambda_q^{\text{PT H-mode}} \leq \lambda_q^{\text{NT L-mode}} < \lambda_q^{\text{PT L-mode}}$
- λ_q represents the "confinement" quality just inside and just outside LCFS
- Hence smaller λ_q reflects larger gradients
- DIII-D recent detachment experiments: SOL heat flux widths approach values typical of inter-ELM H-mode discharges

[R I Morgan et al, Nucl. Fusion \(2025\)](#)



Detachment studies in recent DIII-D NT armor campaign

- Rev BT detaches at lower density
- Since not a problem for H-mode access might be best target solution for FPP design
- Requires new dedicated experiments on confinement, just to make sure
- Confinement degradation probably due to X-point proximity to wall, tbd

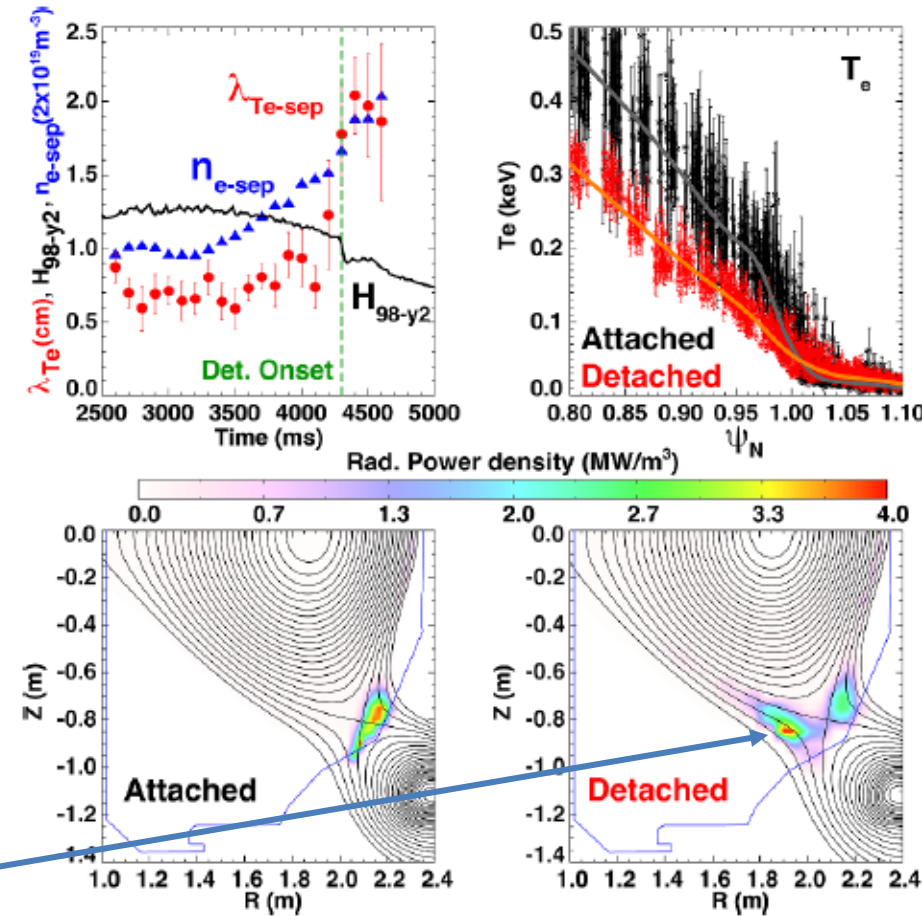
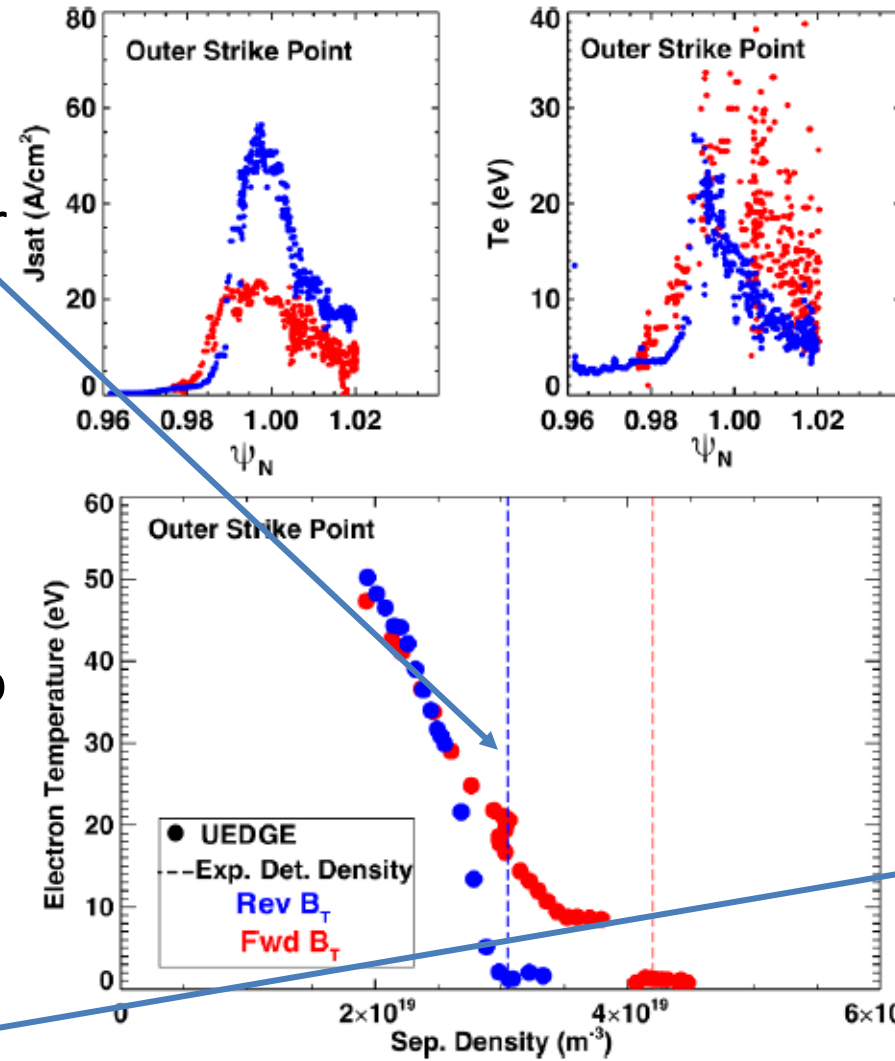
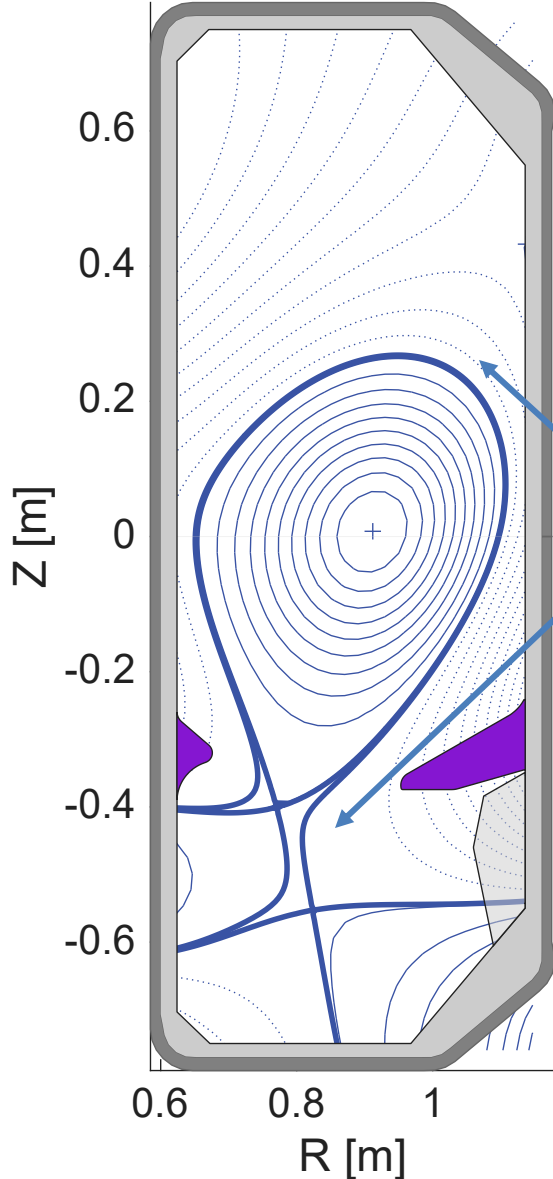


Figure 4. (Top-left) T_e gradient scale length (red) and n_e (blue) at separatrix, H-mode confinement factor (black) as a function of time during an upstream density ramp (194090); (top-right) upstream T_e

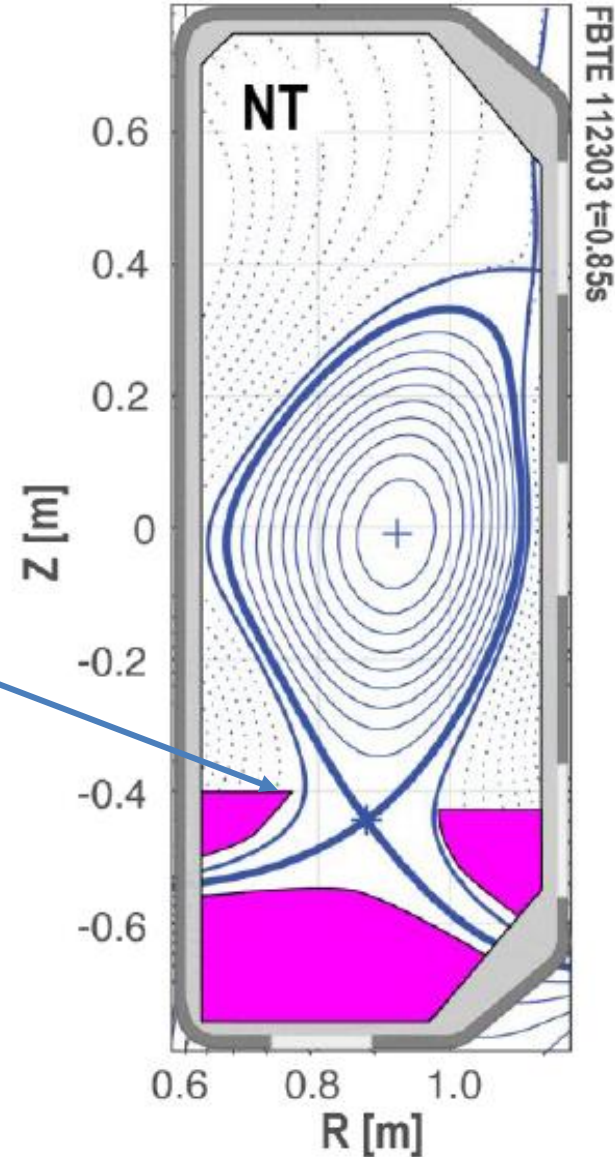
[F. Scotti et al, Nucl. Fusion 64 \(2024\) 094001](#)



Safest at this stage: Combined SND ADC, $\delta > 0$, with top $\delta < 0$



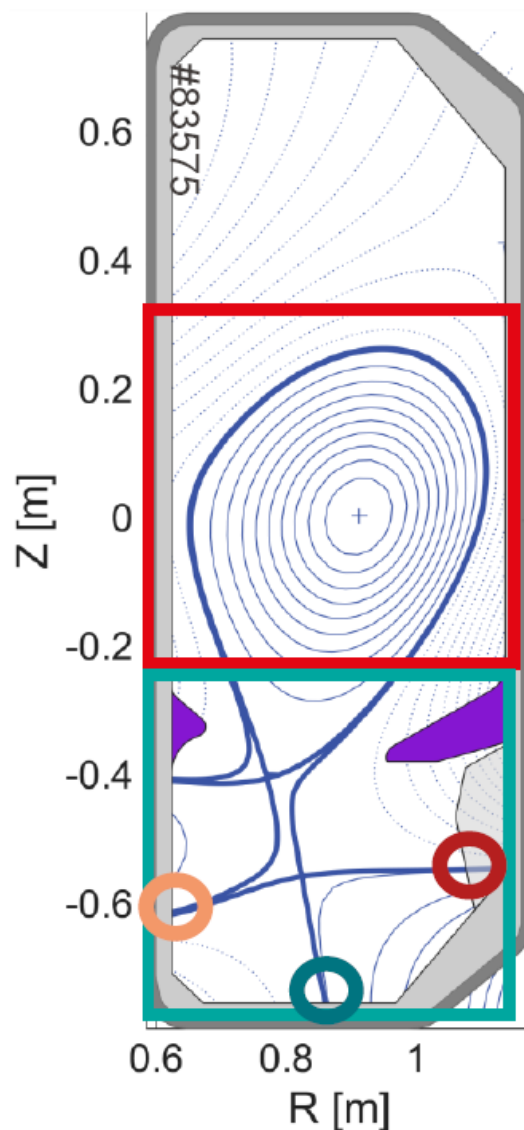
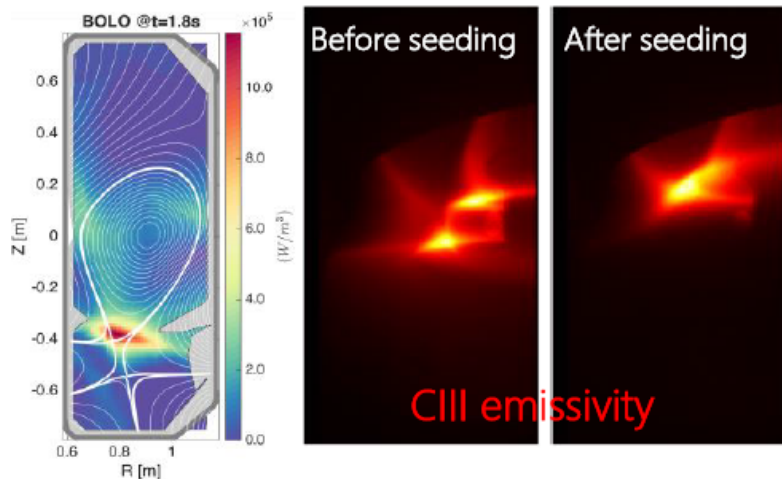
- X-point region "rapidly" uses shape benefits for confinement inside LCFS, hence can use best PT advanced divertor configuration (ADC)
- Non X-point, on the contrary determines the "good confinement" and guarantees the "no ELM" behavior
- Snowflake with negative top δ successfully tested on TCV
- Since NT seem to have lower neutral pressure, additional ADC solutions are needed, TCV can test a dedicated tightly baffled configuration



[1] G. Durr-Legoupil-Nicoud P1-050 EPS 2025

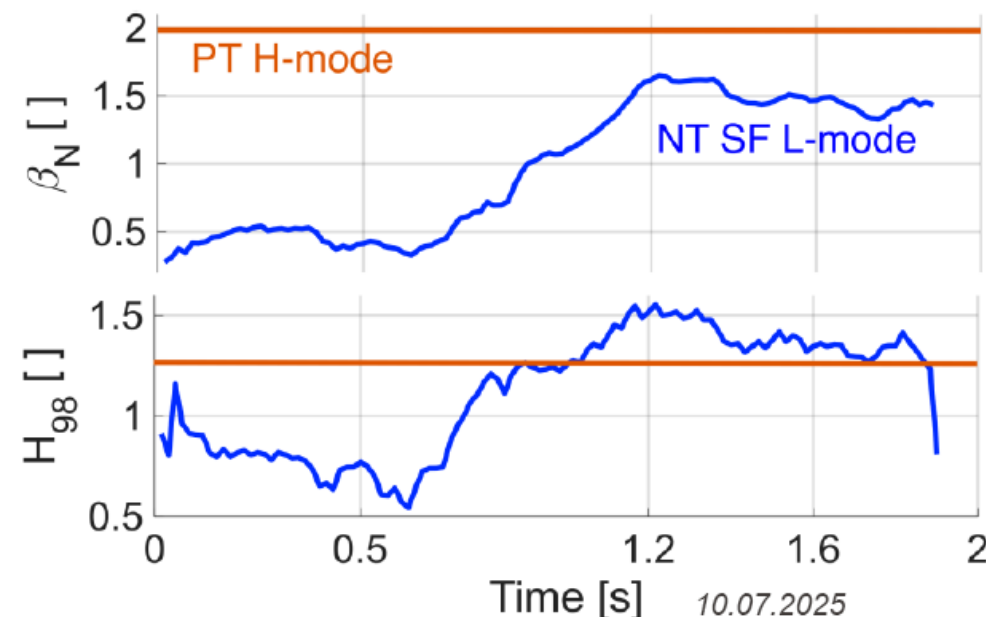
Baffled Snowflake divertor

- Impurity seeding: N_2 ramp
- X-point radiator seen by bolometry and MANTIS
- Detachment of **SP2**, **SP3** and **SP4** seen by wall-embedded Langmuir probes



High performance scenario

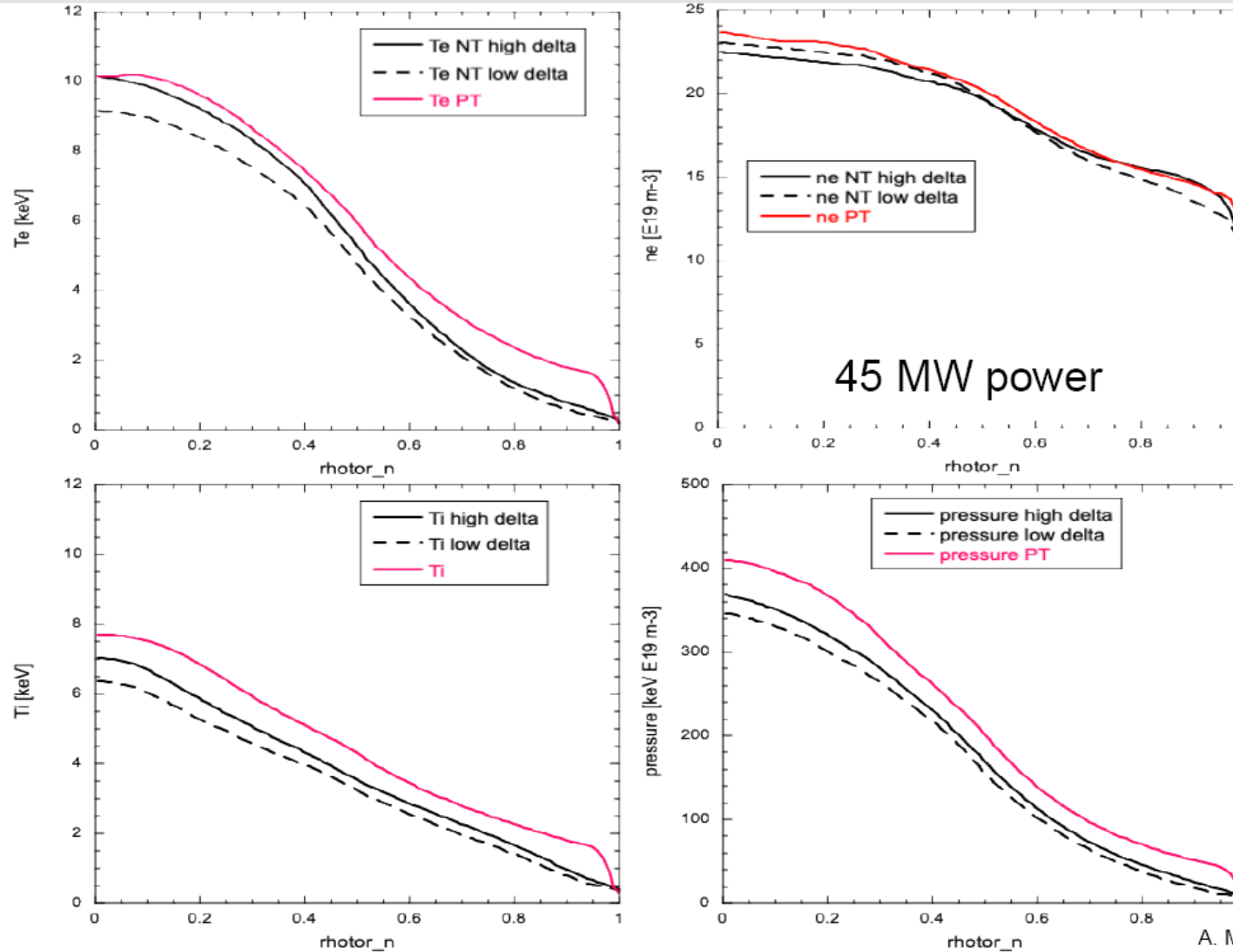
- Performance comparable to PT LSN H-mode with double power
- Core performance degraded by N_2 as in PT H-mode





DTT can test exactly this core-edge integration

DTT higher δ NT predictions : Miller



- Modelling using ASTRA/TGLF SAT2 with Miller geometry up to $\rho=1$ in NT and pedestal top in PT
- Te, Ti, ne, J, Ar, W predicted
- **The high δ shape improves central T values for similar n and radiation**
- NT core pressure is reduced by $\sim 10\%$ wrt PT H-mode

➔ NT scenarios in DTT will allow L-mode edge operation with good core performance



What about "standard" operational limits

- q_{95} down to 2.2-2.4 routinely used on TCV and DIII-D
- No problem with $q_{95} \sim 3$
- $q_{95} > 2$ limit confirmed on both TCV and DIII-D
- No impurity accumulation difficulties observed on neither TCV and DIII-D (even at high P_{rad}), nor JET (ILW) and AUG (W wall) (nor WEST, preliminary results)
- Stationary plasmas with high power easily obtained even up to $> 30\text{MW}$ on JET (*see next slides*)
- Density limit $\gg n_G$ with auxiliary power (DIII-D results, see next slides)
- β_N up to 3 reached on DIII-D in stationary state, near 3 in JET and TCV. Again, basic ideal MHD calculations confirmed
- No "significant" problems with NTMs, except may be when coupling with VDE



Density limit studied in detail in DIII-D armor campaign

Operation above the Greenwald density limit in high performance DIII-D negative triangularity discharges

O Sauter¹, R. Hong², A. Marinoni³, F. Scotti⁴, P. Diamond³, C. Paz-Soldan⁵, D. Shiraki⁶, K. E. Thome⁷, M. A. Van Zeeland⁷, Z. Yan⁸ and the negD-DIII-D Team^x

¹ Ecole Polytechnique Fédérale de Lausanne (EPFL), Swiss Plasma Center (SPC), Lausanne, Switzerland

² University of California, Los Angeles, CA, United States of America

³ University of California, San Diego, CA, United States of America

⁴ Lawrence Livermore National Laboratory, Livermore, CA, United States of America

⁵ Columbia University, New York, United States of America

⁶ Oak Ridge National Laboratory, Oak Ridge, TN, United States of America

⁷ General Atomics, San Diego, CA, United States of America

⁸ University of Wisconsin-Madison, Madison, WI, United States of America

^x see K. Thome et al, Plasma Phys. Control. Fusion **66** (2024) 105018

E-mail: Olivier.Sauter@epfl.ch



<https://doi.org/10.1088/1361-6587/ade185>



Related topics and motivation

- Explore **L-mode** density limit in **high performance** NT plasmas to verify their reactor relevance
- Is Greenwald fraction also "the" scaling to use
- Recent theory motivated by edge turbulence results yields:

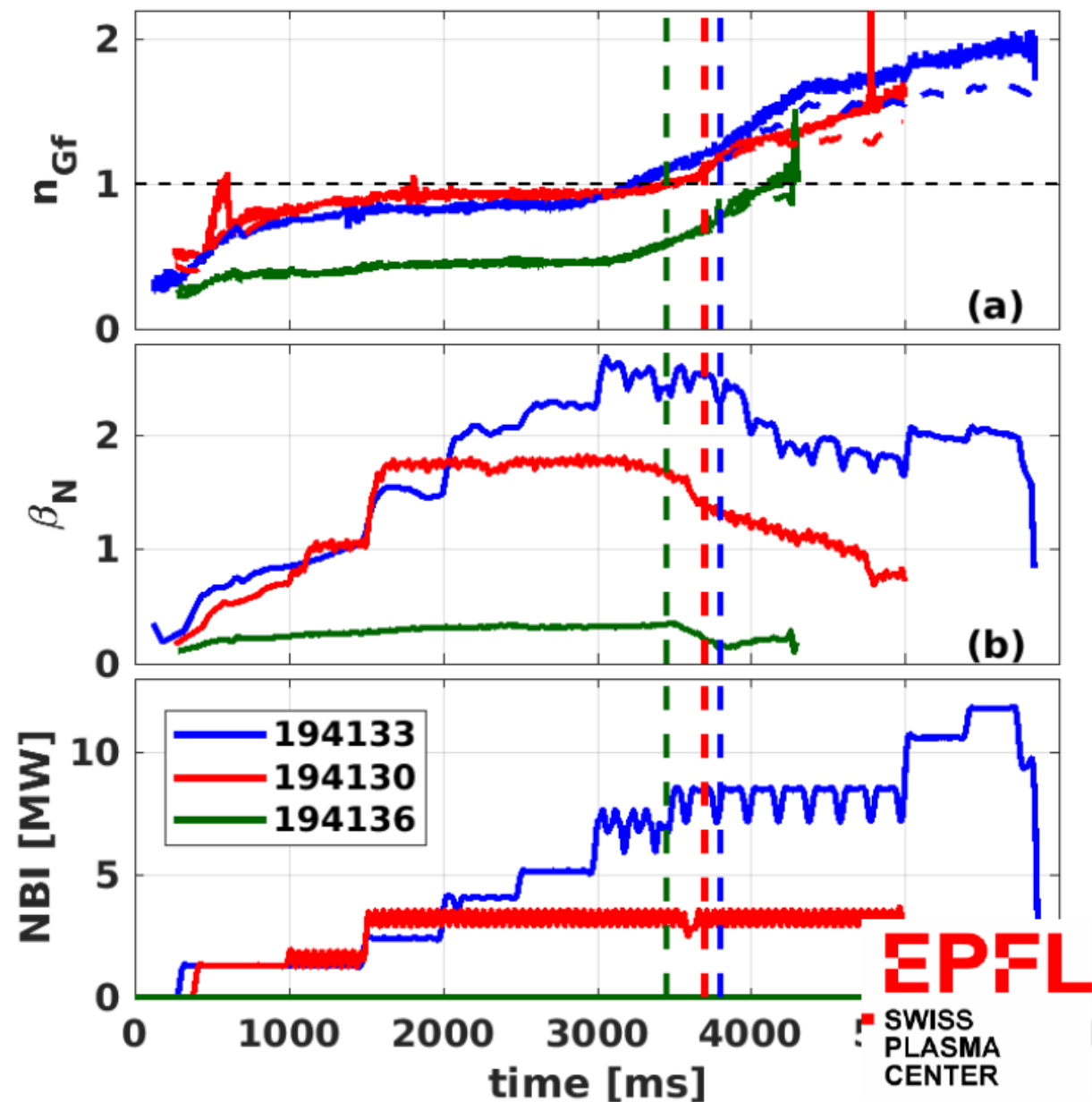
$$n_{\text{lim}} \sim A^{1/6} P_{\text{SOL}}^{10/21} R_0^{1/42} B_T^{-8/21} (1 + \kappa^2)^{-1/3} \frac{I_p^{22/21}}{a^{79/42}} \quad (13)$$

M. Giacomini et al, Phys. Rev. Lett. **128** 185003 (2022)

- With the new armor, DIII-D can test the density limit at high power (at TCV, mainly ohmic and Psep up to 1MW)

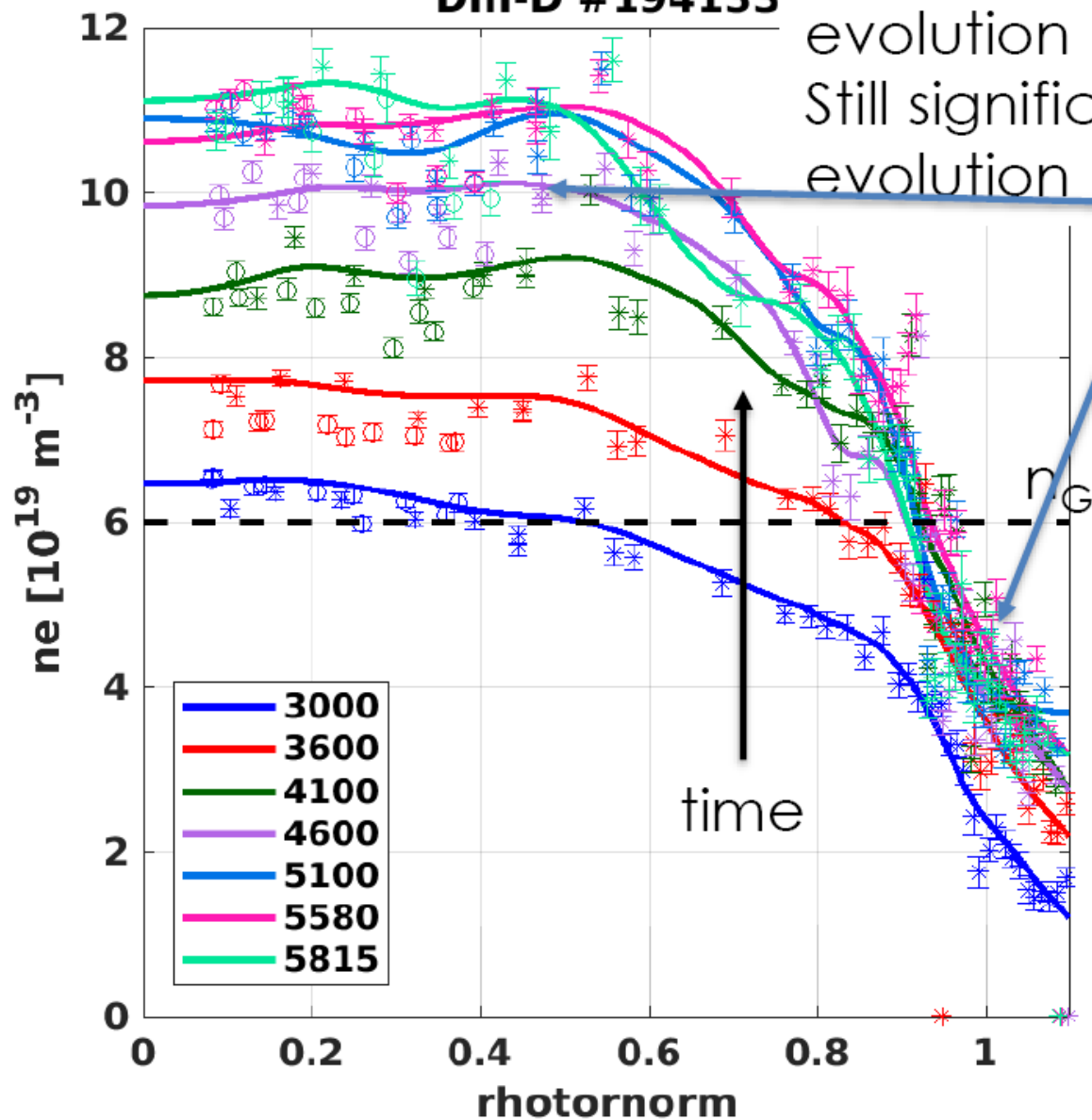
0.6MA: main results: $n_{Gf} \gg 1$ and clear power dependence

- $n_{Gf} = n_{el} / n_G$ (standard in all density limit papers)
- n_{el} = line-averaged density from horizontal FIR "R0" line of sight
- $n_G = I_p [MA] / (\pi a [m]^2)$ (Greenwald NF 28, 2199 (1988))
- Dashed lines: n_{Gf}^{LCFS} from Thomson nel along R0 (integ inside LCFS)
- $n_{Gf} = 1.95$ reached (at 11.8MW)
- $n_{Gf} = 1.7$ with 3.2MW
- $n_{Gf} = 1.2$ in ohmic
- Vertical dashed: start of detachment/Marfe



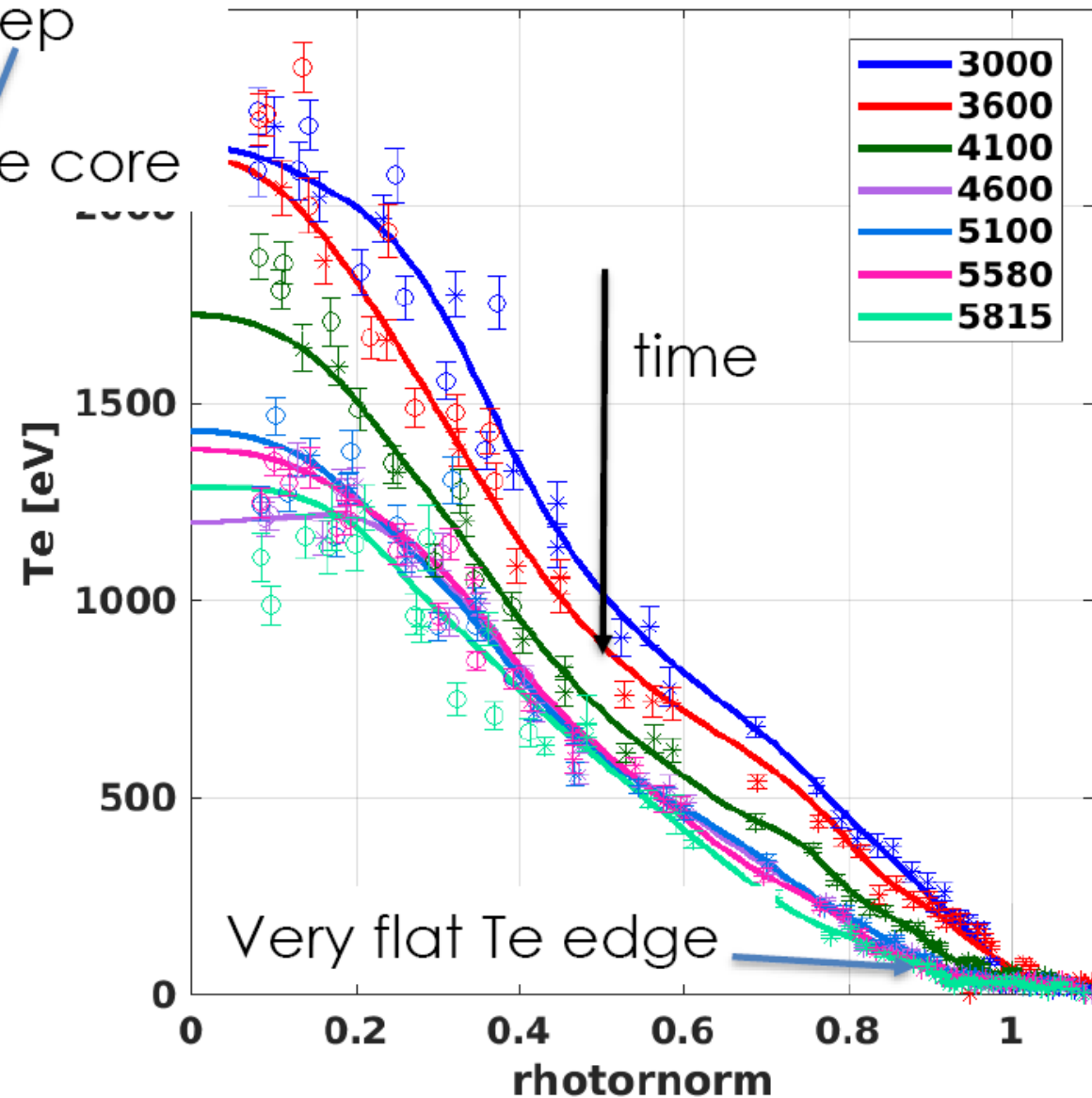
Profiles evolution

DIII-D #194133

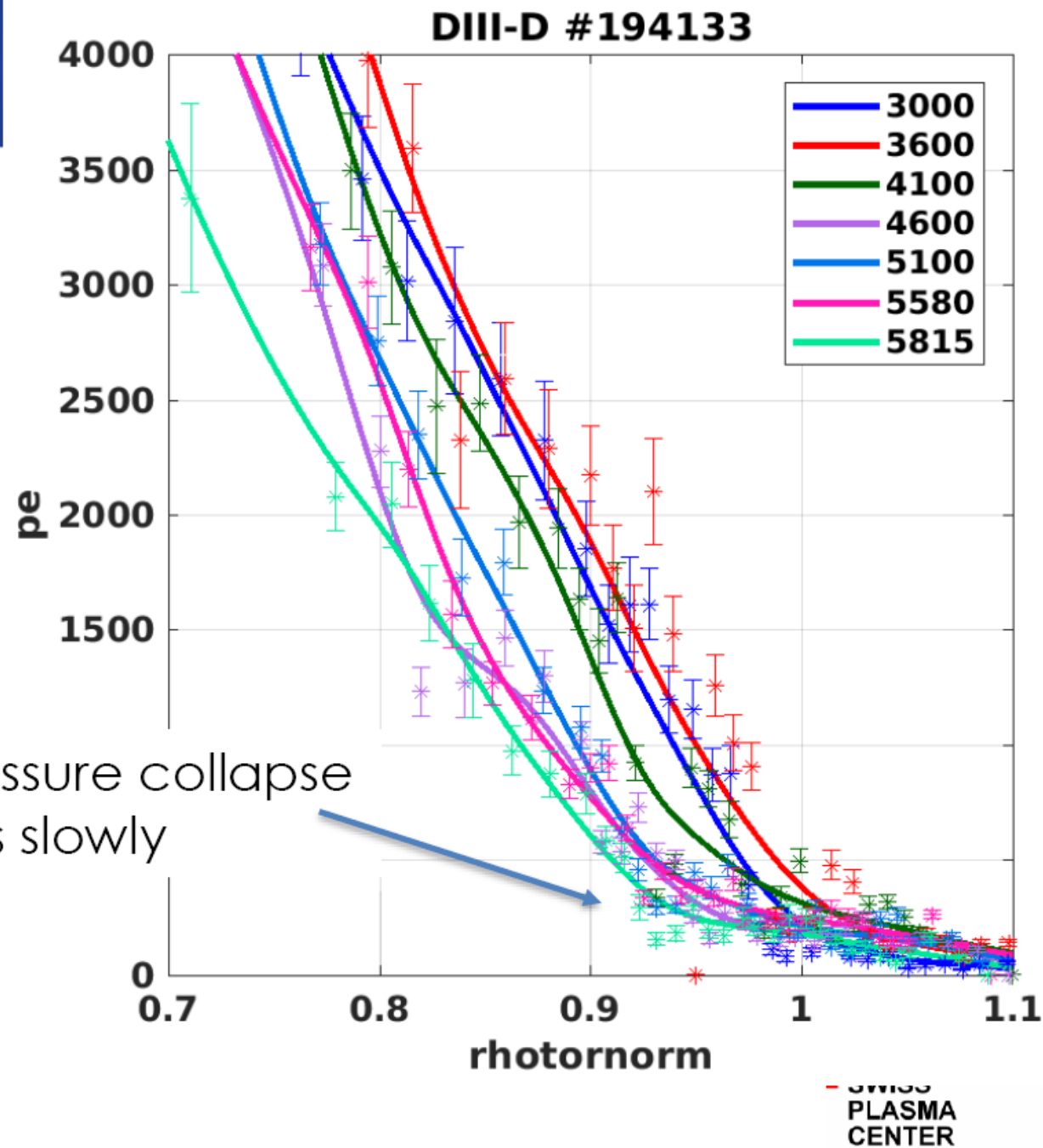
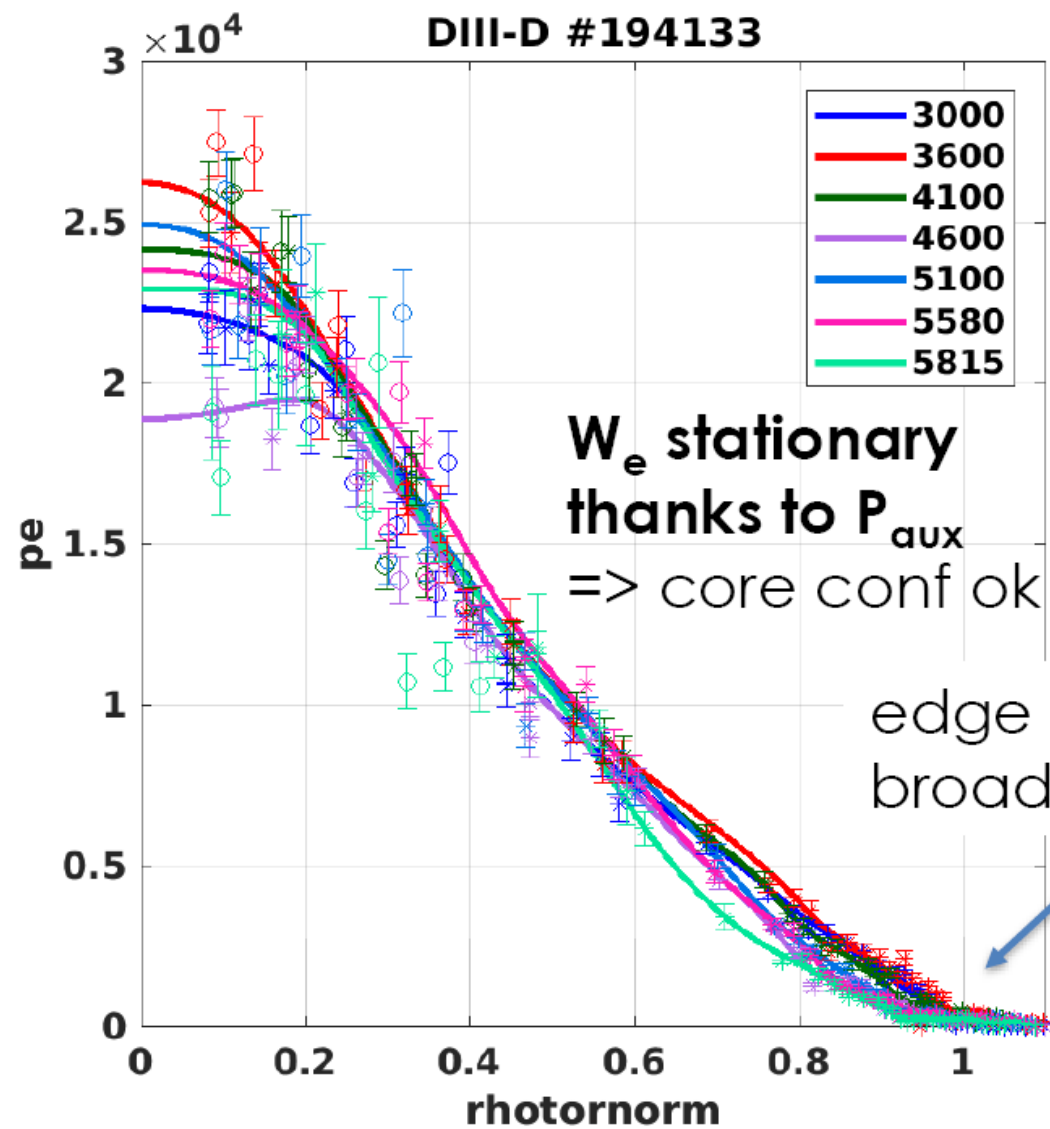


From 4100ms little evolution ne sep
Still significant evolution of ne core

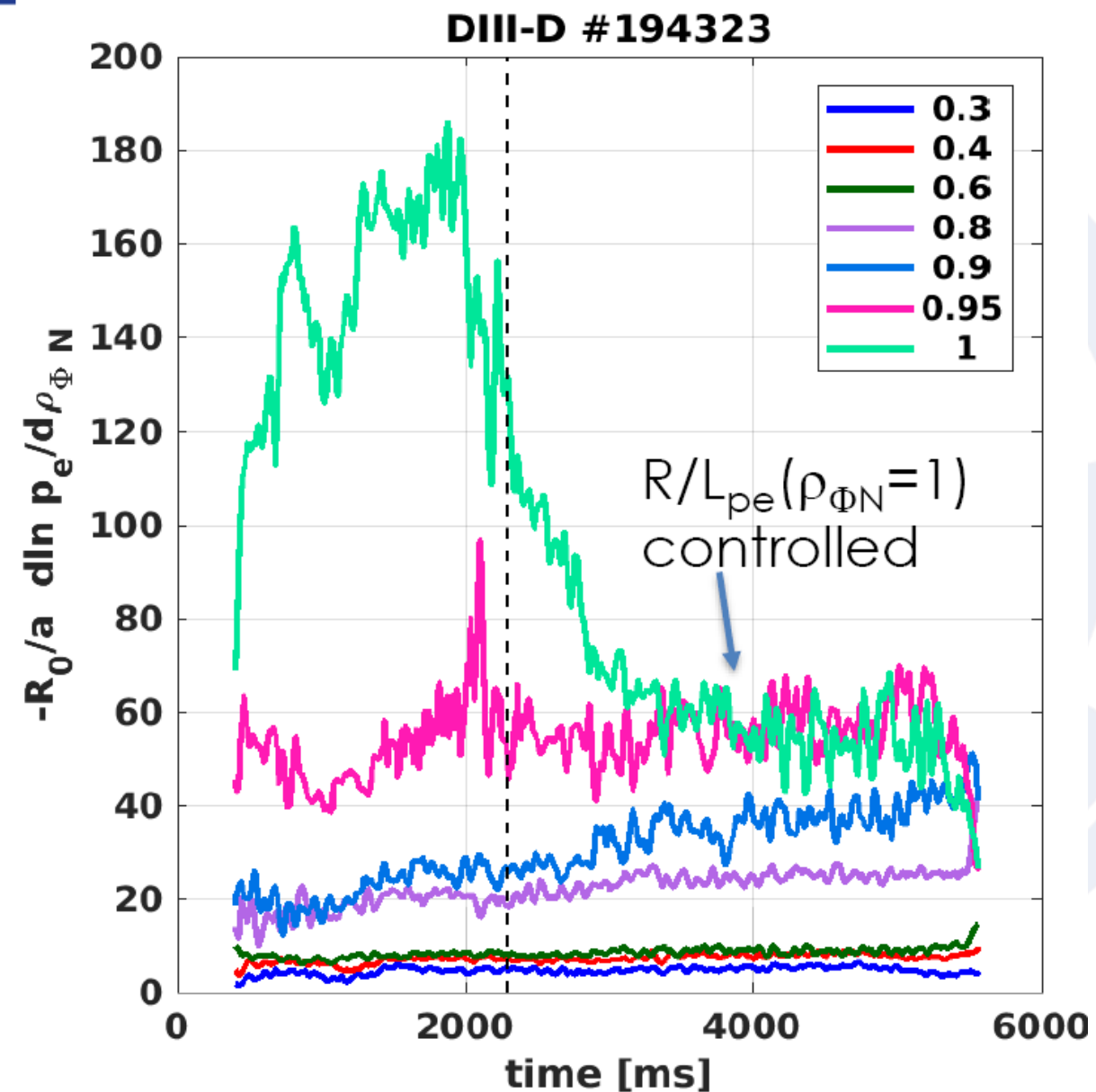
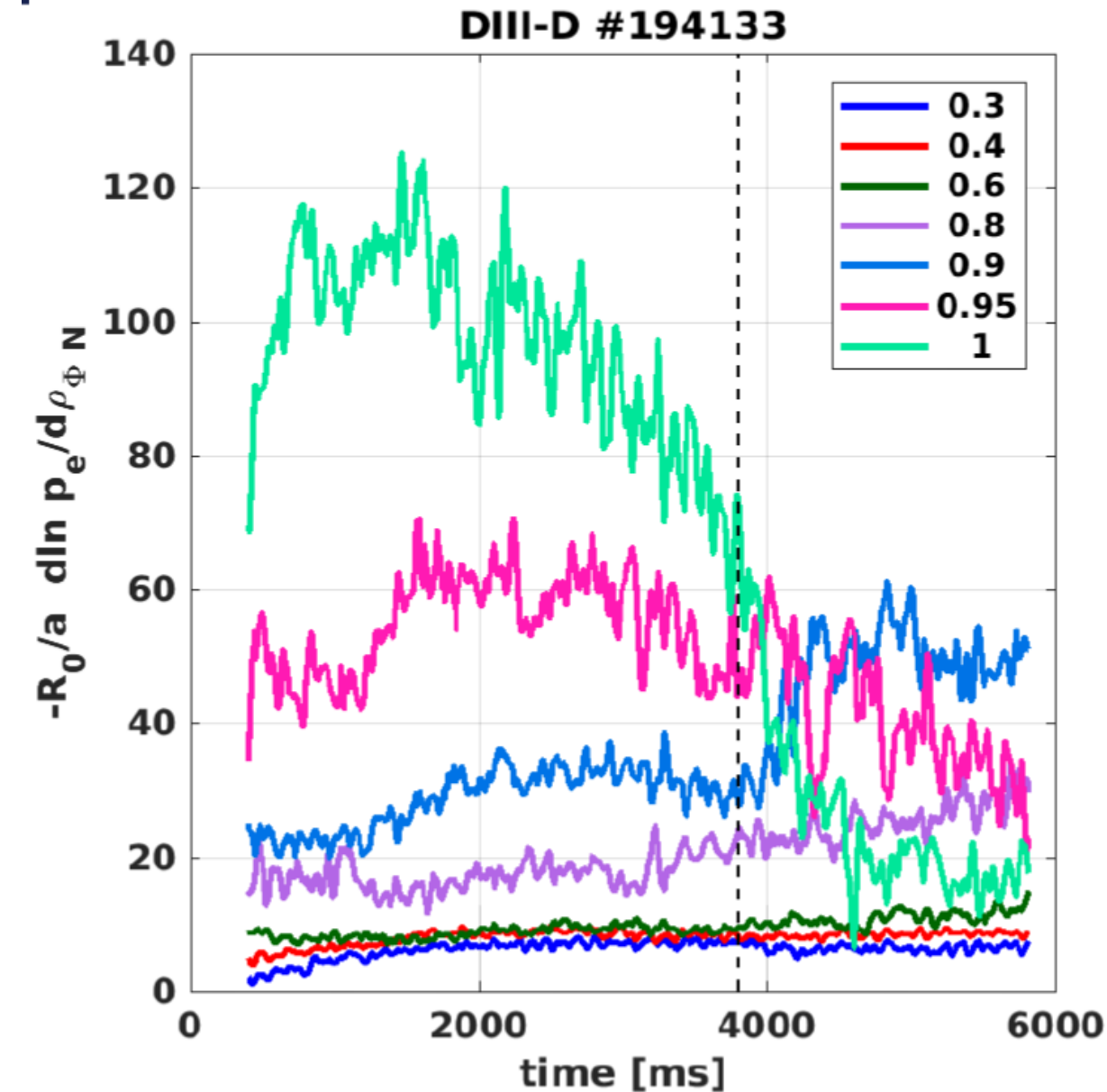
DIII-D #194133



Profiles evolution

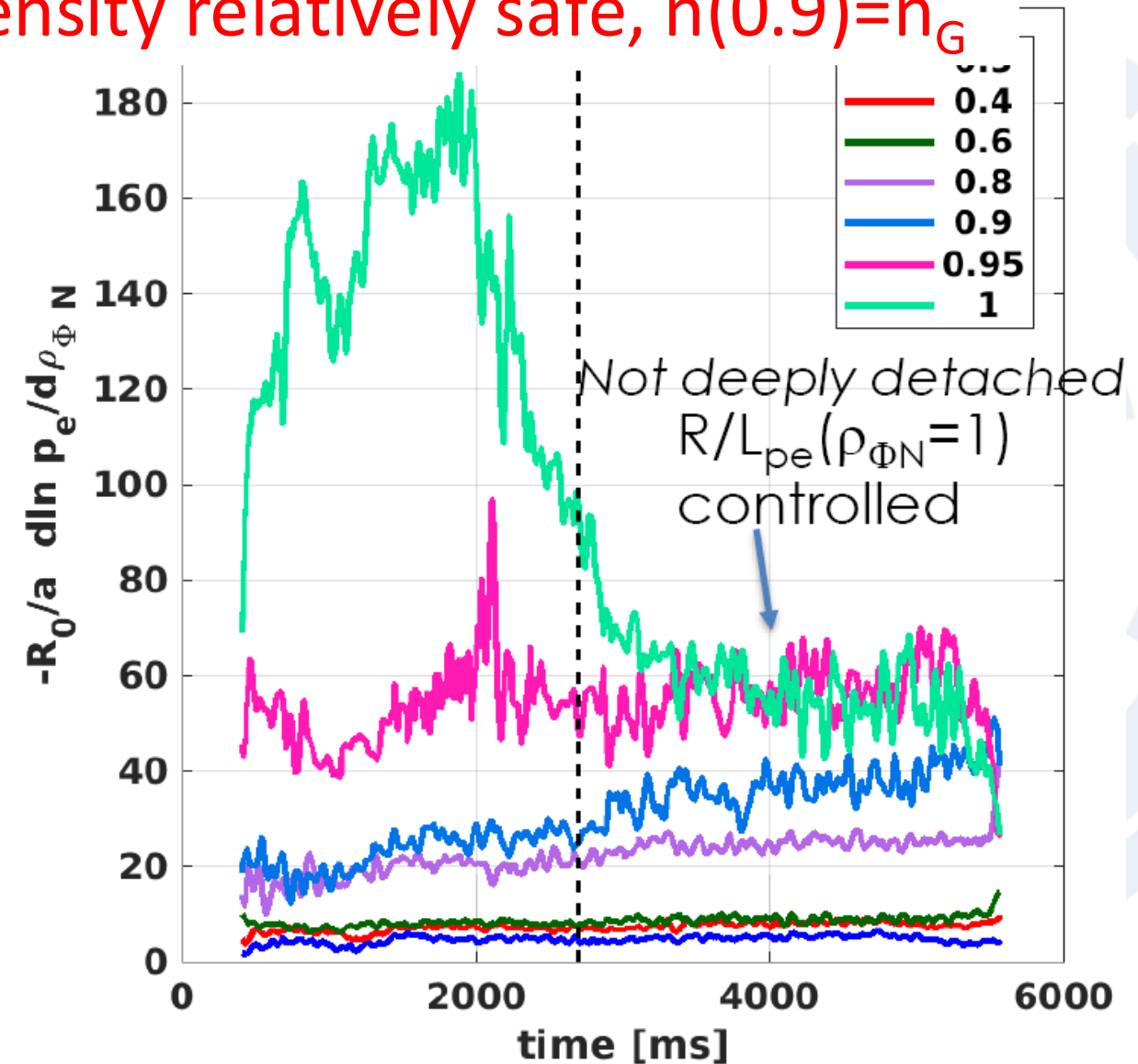
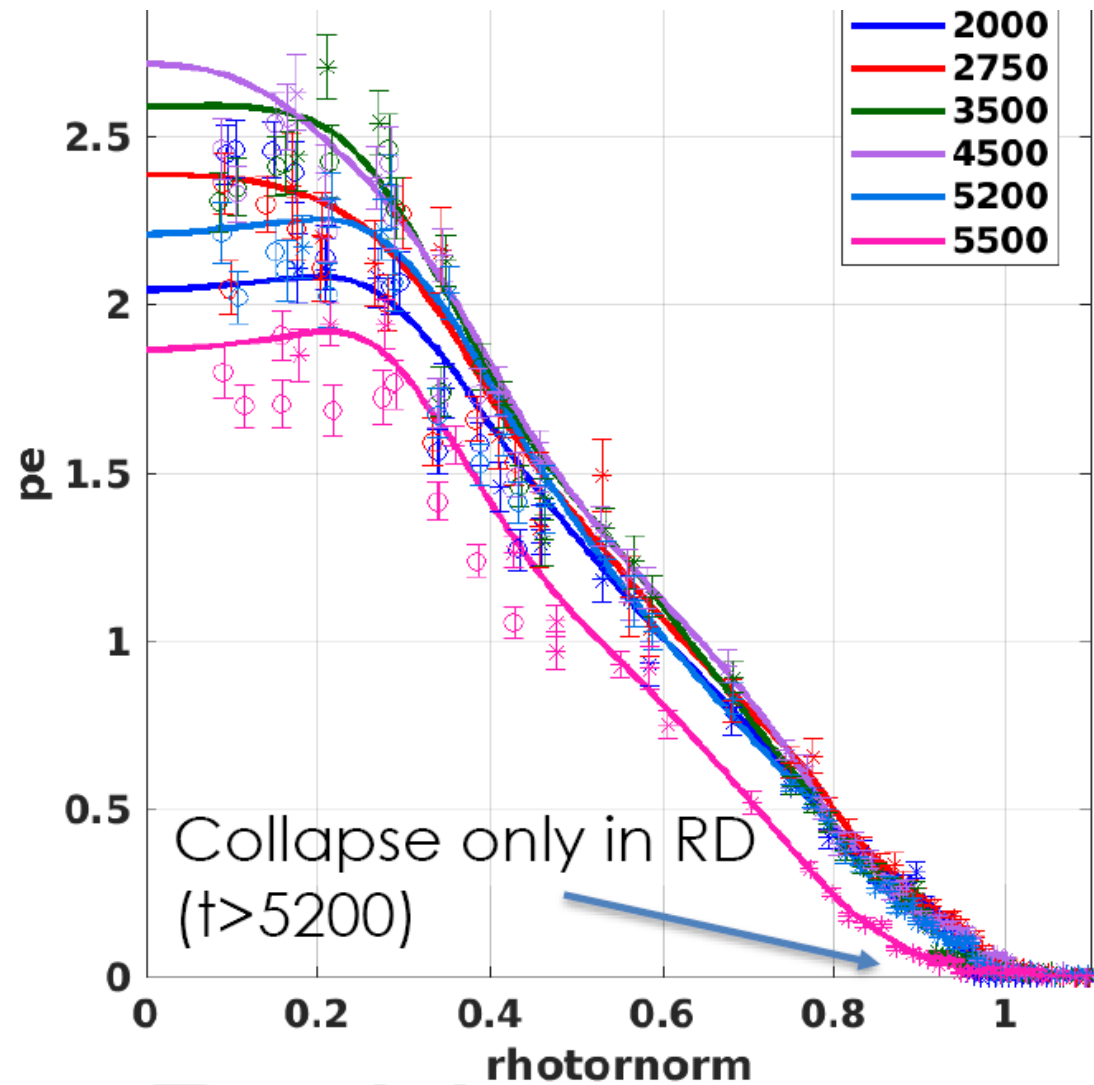


With beta feedback, stationary nGf=1.8, bN=1.8 (194323)



With beta feedback, stationary $n_{Gf}=1.8$, $\beta_N=1.8$ (194323)

NT-FPP: $n_{Gf} \sim 1.5$, with peaked density relatively safe, $n(0.9)=n_G$





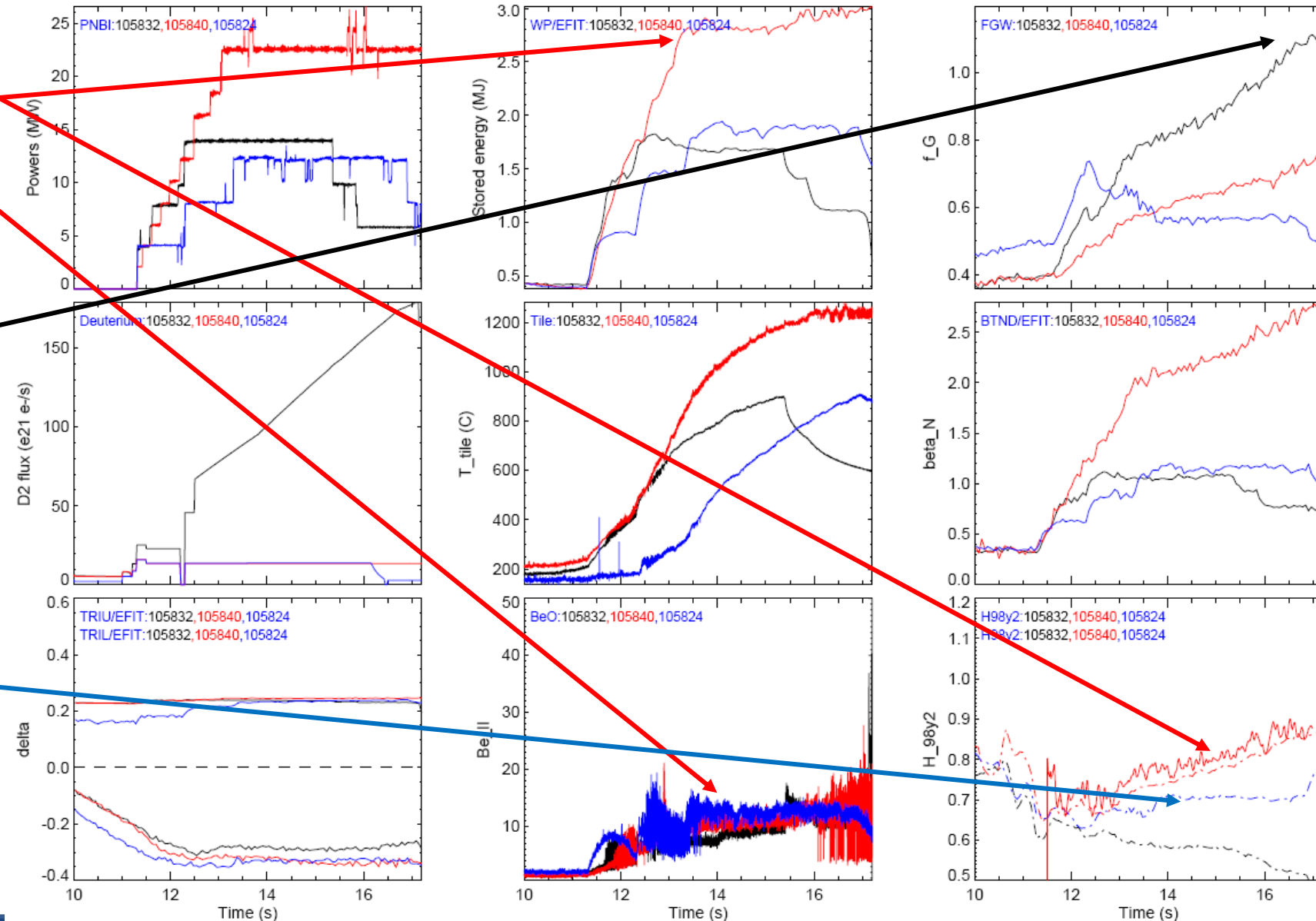
NT at JET

- Very successful given **less than 1 day experiments**
- Up to 32MW, no ELM confirmed, although shape predicted marginal before experiment (residual activity in some cases, still below QCE)
- Since no P>PLH constraint, much easier to operate. Allowed to test from ohmic to full power in a few discharges
- High power cases with significant fueling to be safe. No time for optimization, in particular for confinement
- High density confirmed, at least nG at lowish power
- High β_N (through B0 ramp-down) and low q95 confirmed
- H98 ~0.8 at medium/low gas, but "no gas" cases not really tested, and shape marginal for improved confinement
- GENE simulations confirm/explain improve confinement
- **NT L-mode can be compared with PT H-mode in JET** (*PT L-mode "dismissed" usually*)



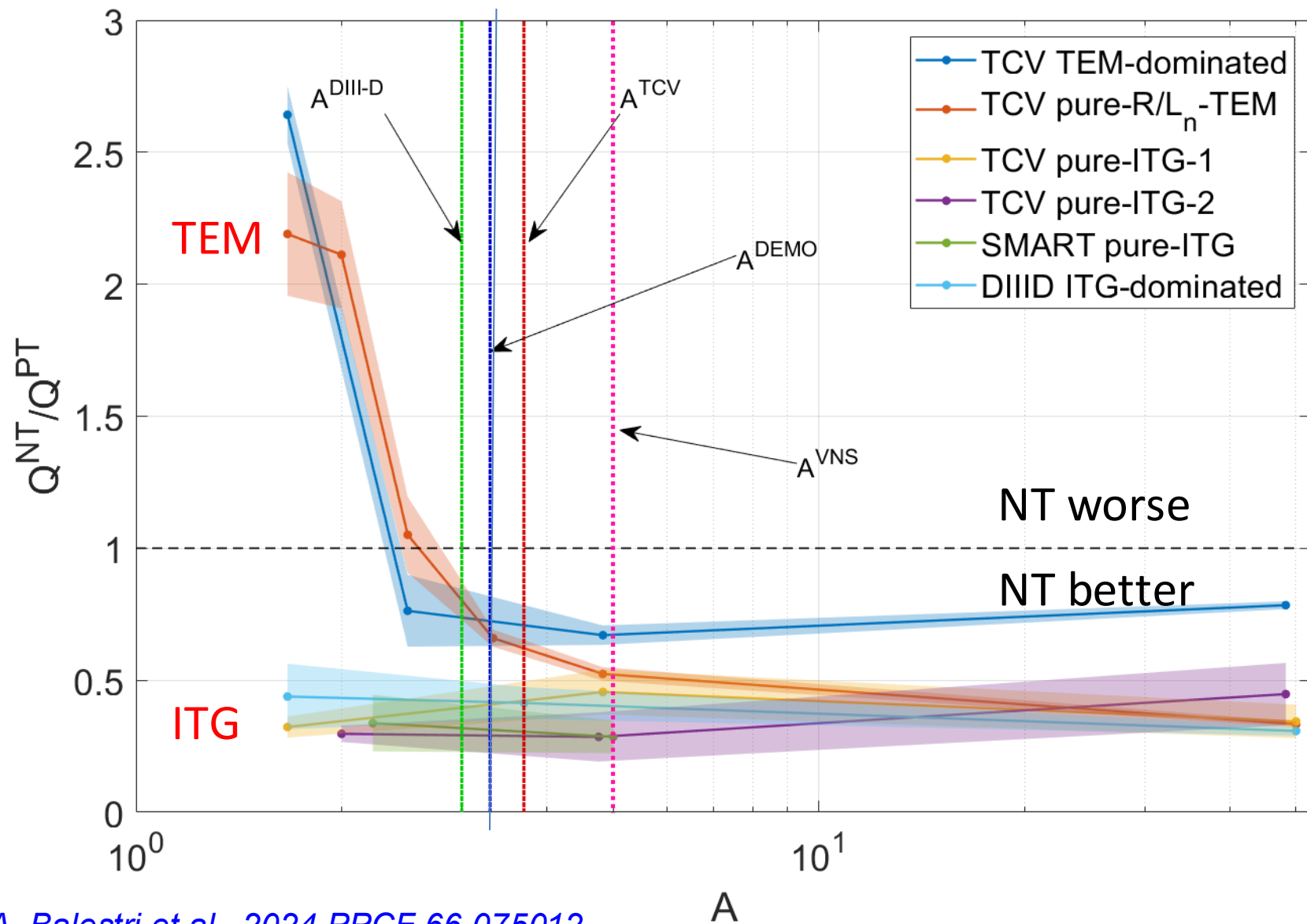
JET NT cases, H values validated (with TRANSP)

- H98 values up to 0.8 at $\beta_N \sim 2-2.5$ obtained in NT-L-mode JET plasmas, lower with stronger gas fueling
- $f_G > 1$ reached with 5MW (only, NBI tripped at high density)
- H lower at lower power, no significant power degradation observed





Some transport properties: Aspect ratio scan



Conventional and large A tokamak

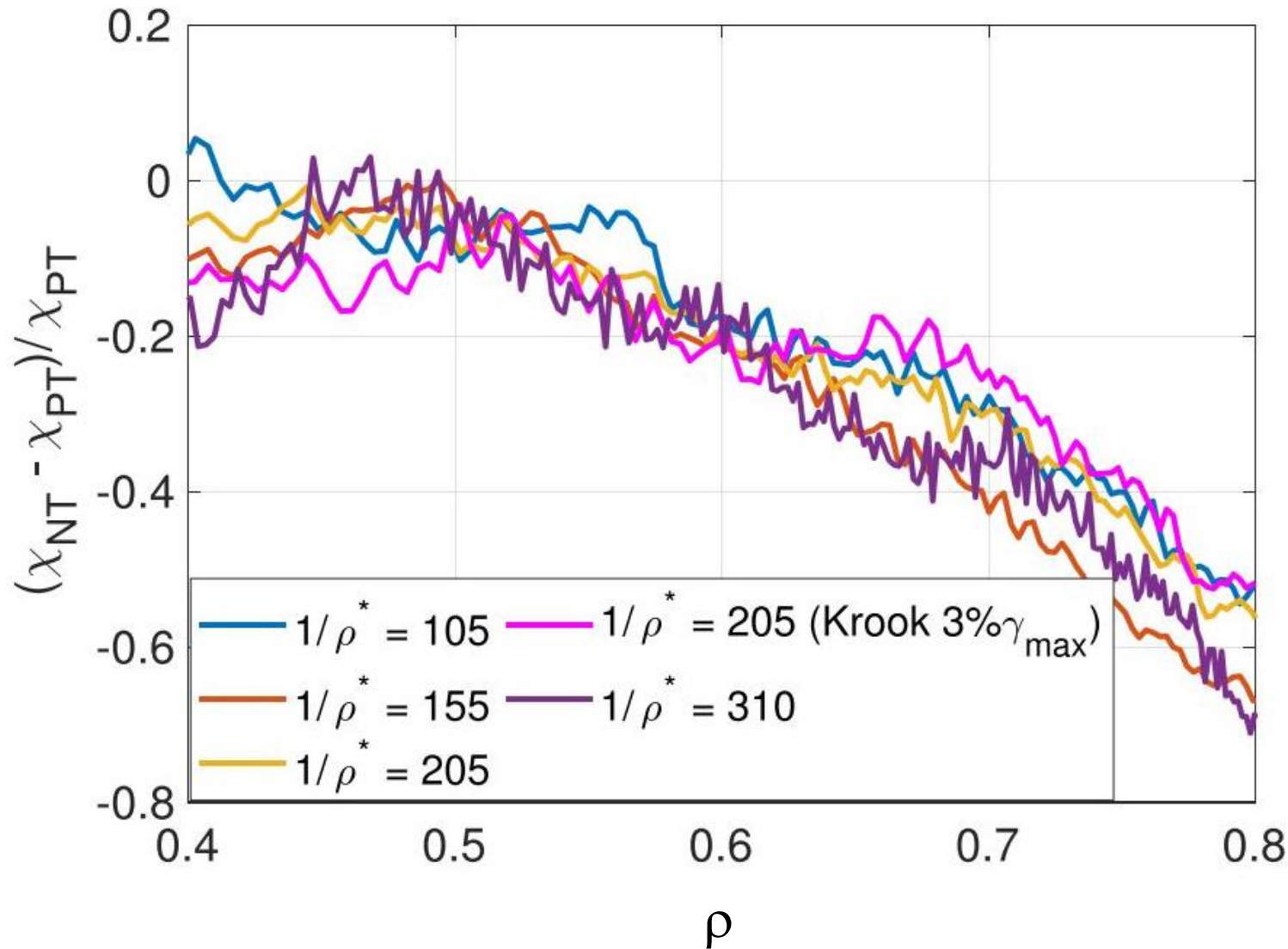
NT has better confinement than PT in ITG and TEM regimes.

Consistent with previous works [1-6] and experimental results on TCV and DIII-D

- [1] A. Marinoni et al., 2009 PPCF 51 055016
- [2] G. Merlo et al., 2015 PPCF 57 054010
- [3] G. Merlo et al., 2023 PoP 30 102302
- [4] A. Mariani et al., 2024 NF 64 046018
- [5] G. Di Giannatale et al., 2024 PPCF 66 095003
- [6] A. Balestri et al., 2024 PPCF 66 065031



Beneficial effect of NT scales to reactor-like machines



Global gradient-driven gyrokinetic simulations performed with the ORB5 code.

ρ^* has been artificially changed

Simulations show no ρ^* effect



Beneficial effect of NT scales to reactor-like machines.

[G. Di Giannatale et al., 2024 PPCF 66 095003](#)

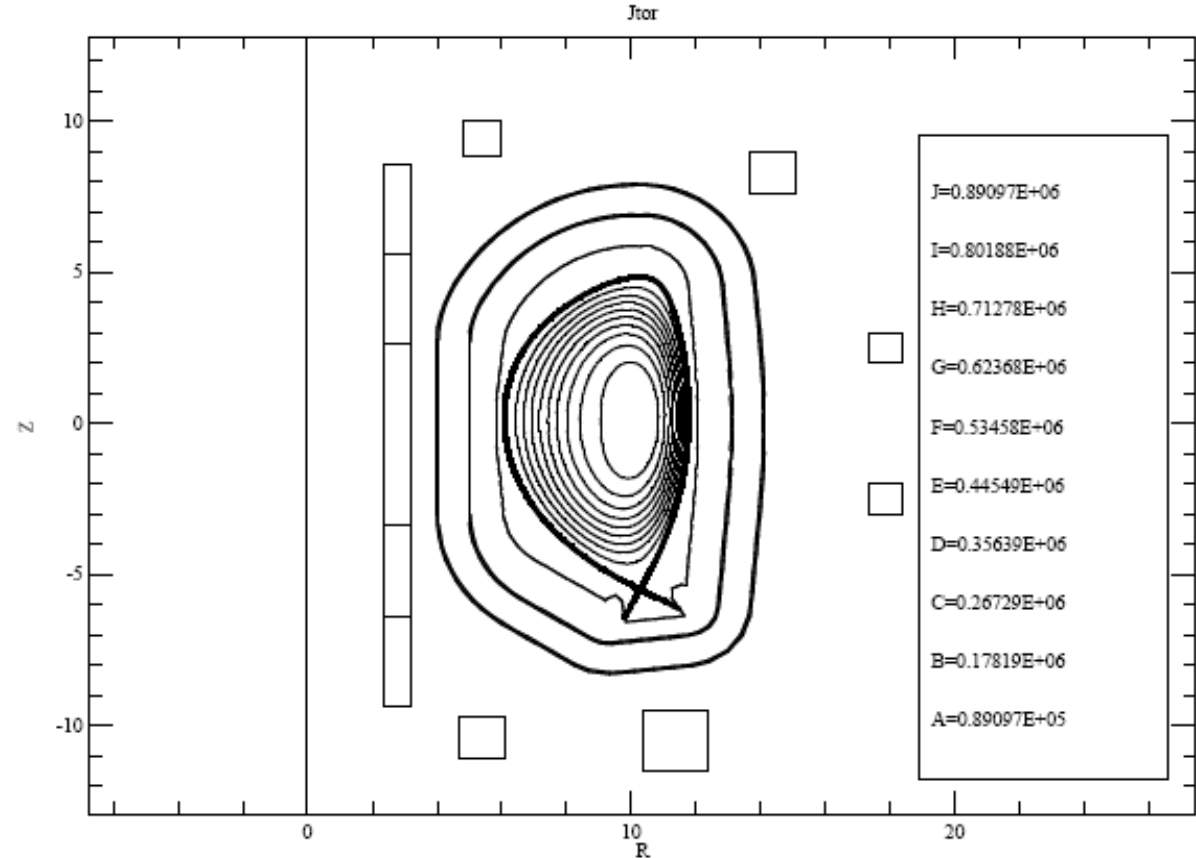
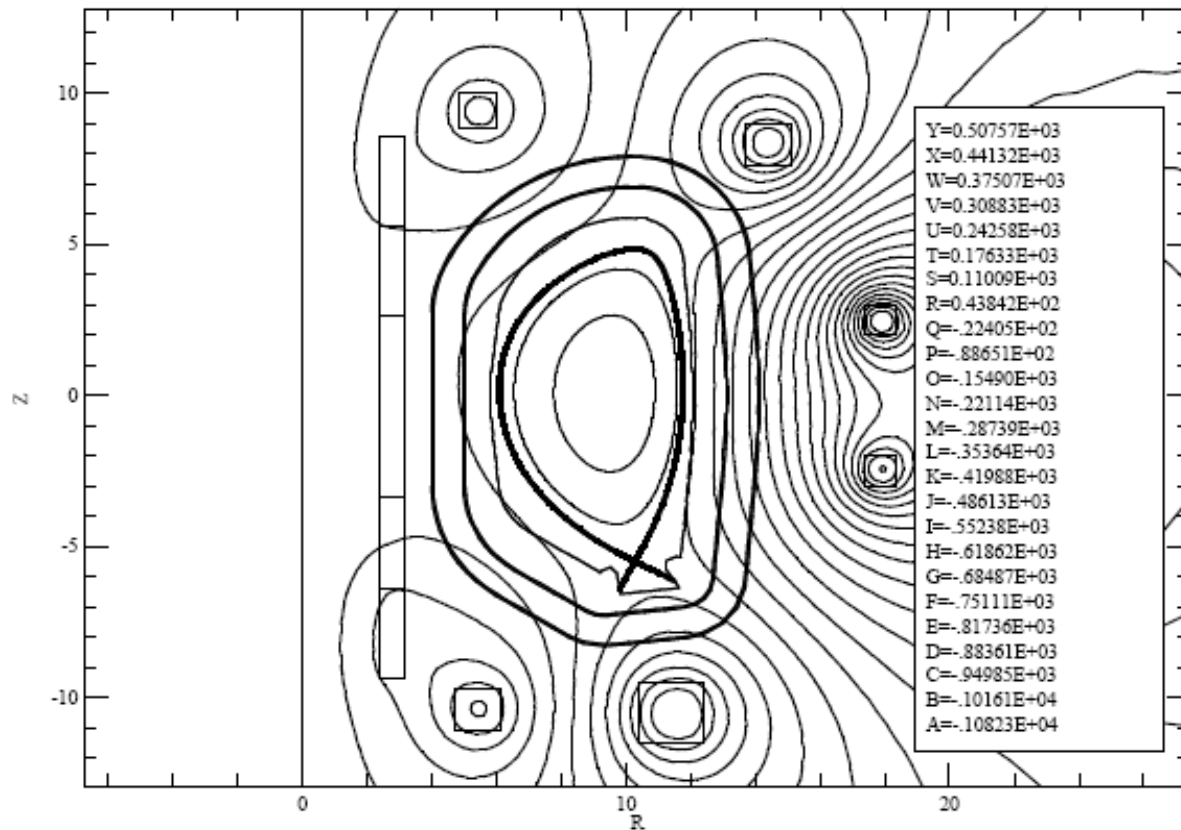


NT-DEMO scenario optimization

- Starting from F. Maviglia initial shape such that avoids access to 2nd stability region for ballooning modes, using MAXFEA and PT-DEMO coils design, checked with CREATE and with some basic forces and currents considerations already accounted for

DEMO Negative Triangularity preliminary, f.maviglia 15.05.2019

STATIC ,dpsi= 0.662E+02,psmm=-0.115E+04,psmx= 0.508E+03[Vs],name=demoutal





RAPTOR modeling assumptions for PT/NT DEMO

- Stationary state solver for poloidal flux ψ , electron temperature T_e and density n_e (\rightarrow relaxed j)
 - Gradient-driven transport model with core $d \log T_e / d \rho$, $d \log n_e / d \rho$, edge $d T_e / d \rho$, $d n_e / d \rho$, free parameter ρ_{ped}
 - T_i is set equal to T_e
 - Prescribed impurity concentrations $n(\text{He})/n_e = 0.02$, $n(\text{W})/n_e = 3 \cdot 10^{-5}$, $n(\text{Xe})/n_e$ controlled to match target for P_{sep}/R_0
 - Impurity radiation calculated with ADAS cooling factors $p_{rad,imp} = n_{imp} n_e L_{imp}(T_e)$
 - Fusion power calculated assuming equal concentrations D and T
 - ECRH gaussian deposition profile in the center
- Iterate with CHEASE
 \rightarrow consistent equilibrium+transport,
for NT DEMO operating points, 'pedestal' ballooning stability verified
 - Iterate with GENE
 \rightarrow consistent heat/particle flux+scalelengths RLT and RLn at $\rho = 0.65, 0.75, 0.85$



RAPTOR PT reference matching EU-DEMO 2018

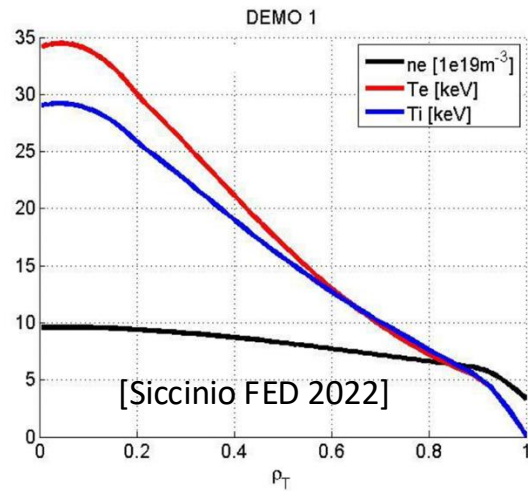
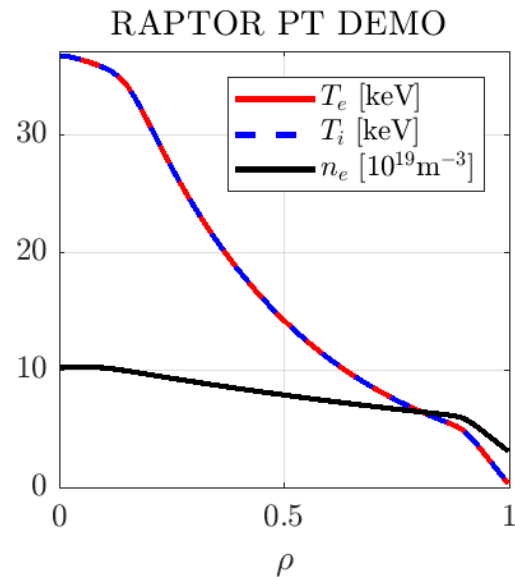


Fig. 3. Density and temperature profiles calculated with ASTRA for DEMO 2018. Figure is taken from [6].



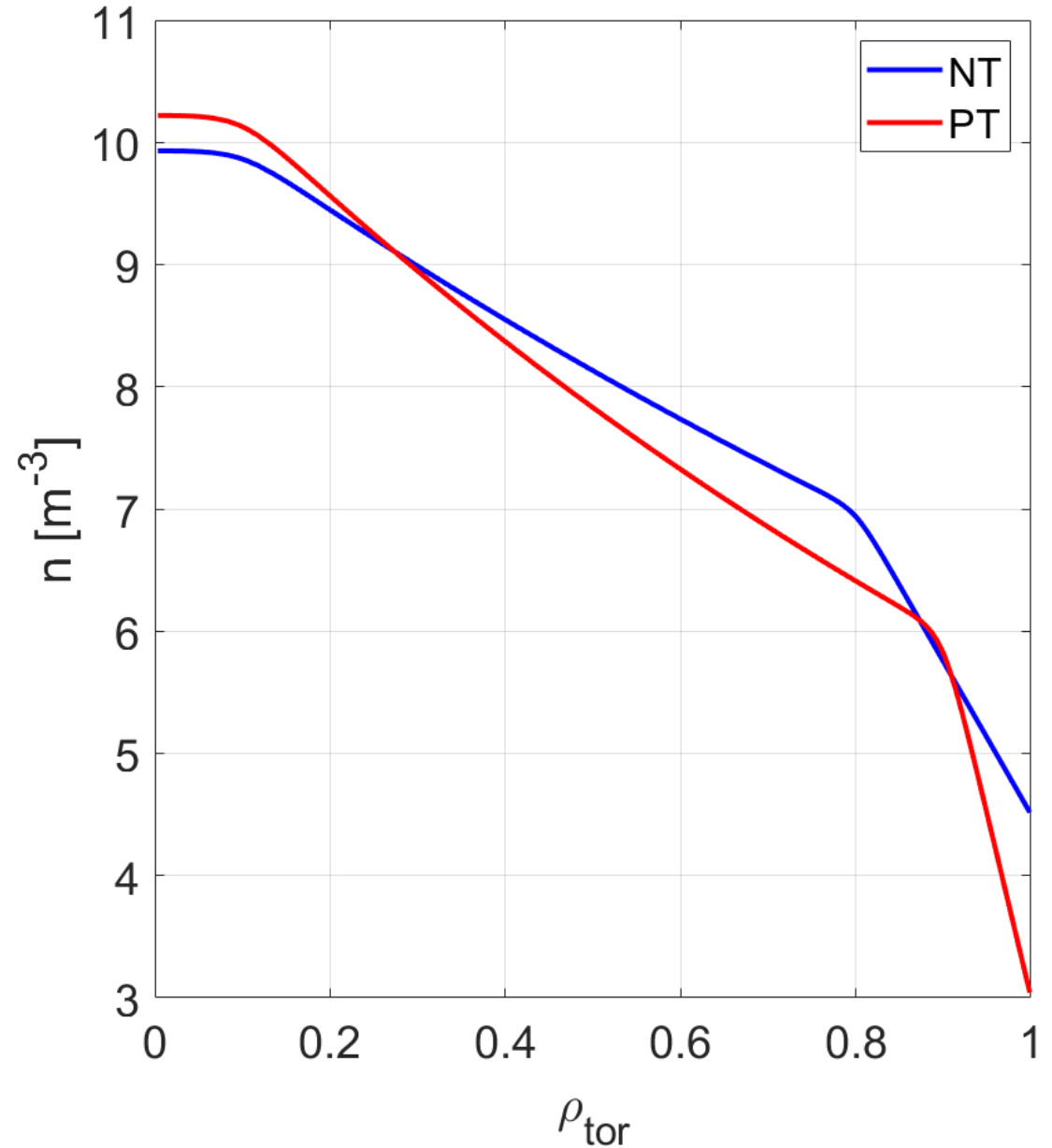
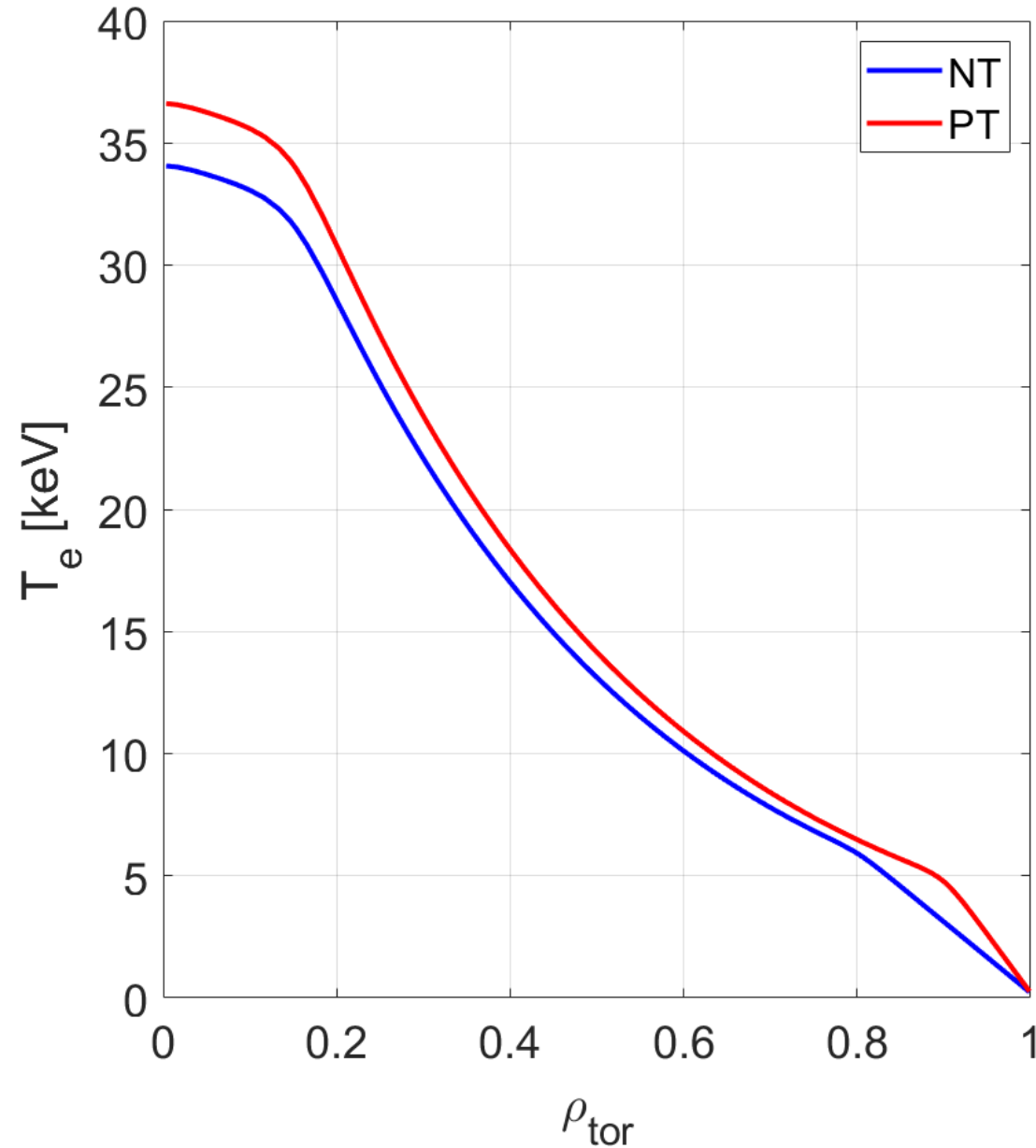
[Siccinio FED 2022]

	EU- DEMO 2015	EU- DEMO 2017	EU- DEMO 2018	EU- DEMO (QH- mode)	EU- DEMO (I- mode)	ITER
R [m]	9.07	8.94	9.07	8.94	9.47	6.2
A	3.1	3.1	3.1	3.1	3.1	3.1
B ₀ [T]	5.66	4.89	5.86	5.74	6.45	5.3
q ₉₅	3.25	3	3.89	3.93	3.87	3
δ ₉₅	0.33	0.33	0.33	0.33	0.33	0.33
κ ₉₅	1.65	1.65	1.65	1.65	1.65	1.7
I _p [MA]	19.6	19.07	17.75	18.27	20.63	15
f _{NI}	0.44	0.5	0.39	0.52	0.219	~0.2
f _{CD}	0.10	0.11	> 0.05	0.16	>0.05	> 0.1
P _{fus} [MW]	2037	1998.3	2012	1871	1274	500
P _{sep} [MW]	154	156.4	170.4	178.5	240	89
P _{aux} [MW]	50	50	50	76	50	50
P _{CD} /P _{aux}	1	1	0	0	0	0
P _{LH} [MW]	121	107.5	120.8	N/A	N/A	52
				P _{LH} = 138 MW	P _{LI} = 265 MW	
H ₉₈	1.1	1.1	0.98	0.89	0.8	1
⟨n⟩/n _{GW}	1.2	1.2	1.2	1.37	0.9	~1
⟨T⟩ [keV]	13.06	12.8	12.49	11.31	10.37	8.9
n _{e,pt} [1e20m ⁻³]	0.67	0.62	0.57	0.63	0.46	~1
T _{e,pt} [keV]	5.5	5.5	3.7	4.6	2.7	~3
β _N [%mT/MA]	2.59	2.889	2.483	2.576	1.35	1.8
Z _{eff}	2.58	2.17	2.12	2.19	1.150	1.78
P _{sep} B/q ₉₅ AR [MW T /m]	9.54	9.2	9.2	9.4	13.6	8.2
P _{sep} /R [MW/m]	17	17.5	18.9	19.8	25.34	14.35
Burn length [sec]	7200	7200	7200	7931	7200	400

	PT
P _{fus} [MW]	1933
P _{ec} [MW]	50
P _{alpha} [MW]	387
Q	38.7
Prad [MW]	262
P _{sep} [MW]	175
PLH	139
P _{sep} /R ₀ [MW/m]	20
ne ₀ /ne _{vol}	1.46
ne _{vol} /n _{GW}	1.06
H ₉₈	0.99
beta _N (th)	2.02
li ₃	0.94
q ₉₅	3.73
V _{loop} [mV]	45

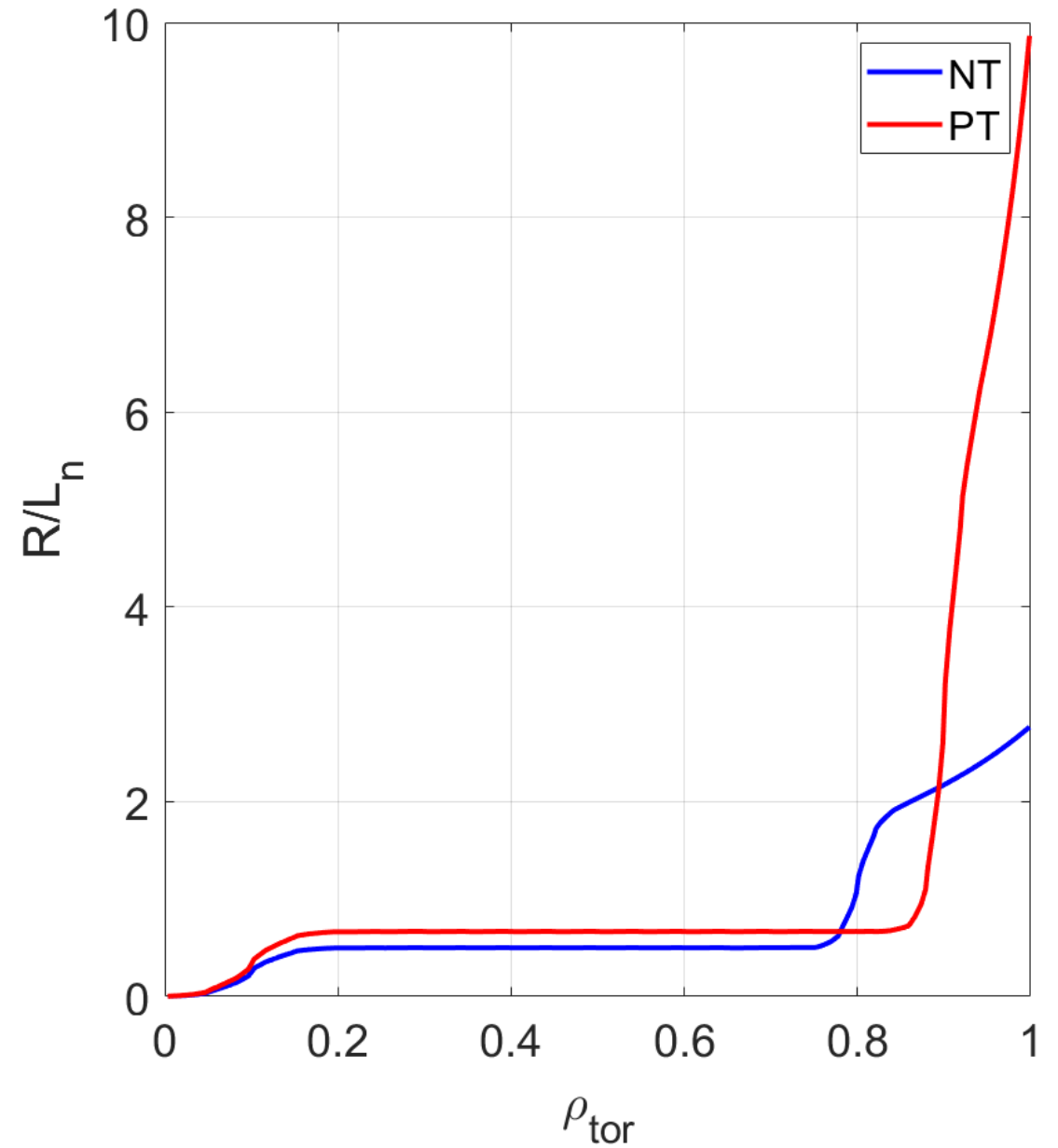
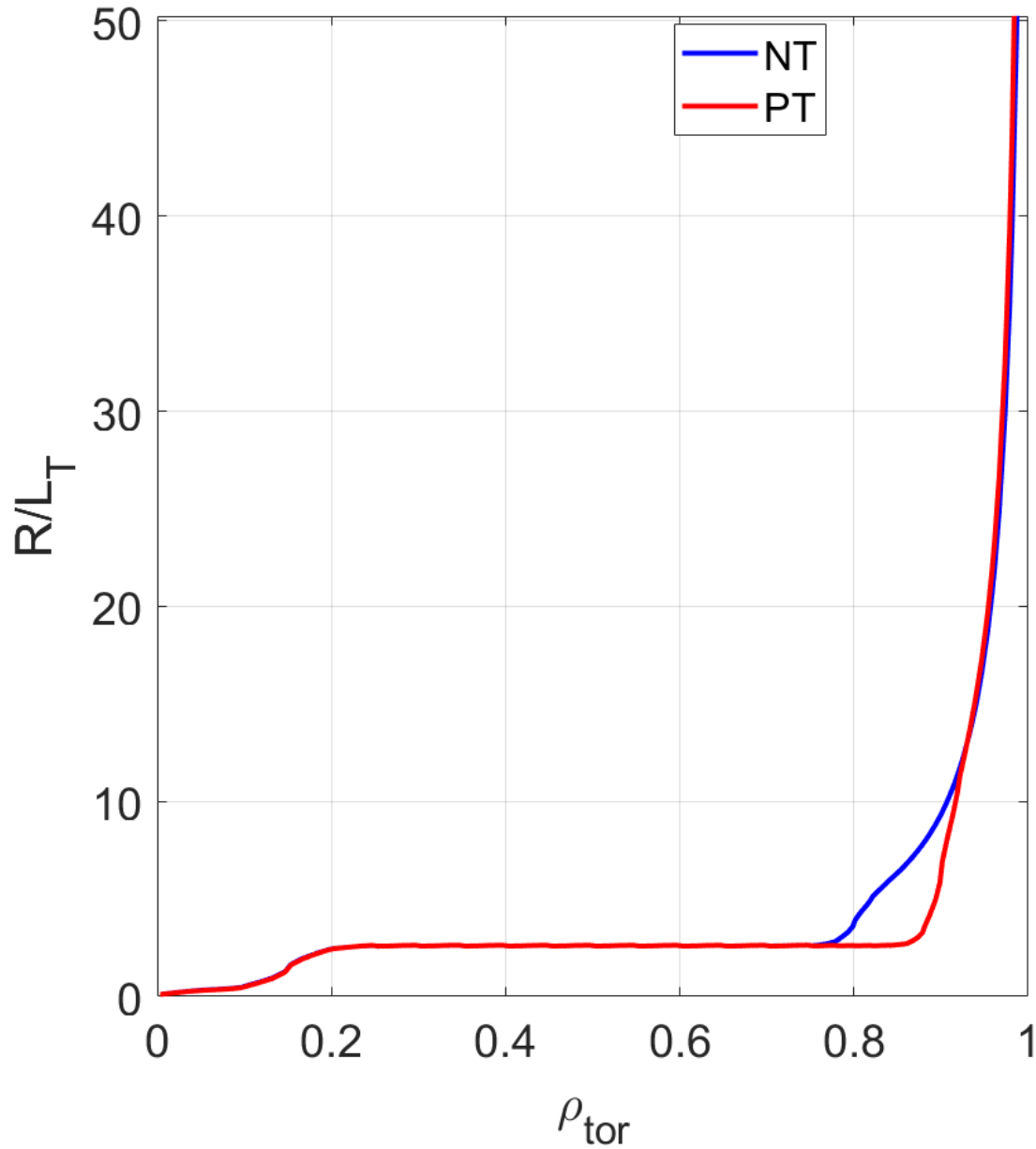


RAPTOR simulations: transport assumptions to match PT-DEMO's





RAPTOR simulations





RAPTOR simulations: PT/NT similar with similar assumptions

	PT	NT
Pfus [MW]	1937	1770
Pec [MW]	50	50
Palpha [MW]	387	354
Q	38.7	35.7
Prad [MW]	263	269
Psep [MW]	175	136
Ne85/nGW	0.95	0.93
H98	0.89	0.83
H98rad	0.98	0.92

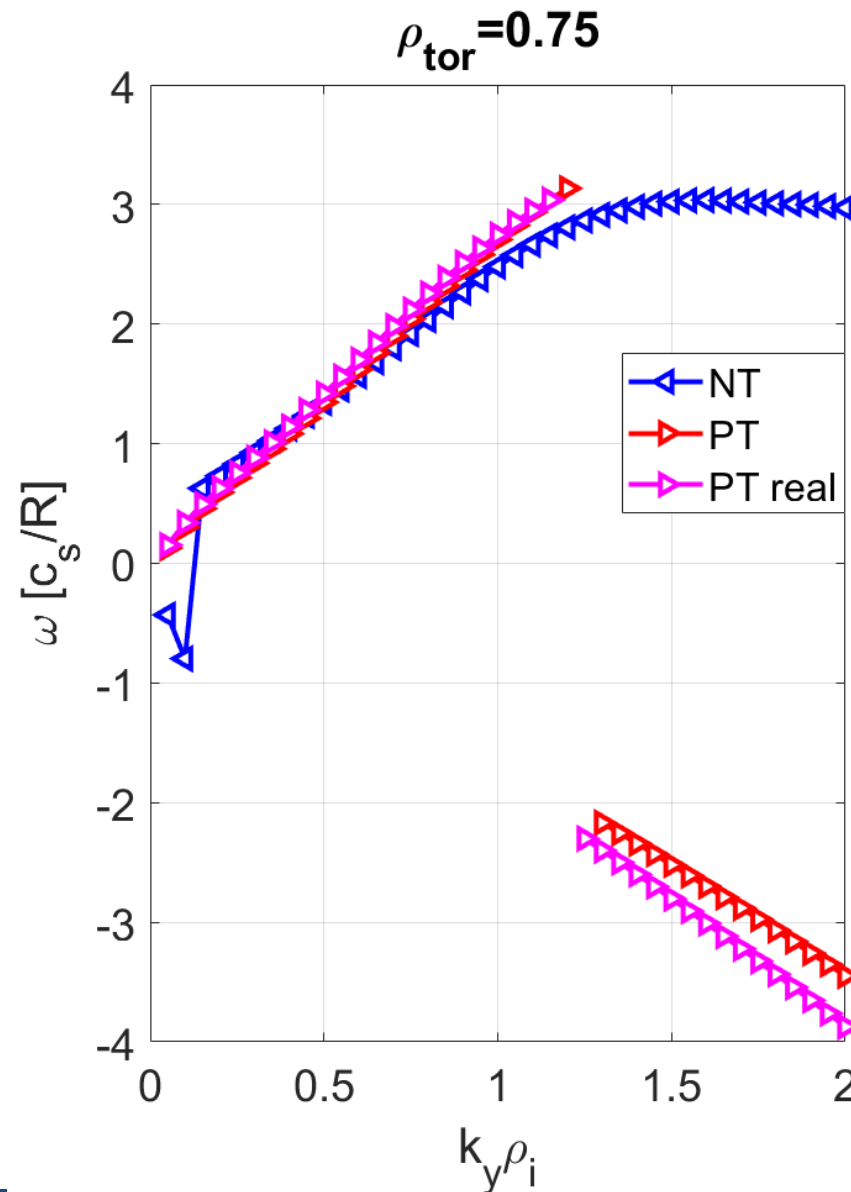
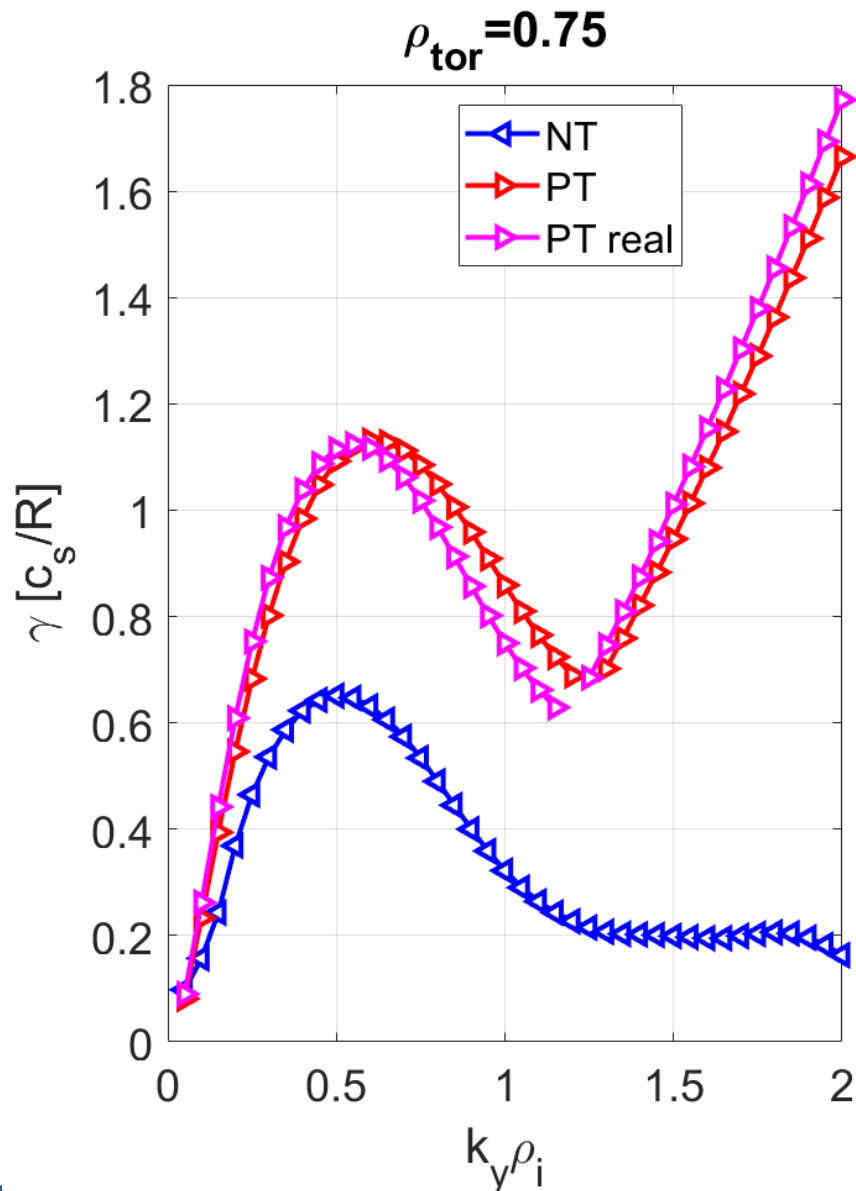


GENE simulations set-up

- Two radii of analysis $\rho_{tor} = 0.75$ and $\rho_{tor} = 0.85$
- Linear simulations to assess the nature of turbulence and have a first comparison between the linear stability of NT vs PT
- Nonlinear simulations to validate the profiles predicted by RAPTOR
- All simulations include kinetic electrons, impurities (He, Xe, W), collisions and electromagnetic effects



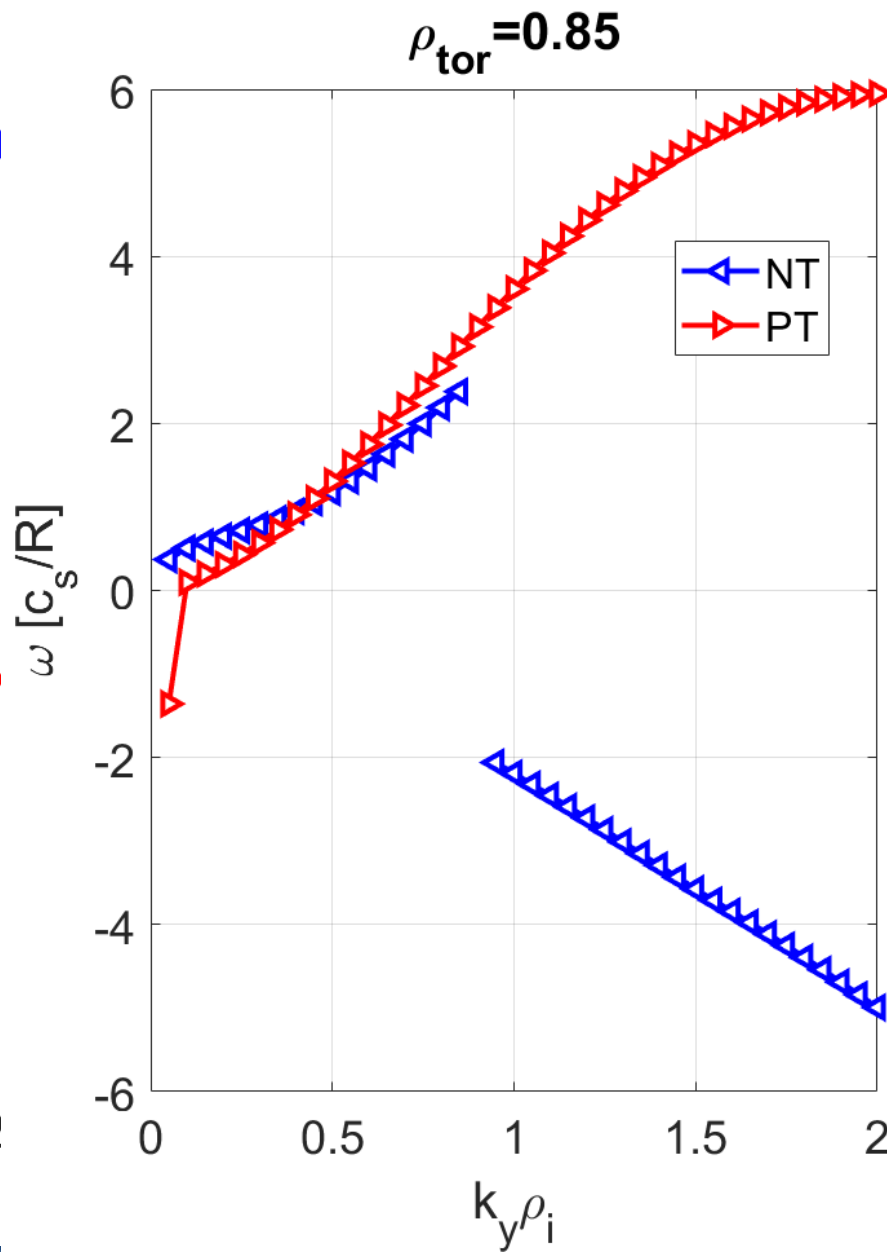
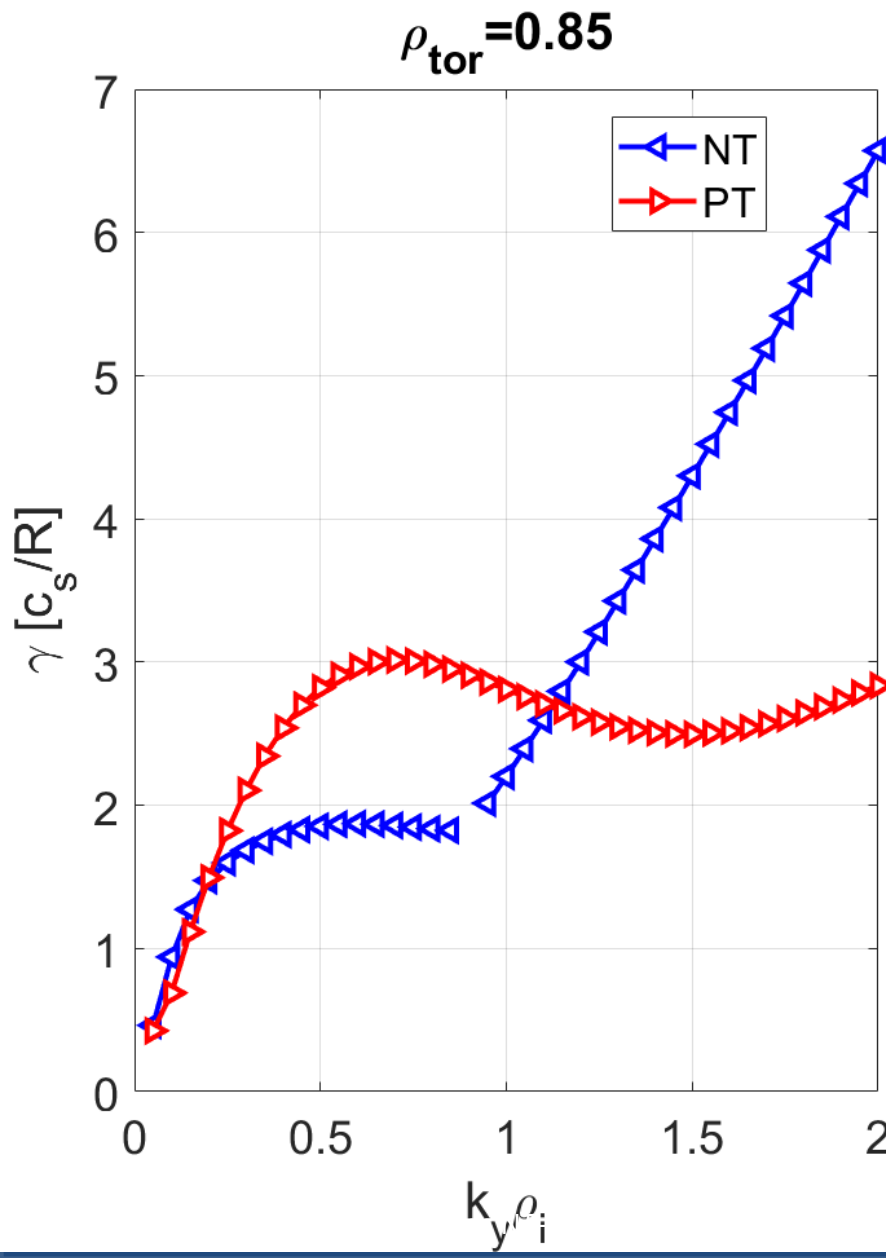
Linear simulations: k_y spectra (ion scale) - $\rho_{tor} = 0.75$



- Scenarios dominated by ITG turbulence
- NT more stable than PT



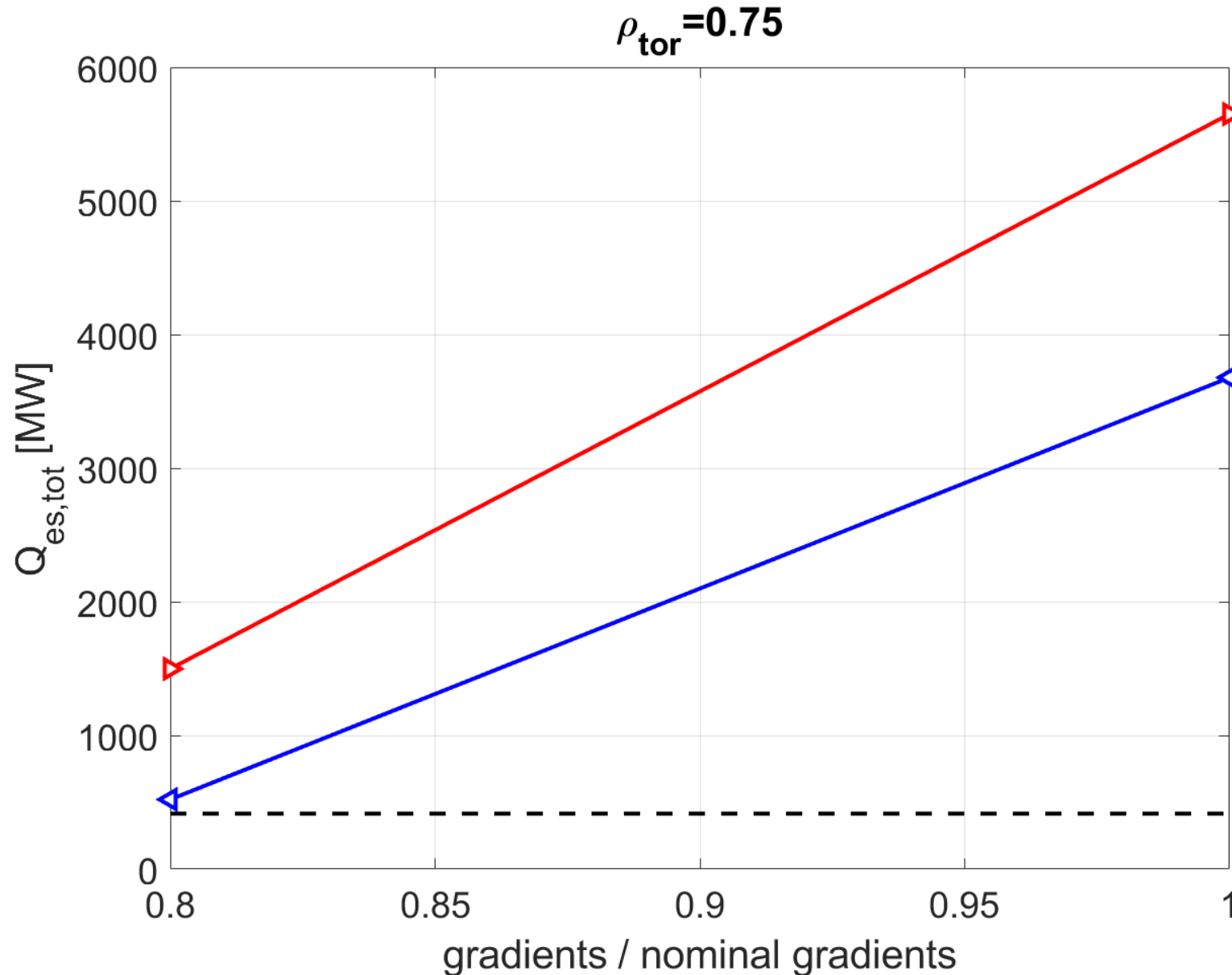
Linear k_y spectra (ion scale) - $\rho_{tor} = 0.85$



- PT dominated by ITG
- NT dominated by mix of ITG/TEM
- NT more stable than PT for the most important k_y



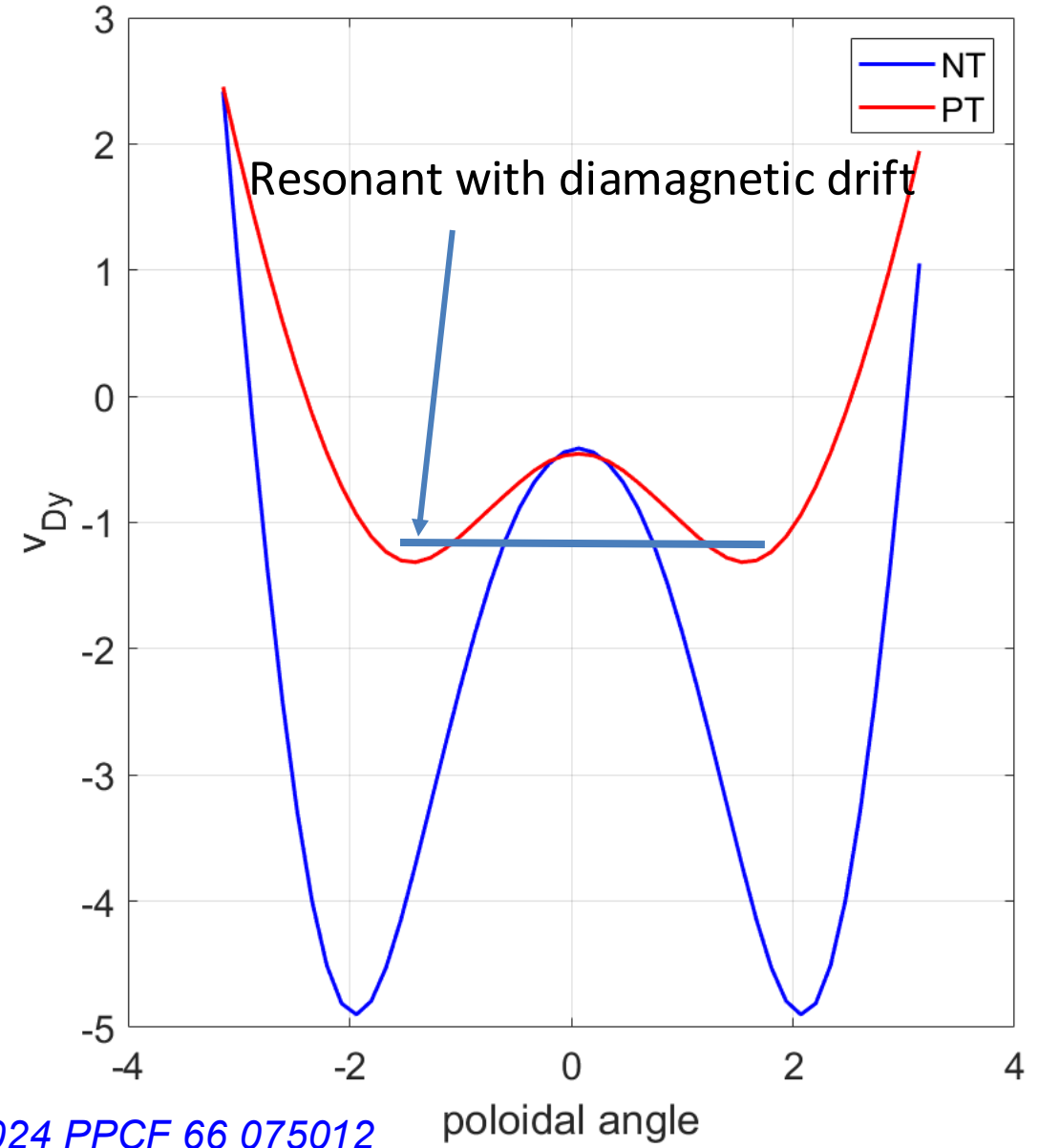
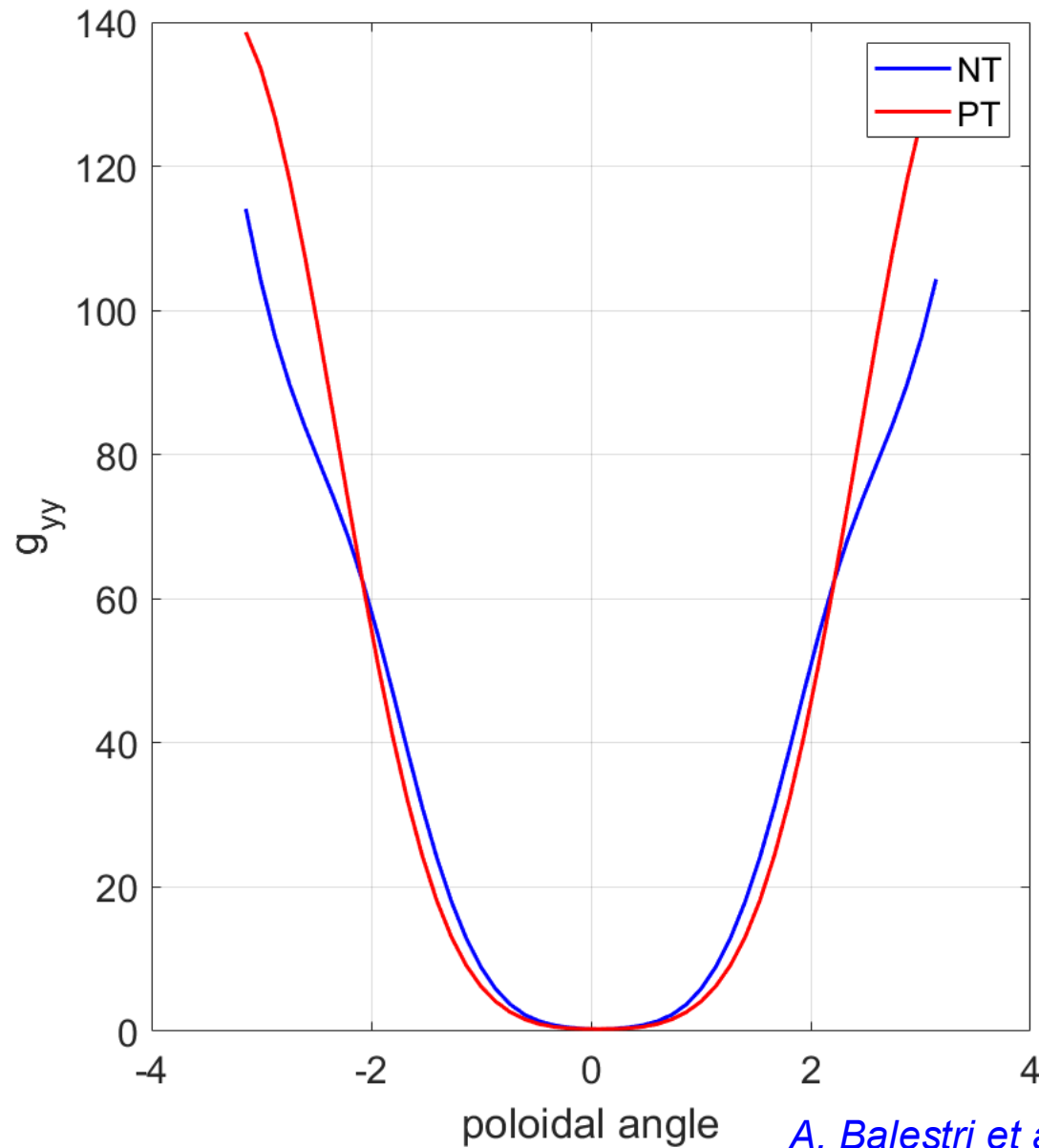
Sensitivity to gradients – with impurities (nonlinear simulations)



- NT is more stable than PT
- 20% reduction of gradients gives reasonable heat fluxes (*for both NT and PT initial profiles!*)



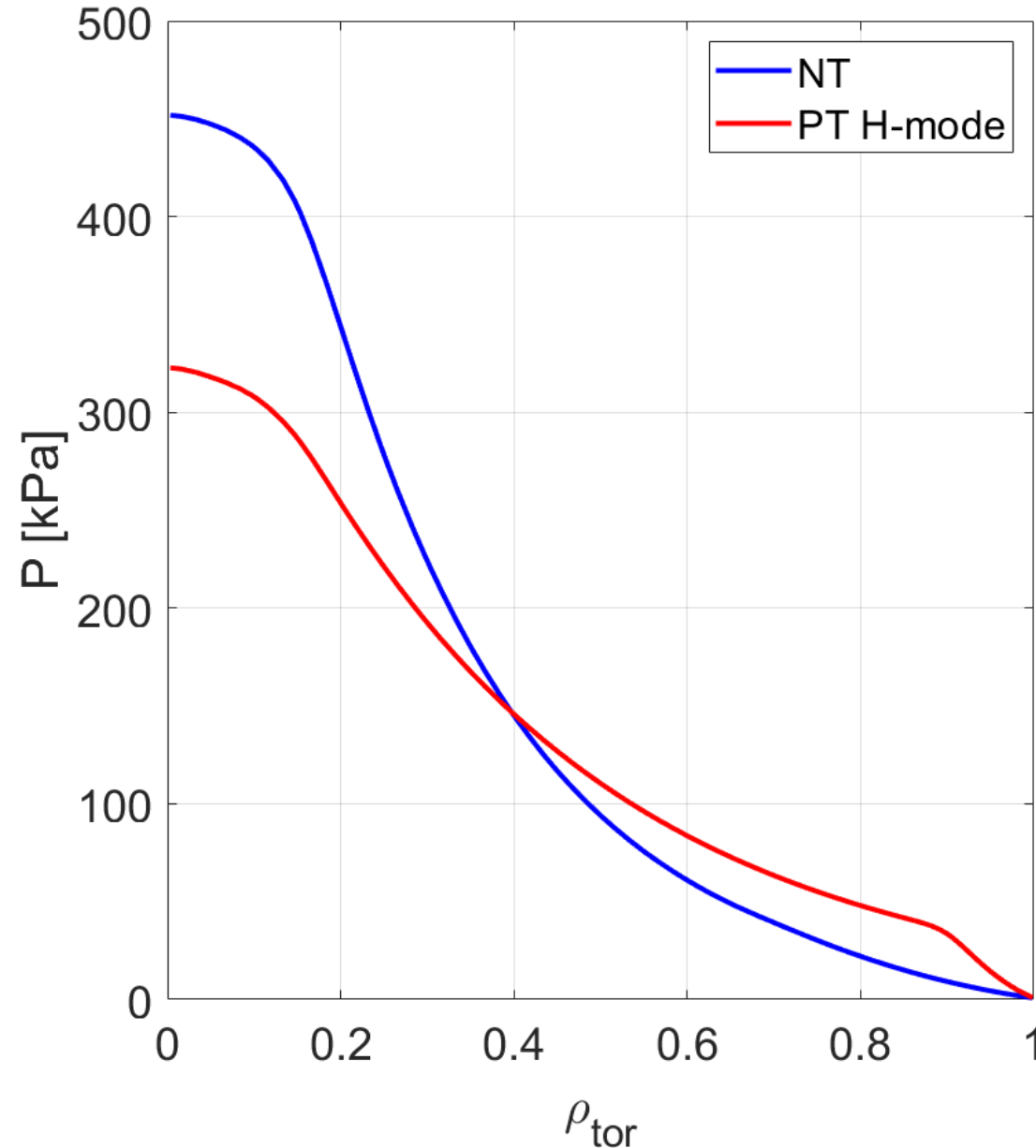
Geometric parameters



[A. Balestri et al. 2024 PPCF 66 075012](#)



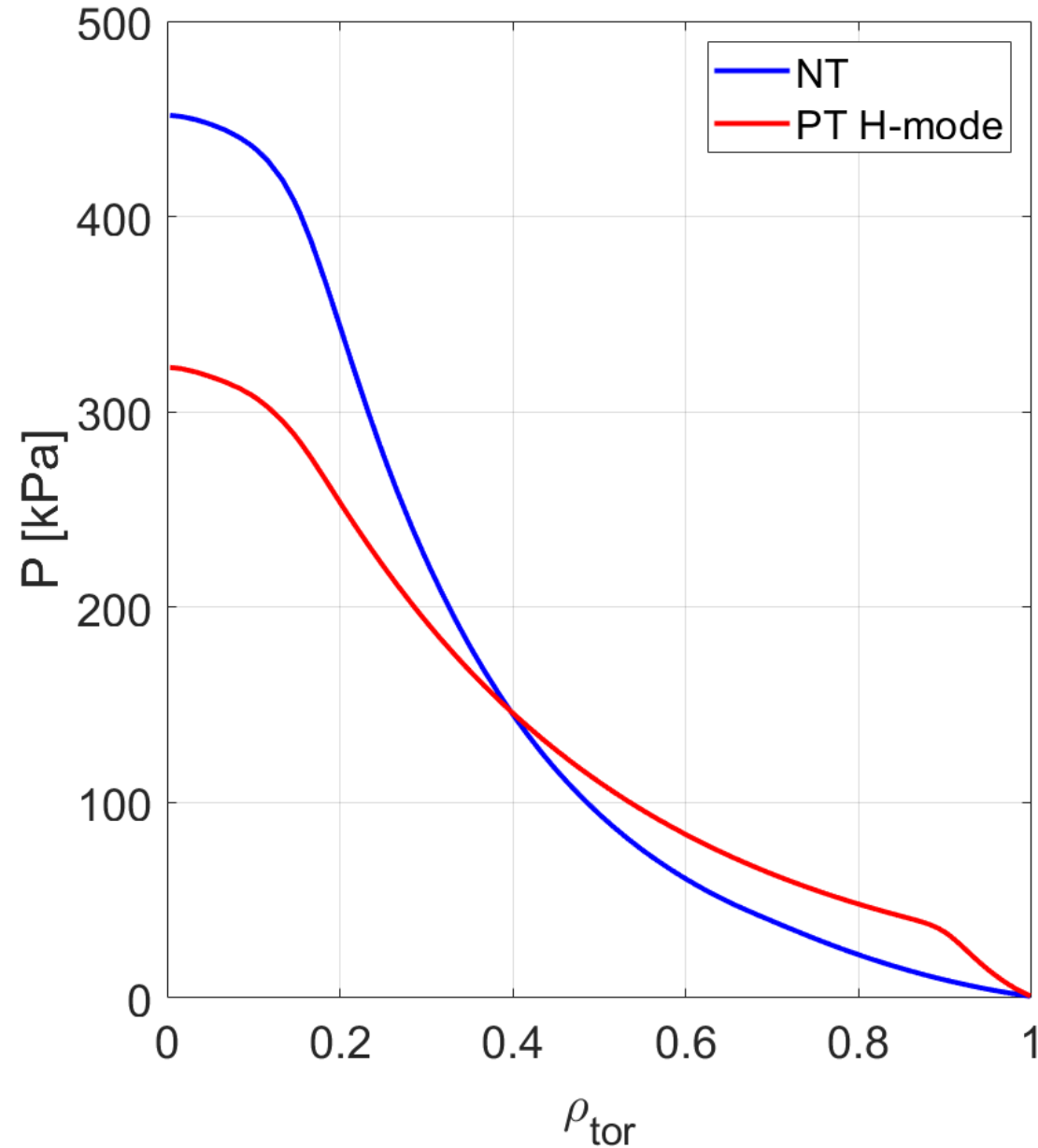
1st iteration: CHEASE+RAPTOR simulations



- Original PT H-mode case core gradients reduced by 15% (optimistic choice). From preliminary GK simulations, lower performance are expected for PT H-mode
- NT edge density and temperature greatly reduced and increased gradients in the core.
- Conservative choice for NT density at the edge



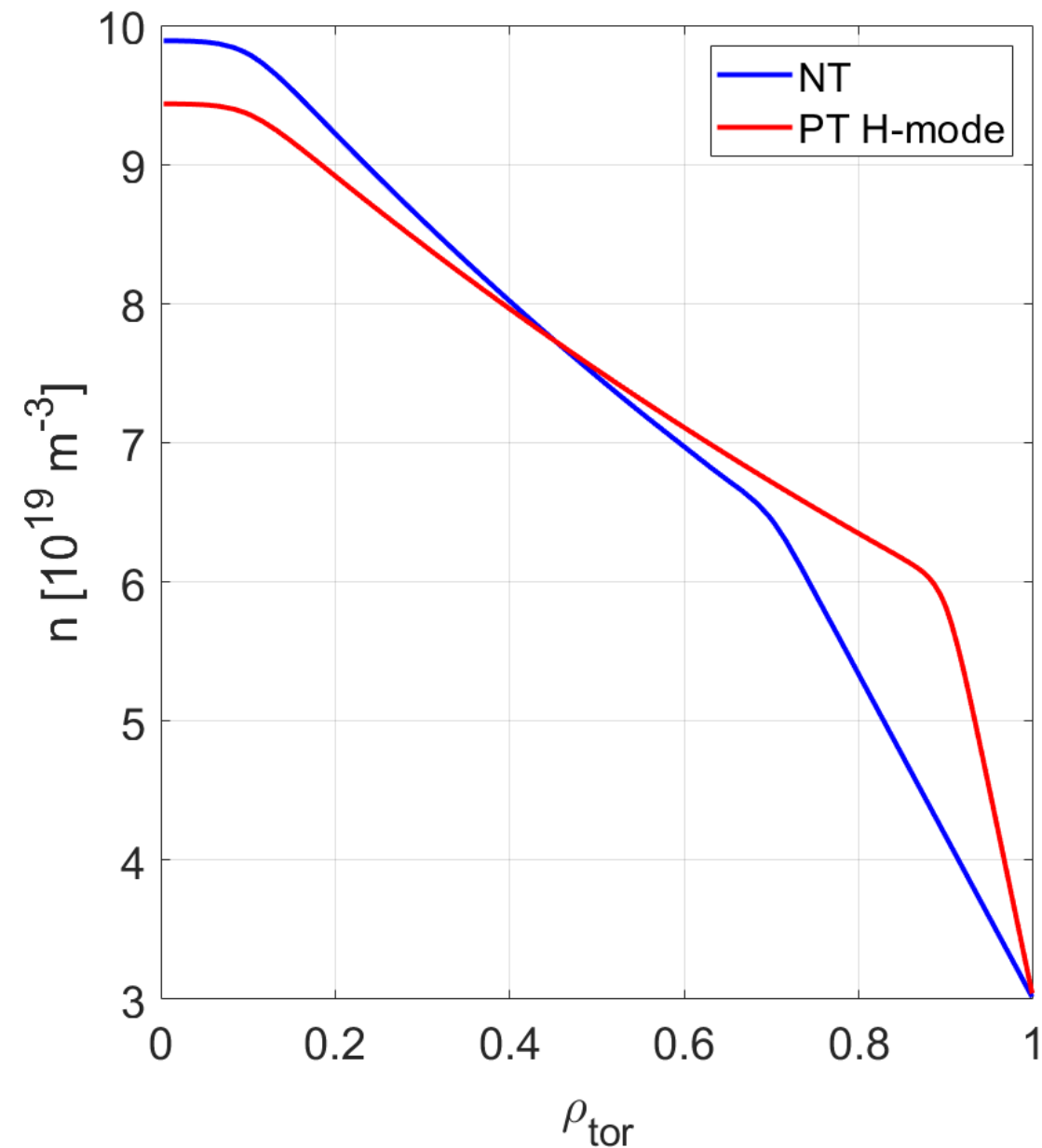
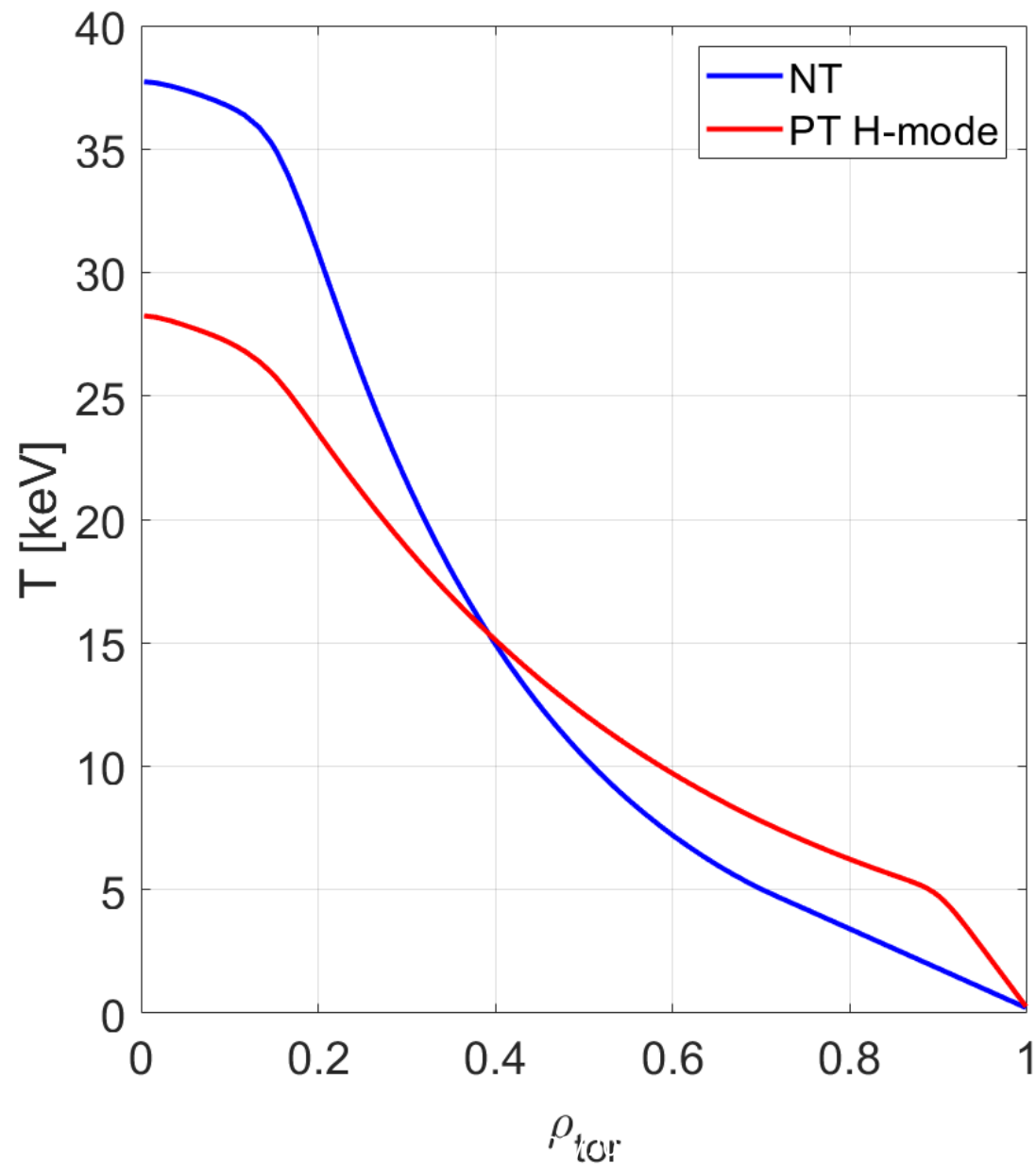
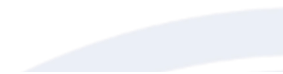
1st iteration: CHEASE+RAPTOR simulations



	PT	NT
Pfus [MW]	1345	1240
Pec [MW]	50	50
Palpha [MW]	269	206
Q	26.9	24.8
Prad [MW]	191	142
Psep [MW]	129	115
Ne85/nGW	0.94	0.7
H98	0.81	0.64
H98rad	0.88	0.7

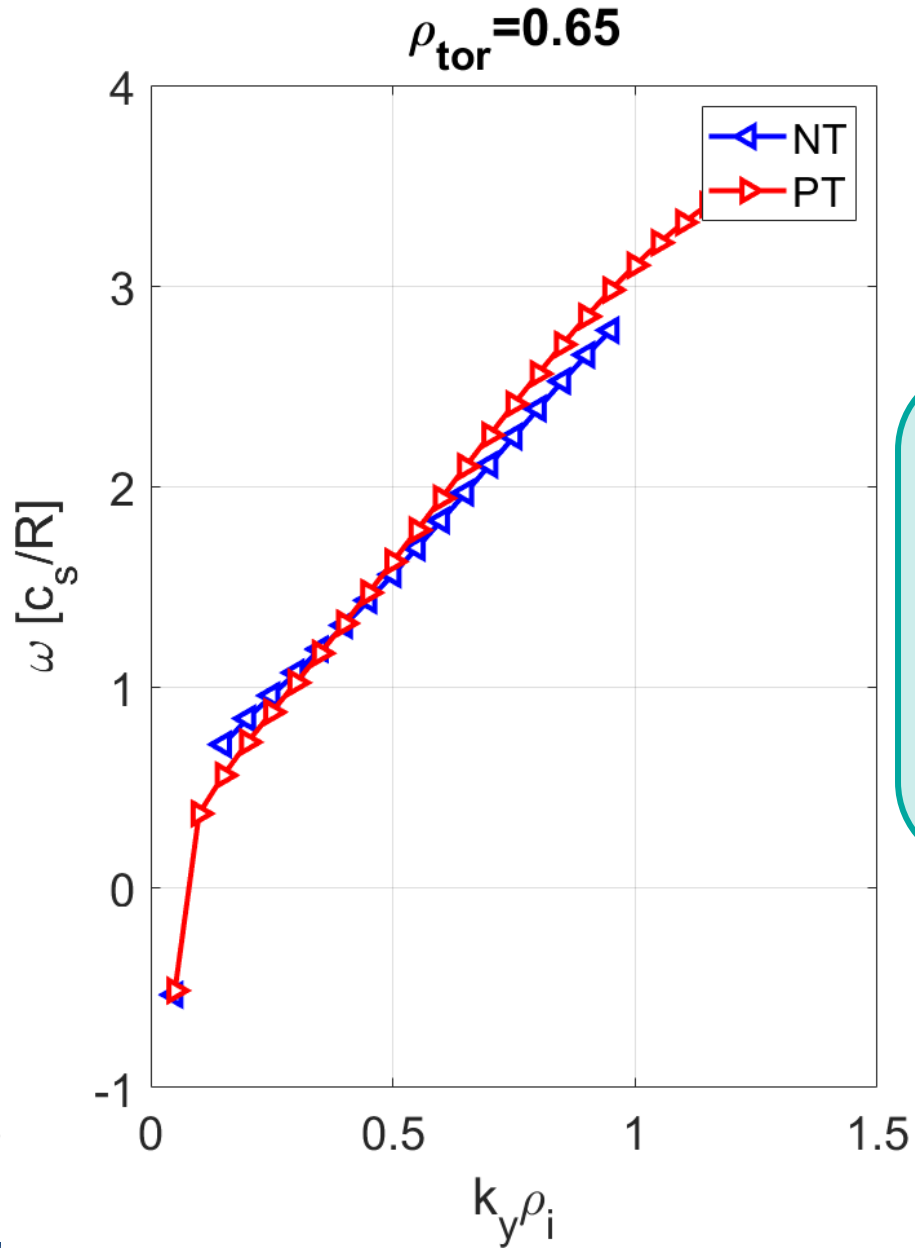
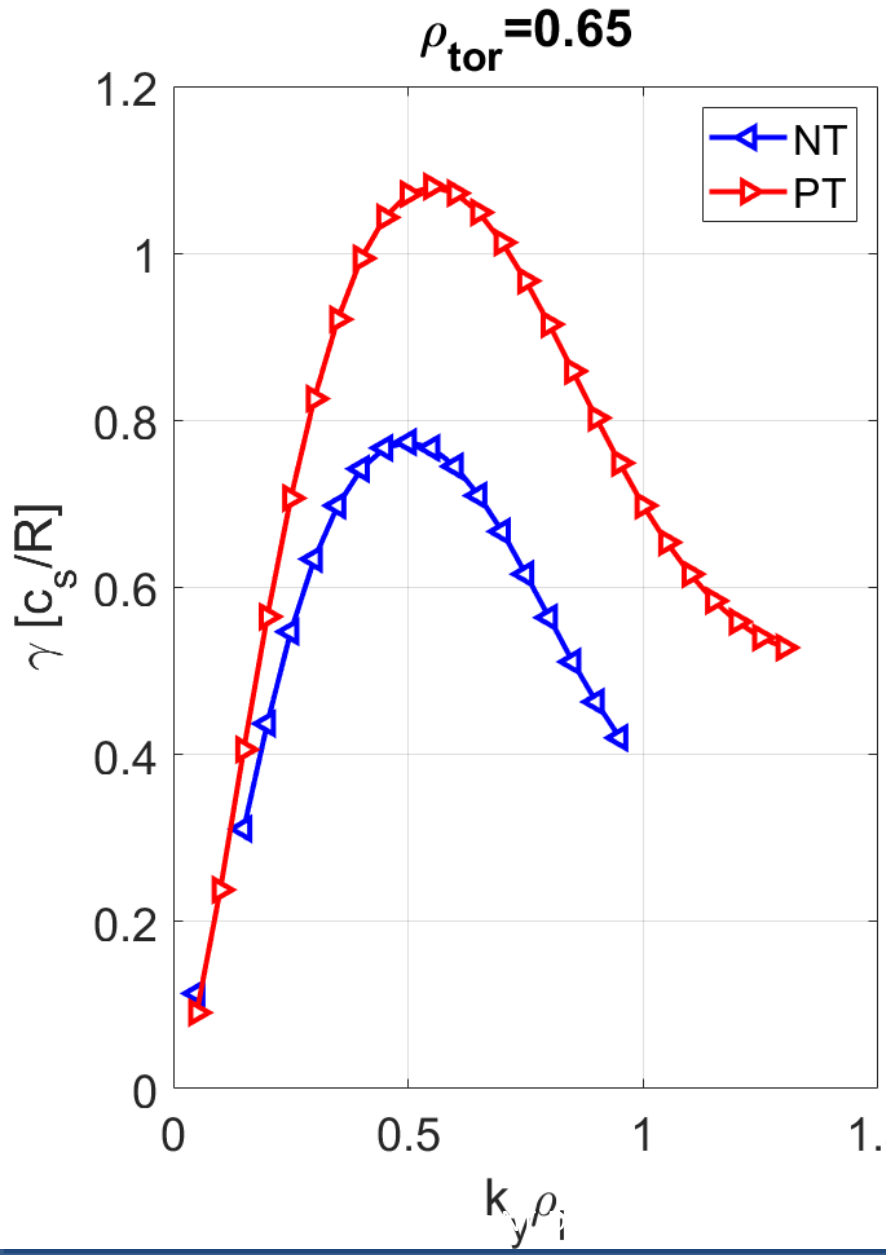


1st iteration: RAPTOR n, T profiles





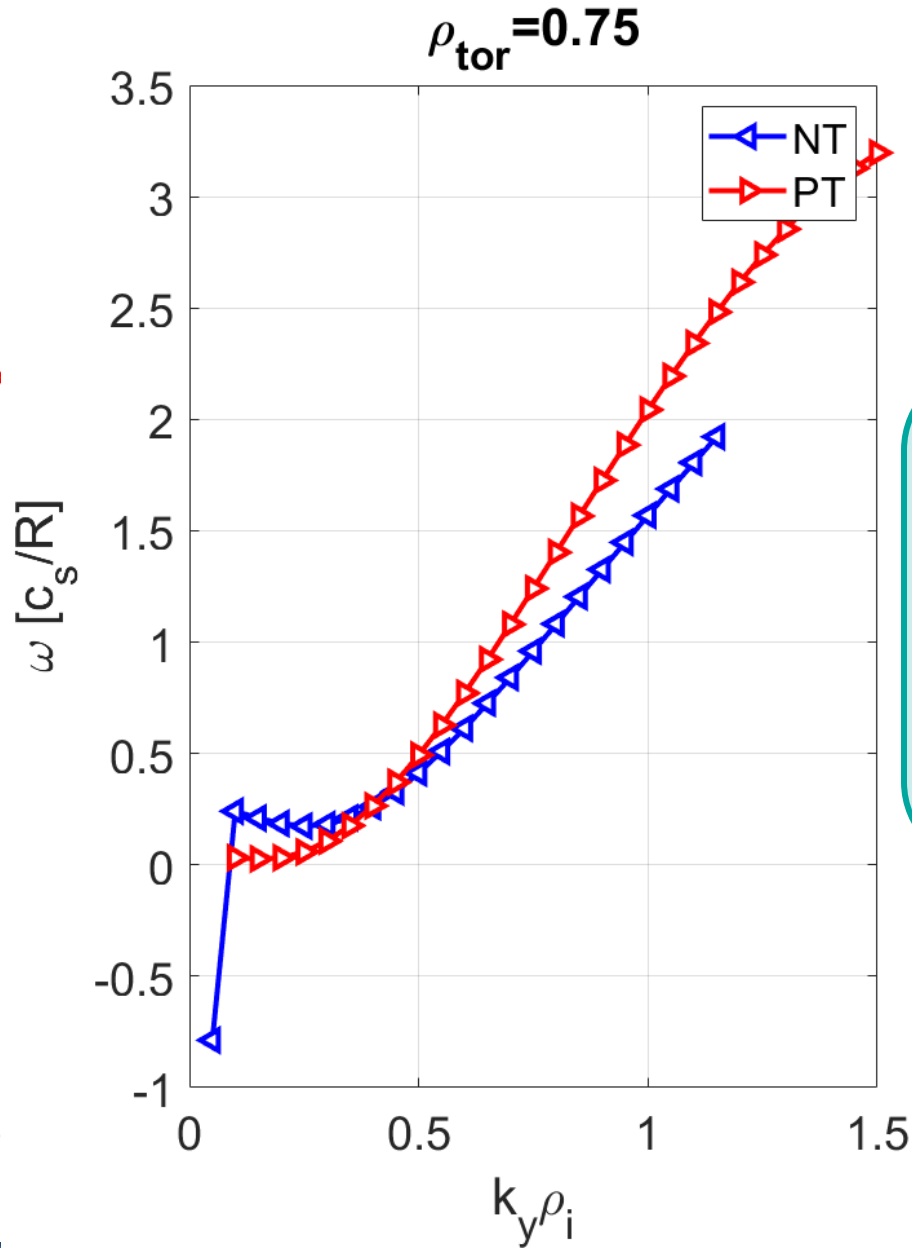
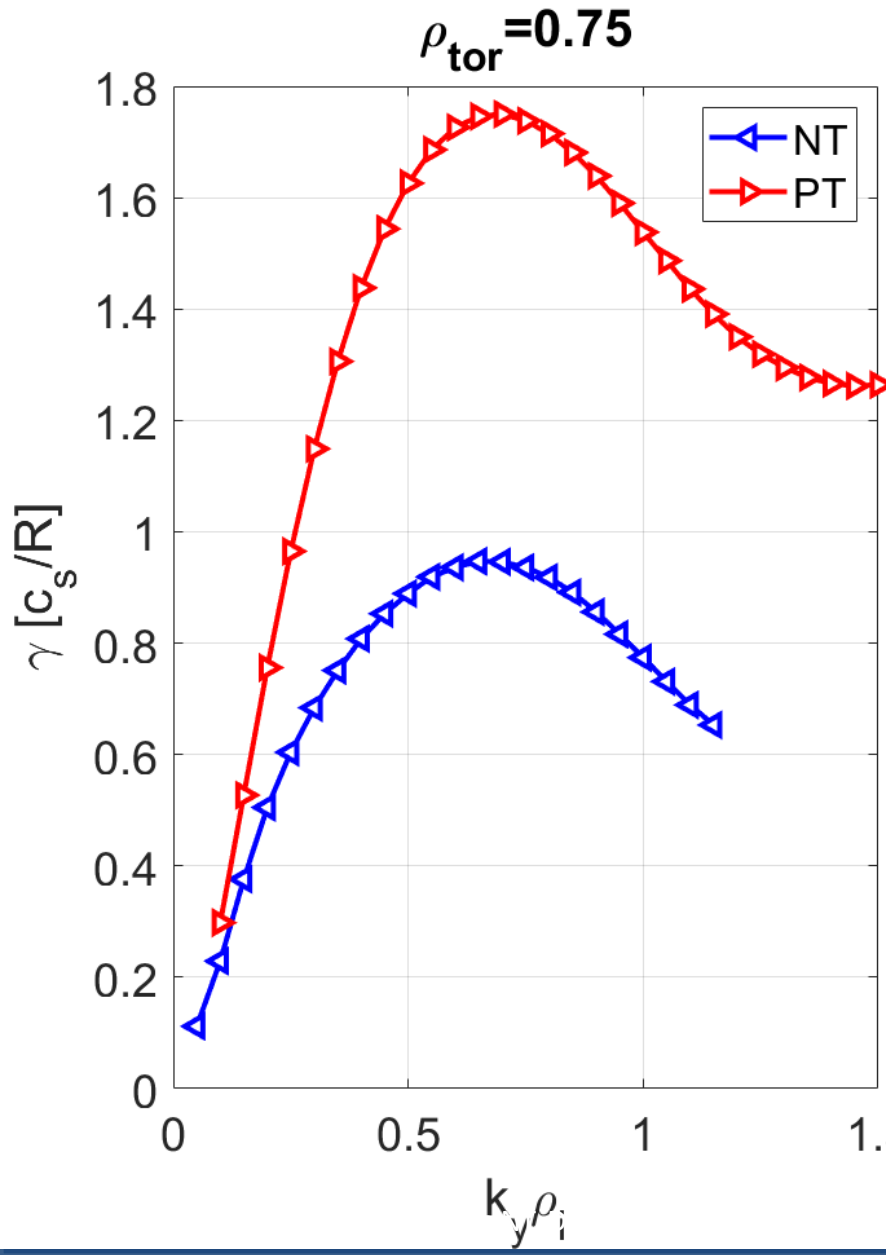
Linear GENE from RAPTOR profiles, k_y (ion scale) - $\rho_{tor} = 0.65$



- Scenarios dominated by ITG turbulence
- NT more stable than PT



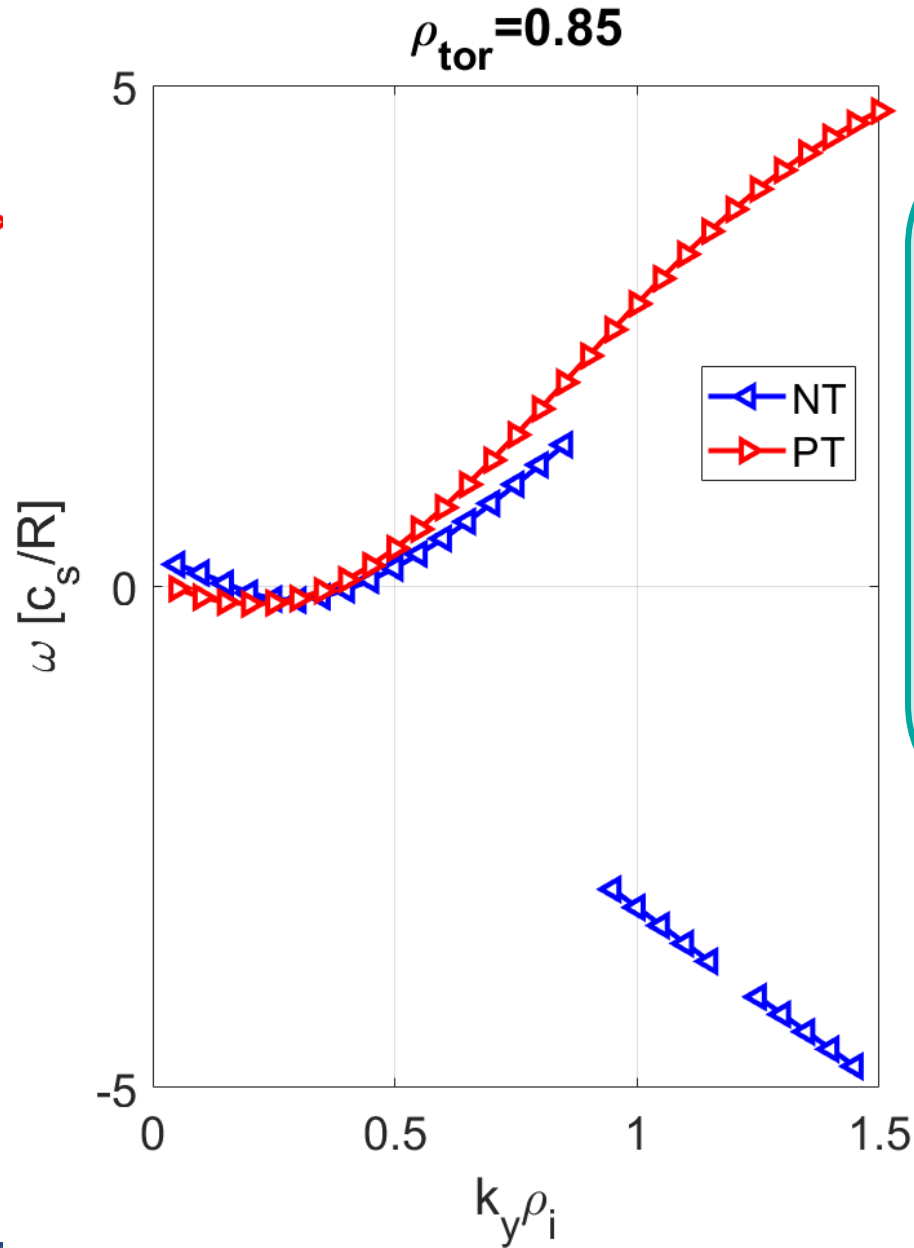
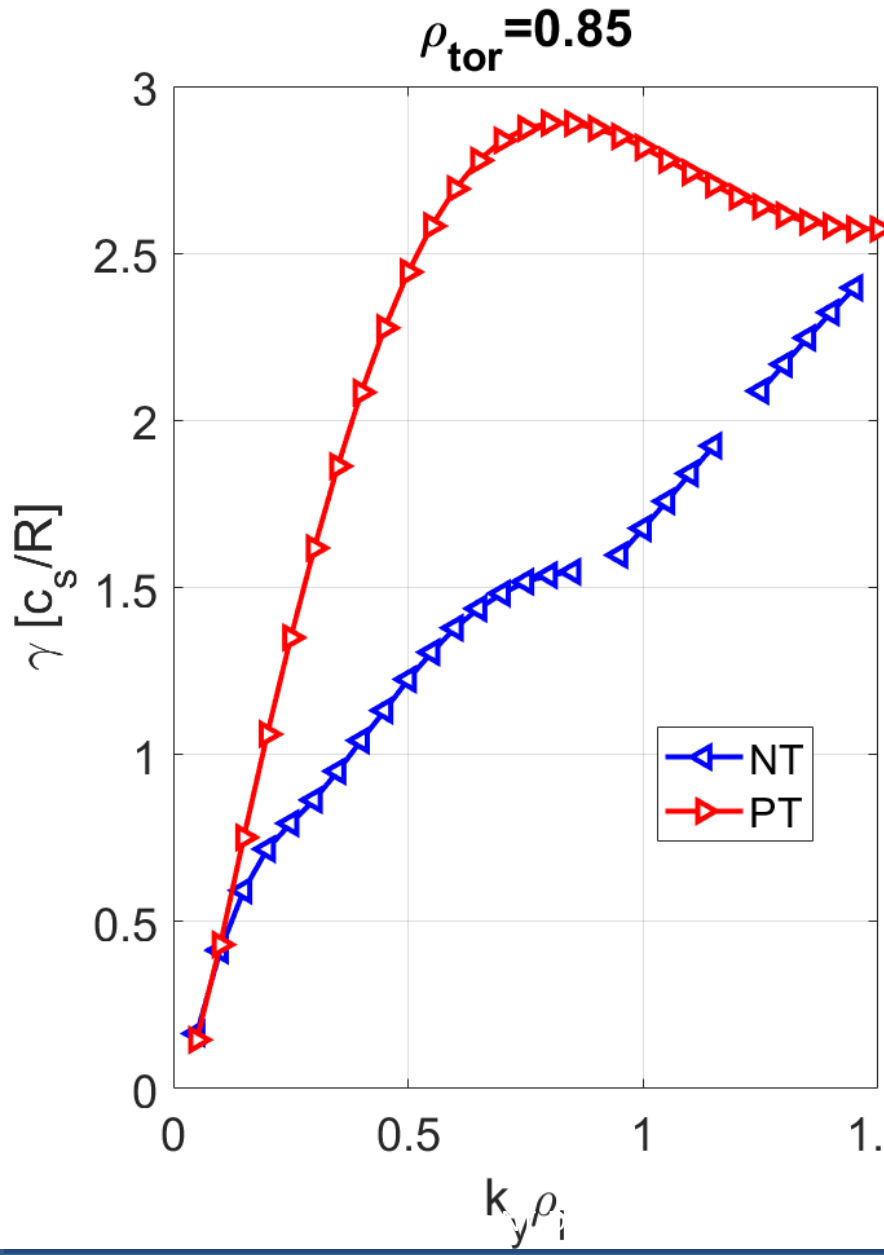
Linear GENE from RAPTOR profiles, k_y (ion scale) - $\rho_{tor} = 0.75$



- Scenarios dominated by ITG turbulence
- NT more stable than PT



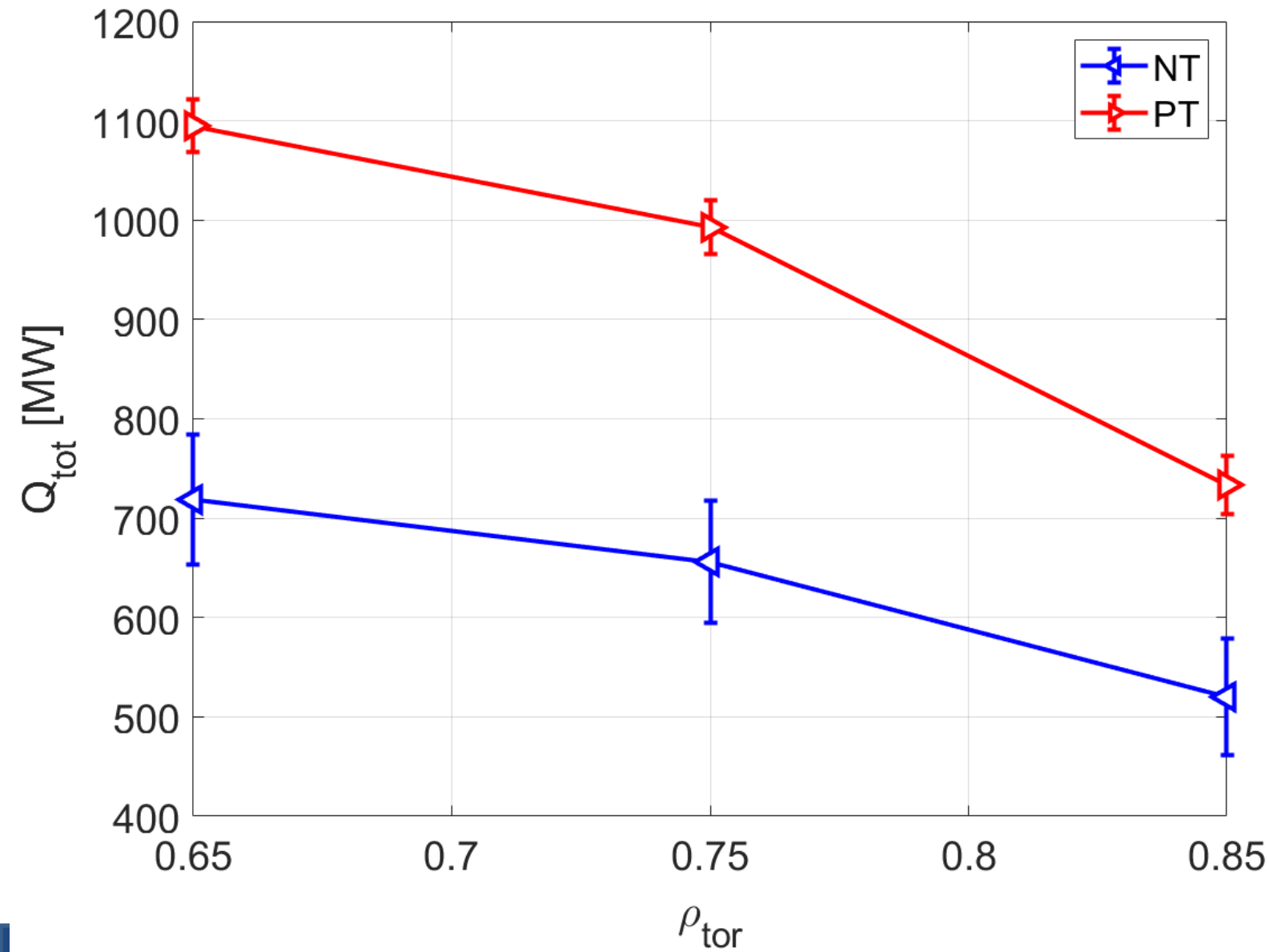
Linear GENE from RAPTOR profiles, k_y (ion scale) - $\rho_{tor} = 0.85$



- PT dominated by ITG
- NT dominated by mix of ITG/TEM
- NT more stable than PT for the most important k_y



Nonlinear GENE: Sensitivity to gradients – with impurities

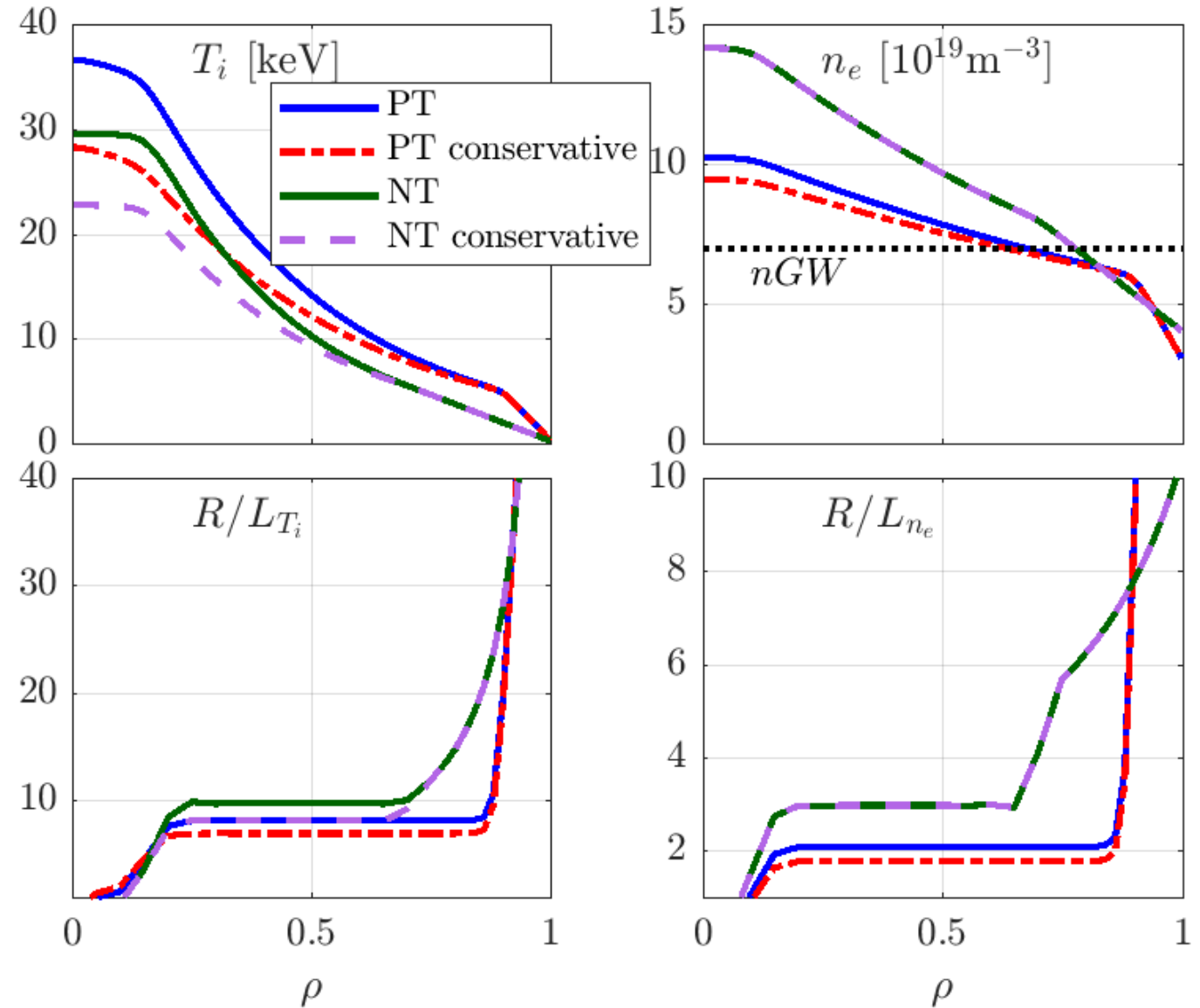


- NT heat flux overestimated between 1.5 and 2. Mostly due to neglect of tungsten
- NT more stable than PT for all radial position. Strong stabilization of turbulence.



RAPTOR PT and NT DEMO next iteration ($I_p=17.75\text{MA}$)

- NT L-mode allows for higher R/L_{n_e} (and $n_e(\text{edge})$ as well)
- NT and NT conservative ok with respect to GENE nonlinear simulations
- Higher density yields high P_{fus} at lower H factor. Hence importance of density limit experiments/theory





RAPTOR PT and NT DEMO operating points (Ip=17.75MA)

	PT	PT conservative	NT	NT conservative
Pfus [MW]	1933	1344	2302	1740
Pec [MW]	50	50	0 - 50	0 - 50
Palpha [MW]	387	269	460	348
Q	38.7	26.9	Inf - 46.1	Inf - 35.1
Prad [MW]	262	189	276 - 330	226 - 280
Psep [MW]	175	131	185 - 182	123 - 122
PLH	139	134	-	-
n(Xe)/ne	$6 \cdot 10^{-4}$	$4 \cdot 10^{-4}$	$3 - 4 \cdot 10^{-4}$	$2 - 3 \cdot 10^{-4}$
Psep/R0 [MW/m]	20	15	14	14
ne0/nevol	1.46	1.39	1.76	1.76
nevol/nGW	1.06	1.03	1.15	1.15
H98	0.99	0.89	0.80	0.76
betaN(th)	2.02	1.63	1.77	1.52
li3	0.94	0.88	1.20	1.12
q95	3.73	3.77	3.05	3.08
Vloop [mV]	45	54	56 - 60	66 - 71

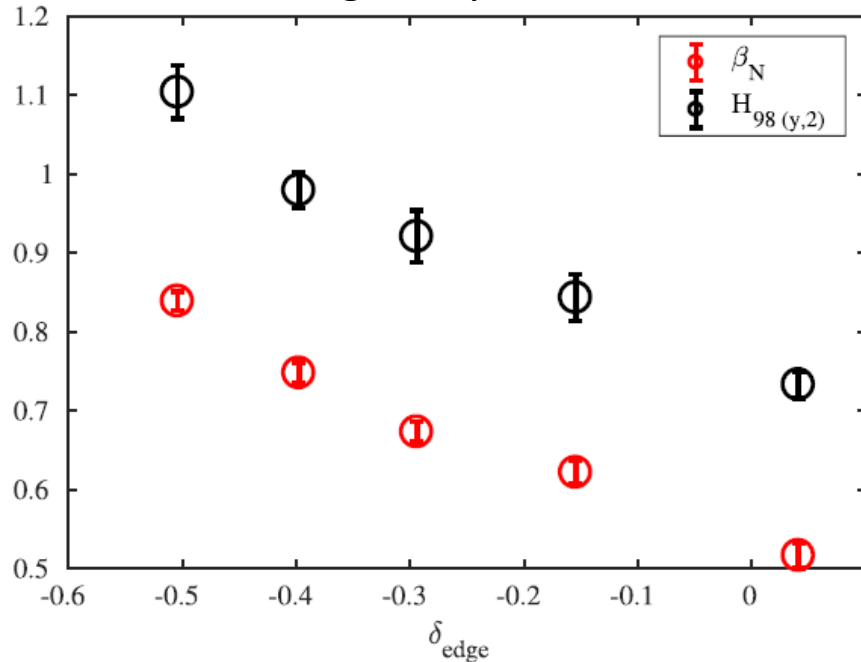
Consistent with GENE nonlinear simulations



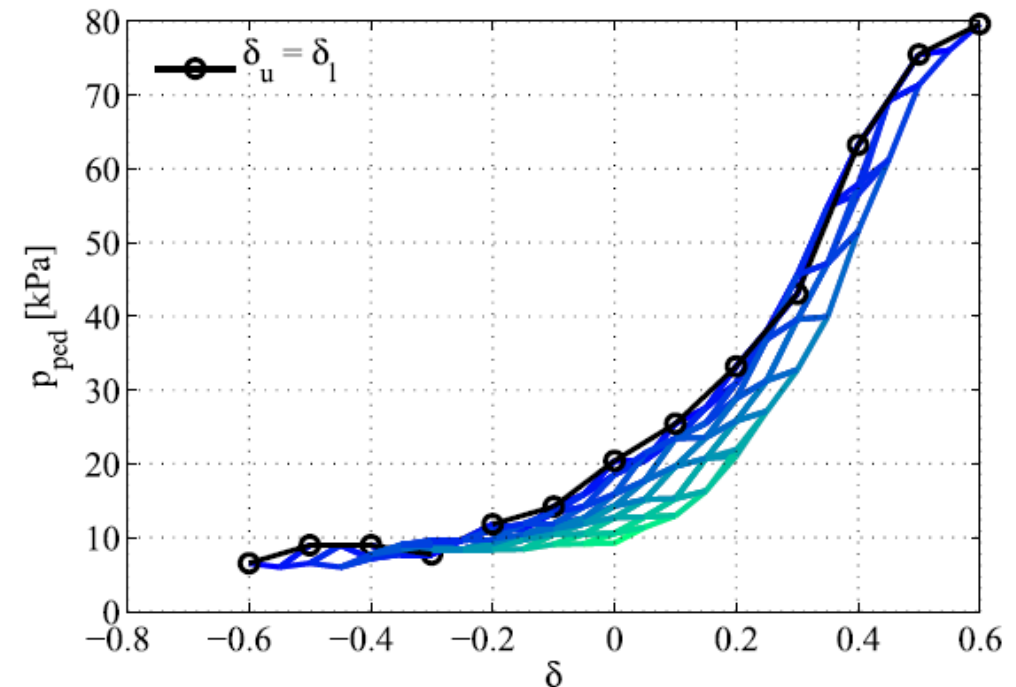
What about NT-VNS ?

- Present design uses small top δ to avoid large ELMs, as expected from A. Merle et al
- But worse confinement in both L-mode and H-mode
- Let's move to $d(\text{top}) < -0.2$: no ELMs large power demonstrated in JET, better confinement
- Win-Win: easier to operate, test NT at large scale

Ohmic TCV triangularity scan: worse conf at $\delta=0$



EPED-CH: still small ELMs at $\delta=0$





Conclusion and Outlook

- All the important questions from the ad-hoc group 2020 have been addressed successfully in present tokamaks. "Last" being resolved is the confinement in the recent AUG experiments (*but clearly better than PT L-mode*)
- Density limit proven better than expected
- Resilience to impurities has proven better than expected. In addition to avoiding constraints on P_{LH}
- Confinement prediction from first principles emerging (*but not really more uncertain than pedestal prediction in PT H-modes, ELM size and core confinement*)
- Next steps:
 - Continue optimization using CHEASE-RAPTOR-GENE for ballooning (L-mode), full discharge 1D system code with transients, GK fluxes
 - Add meq-RAPTOR for free boundary calculations and control issues
 - Optimize NT-DEMO and VNS (*probably best target since avoids ELMs altogether and offers similar to better conf than $\delta=0$, tbd*)